UNIVERSITY OF CALIFORNIA, SAN DIEGO

# Antimicrobial Nanotherapeutics Against *Helicobacter pylori* Infection

A dissertation submitted in partial satisfaction of the requirements for the degree
Doctor of Philosophy

in

Nanoengineering

by

Soracha Thamphiwatana

Committee in charge:

Professor Liangfang Zhang, Chair
Professor Michael J. Heller, Co-Chair
Professor Xiaohua Huang
Professor Marygorret Obonyo
Professor Donald J. Sirbuly

2014

The Dissertation of Soracha Thamphiwatana is approved, and it is acceptable in quality and form for publication on microfilm and electronically:

_____

_____

_____

_____

Co-Chair

_____

Chair

University of California, San Diego

2014

## DEDICATION

This dissertation is dedicated to my mother, Suninath Thamphiwatana, who has made countless sacrifices so I could freely pursue my dreams and always support me in every possible way. My sister, Jinna Thamphiwatana, is always there for me. This work has been possible because of their unconditional love and never-ending support.

## EPIGRAPH

"Imagination is more important than knowledge. Knowledge is limited. Imagination encircles the world."

*Albert Einstein*

## TABLE OF CONTENTS

## LIST OF FIGURES

## LIST OF TABLES

## ACKNOWLEDGEMENTS

I would like to thank Professor Liangfang Zhang first and foremost because this dissertation would not be possible without him. He is undoubtedly the best mentor one could ask for. I thank him for his attention, inspiration, and advice. He gave me a chance to explore novel scientific knowledge with joy and enthusiasm. Working under his guidance, my graduate life here at UCSD has been tremendously memorable.

I thank Professor Marygorret Obonyo who paved the way in the study of *Helicobacter pylori* and always give me a great advice. She always made herself available for me. Working with her is my great pleasure.

All of my colleagues in the Zhang lab have also made a great contribution toward my graduate study. Everyone always shows their willingness to help and gives invaluable suggestion/discussion. Dr. Weiwei Gao is the great scientist and artist. He made all wonderful illustration figures and gave me a lot of useful advice. I learned a lot from working with him. Dr. Dissaya Pornpatananangkul, Dr. Li Zhang, and Victoria Fu had been through a lot with me during the early years of my graduate program. They are not only my great colleagues but also great friends who made me enjoy working with them in the lab days and nights. Dr. Che-Ming Hu, Ronnie Fang, Brian Luk, Cody Carpenter, and Jonathan Cop contributed to many useful discussions and are very supportive. Pavimol Angsantikul, Jingying Zhu, Fei Wang, Dr. Zhiqing Pang, and Yuan Chen added joy to my graduate experience. Thanks so much.

I would love to thank the Ministry of Science and Technology, Royal Thai Government for their financial support through my entire graduate study. I also thank

American Association of University Women for their scholarship that aided me in the third year of my study.

Moreover, I would like to thank all the friendships from Thai community here in San Diego. Thanks for all thier supports and fun stuffs we did together. Our friendships will never been forgotten.

Last by not least, I would like to thank the Nanoengineering department at UCSD, their faculty, and administration staff, for giving me the most memorial, inspiring, and illuminating time of my life.

Chapter 1, in full, is a reprint of the material as it appears in WIREs Nanomedicine & Nanobiotechnology, 2014, Soracha Thamphiwatana, Weiwei Gao, Pavimol Angsantikul and Liangfang Zhang. The dissertation author was the primary investigator and co-author of this paper.

Chapter 2, in full, is a reprint of the material as it appears in Molecular Pharmaceutics, 2012, Soracha Thamphiwatana, Marygorret Obonyo, Li Zhang, Dissaya Pornpattananangkul, Victoria Fu, and Liangfang Zhang, and, The dissertation author was the primary investigator and author of this paper.

Chapter 3, in full, is in a manuscript submitted to Sciences Translational Medicine, 2014, Soracha Thamphiwatana, Weiwei Gao, Marygorret Obonyo, and Liangfang Zhang, and, The dissertation author was the primary investigator and author of this paper.

Chapter 4, in full, is a reprint of the material as it appears in Langmuir, 2013, Soracha Thamphiwatana, Victoria Fu, Jingying Zhu, Dainnan Lu, Weiwei Gao, and

Liangfang Zhang, and, in full, on the material submitted for publication as it may appear in Journal of Materials Chemistry B, 2014, Soracha Thamphiwatana, Weiwei Gao, Marygorret Obonyo, and Liangfang Zhang. The dissertation author was the primary investigator and author of these papers.

## VITA

2006 Bachelor of Pharmaceutical Sciences, Prince of Songkla University

2006-2008 Lecturer at School of Medicine, Prince of Songkla University

2010 Master of Engineering, Biomedical Engineering, Colorado State University

2011 Master of Science, Nanoengineering, University of California, San Diego

2014 Doctor of Philosophy, Nanoengineering, University of California, San Diego

## PUBLICATIONS

1. Obonyo, M.*; Zhang, L.*; Thamphiwatana, S.*; Pornpattananangkul, D.; Fu, V; Zhang, L. "Antibacterial activities of liposomal linolenic acids against antibiotic-resistant Helicobacter pylori", *Molecular Pharmaceutics* 2012, 9, 2677-2685. (*co-first author)

2. Pornpattananangkul, D.; Fu, V.; Thamphiwatana, S.; Zhang, L.; Chen, M.; Vecchio, J.; Gao, W.; Huang, C-M.; Zhang, L. " In vivo treatment of Propionibacterium acnes infection with liposomal lauric acids", *Advanced Healthcare Materials* 2013,2, 1322-1328.

3. Thamphiwatana, S.; Fu, V.; Zhu, J.; Lu, D; Gao, W.; Zhang, L. "Nanoparticle-stabilized liposomes for pH-responsive gastric drug delivery", *Langmuir* 2013, 29, 12228-12233.

4. Gao, W.; Vecchio, D.; Li, J.; Zhu, J.; Zhang, Q.; Fu, V.; Thamphiwatana, S.; Zhang, L. "Hydrogel Containing Nanoparticle-Stabilized Liposomes for Topical Antimicrobial Delivery", *ACS Nano* 2014, 8, 2900-2907.

5. Gao, W.; Thamphiwatana, S.; Angsantikul, P.; Zhang, L. "Nanoparticle approaches against bacterial infections", *WIREs Nanomedicine & Nanobiotechnology* (in press)

6. Thamphiwatana, S.; Gao, W.; Obonyo, M.; Zhang, L. "Phospholipase A2-degradable liposomes for antibiotic delivery against *Helicobacter pylori", Journal of Materials Chemistry B* (manuscript submitted)

7. Thamphiwatana, S.; Gao, W.; Obonyo, M.; Zhang, L. "In vivo treatment of *Helicobacter pylori* infection with liposomal linolenic acid reduces colonization and ameliorates inflammation*", Science Translational Medicine* (manuscript submitted)

## ABSTRACT OF THE DISSERTATION

### Antimicrobial Nanotherapeutics Against *Helicobacter pylori* Infection

by

Soracha Thamphiwatana

Doctor of Philosophy in Nanoengineering

University of California, San Diego, 2014

Professor Liangfang Zhang, Chair
Professor Michael J. Heller, Co-Chair

*Helicobacter pylori* (*H. pylori*) infection with its vast prevalence is responsible for various gastric diseases including gastritis, peptic ulcers, and gastric malignancy. While effective, current treatment regimens are challenged by a fast-declining eradication rate due to the increasing emergence of *H. pylori* strains resistant to existing antibiotics. Therefore, there is an urgent need to develop novel antibacterial

strategies against *H. pylori*. The first area of this research, we developed a liposomal nanoformulation of linolenic acid (LipoLLA) and evaluated its bactericidal activity against resistant strains of *H. pylori*. We found that LipoLLA was effective in killing both spiral and dormant forms of the bacteria via disrupting bacterial membranes. LipoLLA eradicated all strains of the bacteria regardless of their antibiotic resistance status. Furthermore, the bacteria did not develop drug resistance toward LipoLLA. Our findings suggest that LipoLLA is a promising antibacterial nanotherapeutic to treat antibiotic-resistant *H. pylori* infection.

The next step, we investigated the *in vivo* therapeutic potential of LipoLLA for the treatment of *H. pylori* infection. In vivo tests further confirmed that LipoLLA was able to kill *H. pylori* and reduce bacterial load in the mouse stomach. LipoLLA treatment was also shown to reduce the levels of proinflammatory cytokines including interleukin-1β (IL-1β), IL-6, and tumor necrosis factor alpha, which were otherwise elevated due to the *H. pylori* infection. Finally, toxicity test demonstrated excellent biocompatibility of LipoLLA to normal mouse stomach. Collectively, results from this work indicate that LipoLLA is a promising, new, effective, and safe therapeutic agent for the treatment of *H. pylori* infection.

The second area is stimuli-responsive liposomes development. By adsorbing small chitosan-modified gold nanoparticles (AuChi) onto the outer surface of liposomes, we show that at gastric pH the liposomes have excellent stability with limited fusion ability and negligible cargo releases. However when the stabilized liposomes are present in an environment with neutral pH, the gold stabilizers detach

from the liposomes resulting in free liposomes that can actively fuse with bacterial membranes. The reported liposome system holds a substantial potential for gastric drug delivery; it remains inactive (stable) in the stomach lumen but actively interact with bacteria once reaches the mucus layer of the stomach where the bacteria may reside. Another stimulus that can activate drug release from liposomes is virulence factor released from bacteria themselves. We formulate liposomes with a lipid composition sensitive to bacterium-secreted phospholipase $A_2$ ($PLA_2$) degradation and then adsorb AuChi onto their surfaces. The resulting AuChi-stabilized liposomes (AuChi-liposomes) showed prohibited fusion activity and negligible drug leakage. When loaded with doxycycline, AuChi-liposomes effectively inhibit *H. pylori* growth in vitro. Overall, the design of AuChi-liposomes allows for a smart "on-demand" payload delivery: the more enzymes or bacteria at the infection site, which depends on the severity of infection, the more drug will be released. Given the strong association of $PLA_2$ with a diverse range of diseases, the present liposomal delivery technique holds broad application potential for tissue microenvironment-responsive drug delivery.

# Chapter 1

## Introduction

# Introduction

Despite the profound success achieved by the use of antibiotics against infectious diseases, bacterial infections continue to impose significant challenges on global healthcare[1, 2]. Eradication of certain bacterial infections such as tuberculosis remains difficult due to the complex mechanisms of the pathogen in subverting its host's immune system as well as the delivery barriers that prevent antibiotics from reaching sites of infection[3, 4]. Highly potent antibiotics, including certain aminoglycosides and fluoroquinolones, generate severe adverse effects and are reserved only for serious infections[5, 6]. More significantly, the emergence of antibiotic resistance has generated alarming impact, threatening to set back the progress against a range of infectious diseases to the pre-antibiotic era[7, 8]. The widespread drug resistance is further exacerbated by the retreat of the pharmaceutical sector from new antibiotic development[9]. These challenges, together, highlight the demand for alternative and effective antimicrobial strategies.

Over the last few decades, the application of nanotechnology, particularly the use of nanoparticles for drug delivery, has generated significant impact in medicine[10, 11]. Various nanoparticle delivery platforms, especially liposomes, polymeric nanoparticles, dendrimers, and inorganic nanoparticles, have received significant attention (Figure 1.1). Drug molecules loaded into nanocarriers through physical encapsulation, adsorption, or chemical conjugation exhibit an improved pharmacokinetic profile and therapeutic index when compared to their free drug counterparts[12]. Other advantages of nanoparticle delivery systems, including improved

drug solubility, prolonged systemic circulation, sustained and controlled release, precise drug targeting, and concurrent delivery of multiple drugs, have also been validated in various studies[13]. As a result, a number of nanoparticle-based drug delivery systems have been approved for clinical use to treat a variety of infectious diseases, and many other antimicrobial nanoparticle formulations are currently under various stages of pre-clinical and clinical tests[14].

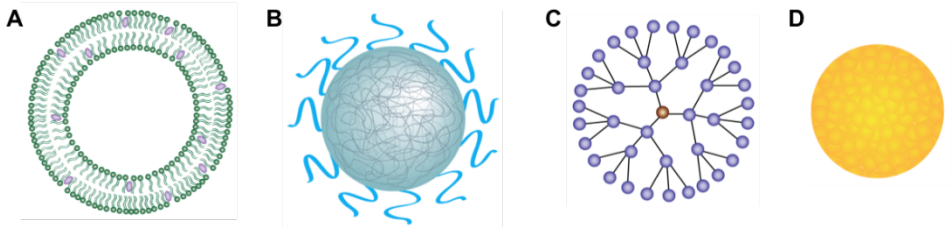


**Figure 1.1** Major nanoparticle-based delivery platforms for treating bacterial infections: (A) liposome, (B) polymeric nanoparticle, (C) dendrimer, and (D) inorganic nanoparticle.

As the ability to engineer multifunctional nanoparticles continually advances, numerous innovative approaches have emerged, further improving on nanoparticle therapeutic efficacy against bacterial infection. In this review article, we select five areas where nanoparticle approaches hold significant potential to improve upon current treatments. These areas include: (1) targeted antibiotic delivery, (2) environmentally responsive antibiotic delivery, (3) combinatorial antibiotic delivery, (4) nanoparticle-enabled antibacterial vaccination, and (5) nanoparticle-based bacterial detection. In each area we review the current and forthcoming nanoparticle platforms and the progress made against bacterial infections.

## 1.1 Targeted antibiotic delivery

Bacterial infection increases vascular permeability, which makes passive targeting possible. At the infection sites, the release and accumulation of bacterial components such as bacterial protease and lipopolysaccharide from gram-negative bacteria or lipoteichoic acid from gram-positive bacteria are known to trigger various inflammatory mediators that directly stimulate vascular permeability[15, 16]. These bacterial components also activate immune cells, which in turn interact with vascular endothelium through multiple inflammatory and vascular mediators, leading to gap widening, barrier dysfunction, and eventually increased permeability[17]. Moreover, dysfunctional lymphatic drainage has also been reported in bacterial infection, which potentially promotes nanoparticle accumulation at the sites of infection[18]. These features of bacterial infection suggest that the enhanced permeation and retention (EPR) effect can be harnessed by nanoparticles for targeted antibiotic delivery[19]. In fact, both uncoated liposomes and PEGylated liposomes have been shown to accumulate selectively at soft tissue infected by *Staphylococcus aureus* (*S. aureus*), and their retention times correlated closely with size[20-23]. Similar results were observed for superparamagnetic iron oxide nanoparticles (SPIONs) at the soft tissue of rats and in the lungs of mice infected by *S. aureus*[24].

Pathogenic bacteria maintain a negative surface charge under physiological conditions. Therefore, cationic nanoparticles capable of binding with bacteria via electrostatic interactions have been explored for effective bacterial targeting[25, 26]. This strategy is attractive for its multivalent effect and the ability to target polymicrobial

infections. As a result, a diverse range of bactericidal polymers and peptides has been incorporated into various nanoparticle designs for antibacterial applications[27]. More importantly, nanoparticle formulation can increase the local charge and mass densities of the bactericidal components, resulting in enhanced therapeutic index. For example, a self-assembled cationic peptide nanoparticle has shown strong antimicrobial properties while inducing minimal systemic toxicity[28]. Furthermore, improving the biodegradability of the nanoparticles can further reduce cationic charge related toxicity. In this perspective, cationic nanoparticles self-assembled from polycarbonate-based block co-polymers with high biodegradability have been shown to kill bacteria without inducing obvious hemolytic activity and systemic toxicity[29].

Active targeting with pathogen-binding ligands directly conjugated to the surface of nanoparticles is another strategy to target bacteria. For example, small molecules such as vancomycin have been conjugated to the surfaces of dendrimers[30], iron oxide nanoparticles[31], gold nanoparticles[32], and porous silica nanoparticles[33], resulting in preferential binding of nanoparticles to gram-positive bacteria. The targeting efficiency of small molecules was also found to be strongly dependent on molecular orientation, surface density, and length of the spacer used in conjugation[34]. In addition to small molecules, lectins, particularly those with selective agglutination activities, have also been used as ligands to target bacteria[35]. Polymeric nanoparticles conjugated with mannose-specific or fucose-specific lectins showed enhanced binding affinity to the carbohydrate receptors on *Helicobacter pylori* (*H. pylori*) surfaces, suggesting a promising approach for site-specific and gastroretentive drug delivery to

treat *H. pylori* infection[36]. Besides lectins, other protein ligands such as single-domain antibodies[37] and bacteriophage tailspike proteins[38] are highly specific targeting ligands and their conjugation to nanoparticles has resulted in targeted delivery platforms effective against a variety of bacterial infections. Furthermore, aptamers have also become a class of attractive targeting moieties owing largely to the advancement in bacterium-based aptamer selection techniques, which continually improve aptamer binding affinity and specificity. These targeting molecules have been extensively explored to target nanoparticles to pathogenic bacteria such as *Salmonella typhimurium* (*S. typhimurium*) and *Mycobacterium tuberculosis* (*M. tuberculosis*)[39, 40].

Moreover, bacteria can survive ingestion by phagocytic cells such as macrophages, hence evading the immune system and the bactericidal action of antibiotics[3]. However macrophages are able to transport drugs to the site of infection by a chemotactic mechanism[41, 42]. Therefore, targeting antimicrobial nanoparticles to macrophages as opposed to bacteria has become an attractive strategy for improving antibiotic therapy, particularly to treat intracellular bacterial infection[43]. It has been observed that following passive targeting to the infection sites, nanoparticles could preferentially be taken up by macrophages due to the spontaneous scavenging feature of macrophages[23, 24]. Such macrophage uptake could be further enhanced by attaching targeting ligands onto the nanoparticles[44, 45]. In this regard, various ligands, including mannose, maleylated bovine serum albumin and O-steroyl amylopectin, have been applied to successfully enhance macrophage uptake of nanoparticles for the treatment of intracellular infection[46, 47].

## 1.2 Environmentally responsive antibiotic delivery

To further improve upon the therapeutic efficacy of antimicrobial nanoparticles, researchers have explored environmentally responsive nanoparticles that remain inactive until they are triggered by cues found in the microenvironment of infection sites. These external stimuli can be physical signals such as temperature, electric field, magnetic field, and ultrasound; they can also be chemical signals such as pH, ionic strength, redox potential, and enzymatic activities [48].

Among these environmental stimuli, pH gradients have been widely used to design novel, responsive nanoparticles for antibiotic delivery. At the organ level, nanoparticles have been designed to respond to the pH gradient along the gastrointestinal (GI) tract[49] and the acidic environment of human skin[50] for site-specific antibiotic delivery. At the intracellular level, nanoparticles have been formulated to respond to the acidic pH inside the endolysosomal compartments for triggered drug release[51-53]. In addition to pH gradient, bacterial enzymatic activities, including those of secreted toxins, have also been used to trigger the release of antimicrobial agents to inhibit the growth of the target bacteria.

Charged polymers have been adsorbed onto liposome surfaces with opposite charge to stabilize the liposomes [54, 55]. Such stabilization is pH sensitive and has been extensively used to treat various intracellular bacterial infections including *Salmonella enterica (S. enterica)* [56, 57] as well as cases of septic shock [58, 59]. Based on a similar mechanism, ionic liposomes can be employed to carry oppositely charged drug molecules for pH-sensitive drug release. In addition, loading liposomes with

membrane disrupting toxins such as hemolysin [60] and listeriolysin that are responsive to endosomal acidification has also shown potential for the treatment of intracellular infections [61].

Recently, a new environment-responsive delivery strategy has emerged that involves the attachment of small charged nanoparticles onto liposome surfaces for liposome stabilization and triggered antimicrobial delivery (Figure 1.2). The nonspecific adsorption of charged nanoparticles onto phospholipid bilayers provided steric repulsion that inhibited liposome fusion. It also reduced liposome surface tension and thus further enhanced liposome stability [62, 63]. Intriguingly, the charge and charge density of both the nanoparticle stabilizers and the liposomes could be precisely tailored to enable stimulus-responsive binding and detachment of the nanoparticles, thereby allowing for an on-demand control over liposome fusion activity for smart drug delivery. For instance, cationic liposomes bound with negatively charged gold nanoparticles only fused with bacteria at acidic pH, which made them suitable for treating various skin pathogens that thrive in acidic infection sites such as the case with *Propionibacterium acnes* (*P. acnes*)[64]. Conversely, anionic liposomes stabilized by positively charged gold nanoparticles were highly stable in gastric acid, but capable of fusing with bacteria at physiological pH, making them suitable to treat gastric pathogens such as *H. pylori* [65]. Even in the absence of such stimulus-induced detachment of the nanoparticle stabilizers, these liposomes still had a substantial fraction of their surface areas exposed and highly accessible to bacterial toxins. This feature allowed the liposomes to respond to various bacteria such as *S.*

*aureus* that secret pore-forming toxins to trigger drug release from the liposomes [66]. Aimed at improving the topical applications of nanoparticle-stabilized liposomes, a hydrogel form of the delivery system was recently developed, which not only preserved the structural integrity of the nanoparticle-stabilized liposomes, but also allowed for controllable viscoelasticity and tunable liposome release rate [67].

Meanwhile, polymeric nanoparticles have been extensively studied for responsive antibiotic delivery. For example, tri-block copolymer nanoparticles composed of poly(lactic-*co*-glycolic acid) (PLGA), poly(L-histidine) and poly(ethylene glycol) (PEG) have been reported for acid-responsive antibiotic delivery [68]. These nanoparticles maintained a negative charge at neutral pH; however, when exposed to an acidic pH, the protonation of the imidazole groups switched the surface charge to a positive one, resulting in enhanced bacterial binding and improved antibacterial efficacy. As another example, heparin and chitosan have been applied to form base-sensitive nanoparticles for treating gastric pathogens such as *H. pylori*. The polymers self-assembled to form nanoparticles at pH 1.2-2.5; however, upon contact with *H. pylori* at the gastric epithelium with physiological pH, the chitosan deprotonated, causing nanoparticle disassembly and release of drugs for bacteria killing[69]. Moreover, by tailoring the pKa of amphiphilic copolymers, a wide range of polymeric nanoparticles has been engineered, which precisely respond to the subtle changes of pH along the GI tract for site-specific antibiotic delivery. Enzyme-sensitive polymeric nanoparticles have also been developed for intracellular delivery in macrophages. For example, a triple-layered nanogel formulation has been reported,

which contained a bacterial lipase-sensitive poly(ε-caprolactone) interlayer between the cross-linked polyphosphoester core and the PEG shell [70]. Following macrophage uptake, the presence of bacterial phosphatase or phospholipase triggered rapid drug release, which subsequently inhibited the growth of *S. aureus* [47].

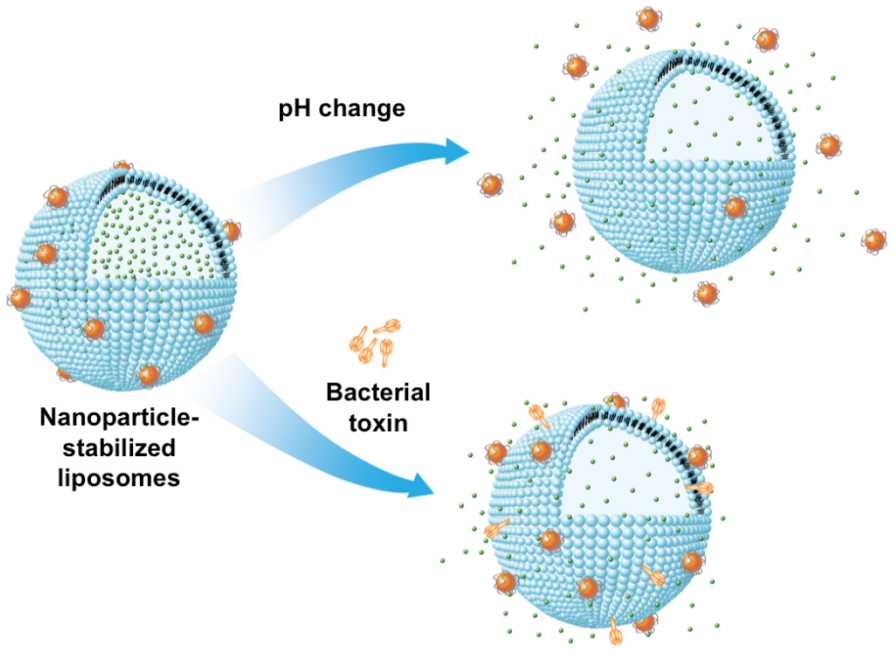


**Figure 1.2** Schematic illustration of a phospholipid liposome stabilized by charged gold nanoparticles and its drug release in response to pH change or the presence of bacterial toxin.

## 1.3 Combinatorial antibiotic delivery

Combining two or more distinct antibiotics represents a common strategy in treating bacterial infections with the aim to broaden the antimicrobial spectrum, generate synergistic effects, and counteract antibiotic resistance. However, varying pharmacokinetics, biodistributions, toxicity profiles, and membrane transport

properties among different drug compounds complicate dosing and scheduling optimization, which in turn compromise drug synergy *in vivo* [71]. In this regard, nanoparticles offer unique properties to enhance combinatorial antibiotic delivery and numerous applications have been investigated to address a variety of bacterial infections (Table 1.1).

Liposomes are a highly versatile platform for combinatorial delivery. Hydrophilic drugs can be directly encapsulated in the aqueous compartments of liposomes, while hydrophobic drugs can be incorporated into the lipid bilayer membranes[72]. For example, isoniazid and rifampicin, first line antitubercular drugs, have been loaded in the aqueous compartment and the lipid bilayer, respectively. The resulting liposomal formulation has shown increased efficacy compared to free drug counterparts at the same dosages[73-75]. Liposomal formulation can also reduce drug toxicity to the host cells, thereby allowing for co-delivery of combinatorial antibiotics that are otherwise too toxic in their free forms. For example, drug compounds such as gallium (Ga) and bismuth derivatives are antibiotics that inhibit bacterial growth by interrupting their iron uptake. Although they have shown synergetic effects in combination with other antibiotics, their usage has been limited by severe toxicity[76]. To address this challenge, $Ga^{3+}$ was combined with gentamicin and loaded into liposomes. The formulation reduced Ga toxicity and improved efficacy against highly resistant *Pseudomonas aeruginosa (P. aeruginosa)* [77]. Similarly, bismuth-ethanedithiol (BiEDT) was encapsulated together with tobramycin into liposomes, resulting in the elimination of BiEDT's toxic effect on human lung cells while

increasing its antibacterial efficacy against *P. aeruginosa* and *Burkholderia cepacia (B. cepacia)* [78-80]. A recent *in vivo* study showed that the same drug combination in a liposome formulation enhanced efficacy in reducing bacterial burden in rats chronically infected with *P. aeruginosa* [81].

Moreover, liposomal formulation of combinatorial antibiotics enables ratiometric control over the drugs and thus unifies the pharmacokinetics of different drug molecules and ensures parallel tissue distribution. These advantages serve to enhance the antimicrobial efficacy of the drugs. For example, using the dosage and dosing schedule derived from *in vitro* studies, the co-administration of gentamicin and ceftazidime only resulted in an additive effect in a rat model of an acute unilateral *Klebsiella pneumoniae* (*K. pneumoniae*) infection [82]. In contrast, the corresponding liposomal formulation encapsulating both gentamicin and ceftazidime showed a synergistic effect that led to a shorter course of treatment at lower cumulative doses [83]. The benefit of ratiometric delivery using liposomes was also reported in other combination therapies in treating *S. aureus* [84, 85], *M. tuberculosis*[73, 74], *Mycobacterium avium (M. avium)* [86, 87], and *H. pylori*[88, 89].

Polymeric nanoparticles represent another emerging platform for combinatorial antibiotic delivery to treat bacterial infection. In general, drug molecules can be directly encapsulated into the polymeric cores. For precise ratiometric loading and controlled drug release, multiple drugs can be covalently conjugated to the polymer backbone followed by nanoparticle preparation[90-92]. In addition, using emulsion techniques, both hydrophobic and hydrophilic drug molecules can be co-encapsulated

into the polymeric cores[93, 94]. As a result, several polymeric nanoparticle systems have been reported for delivering antibiotic combinations. For example, the combination of rifampin and azithromycin was delivered with PLGA nanoparticles and showed better efficacy *in vitro* compared to free drugs in treating persistent chlamydial infection[95]. Galiadin nanoparticles co-encapsulating clarithromycin and omeprazole showed better efficacy against *H. pylori* bacteria in rats [96, 97]. The gliadin nanoparticles were further conjugated with lectin and used in triple therapy with amoxicillin, clarithromycin, and omeprazole [98], resulting in superior *in vivo* clearance of *H. pylori* compared to the non-conjugated formulation and free drugs. Moreover, PLGA nanoparticles were also used for oral delivery of anti-tuberculosis drugs (ATDs) [99, 100]. In these studies, three or four frontline ATDs, including rifampicin, isoniazid, pyrazinamide and ethambutol, were co-encapsulated inside PLGA nanoparticles through an emulsion technique, and the resulting nanoparticle formulation improved bacterial clearance in *M. tuberculosis* infected mice and guinea pigs via oral administration.

**Table 1.1** Combinatorial nanoparticles for antibacterial drug delivery

| Platform | Formulation | Drug Combination | Targeted bacteria | References |
|---|---|---|---|---|
| Liposomes | DPPC, DMPG and cholesterol | Gallium and gentamicin | *P. aeruginosa* | [77] |
| | DSPC and cholesterol | Bismuth-ethanedithiol (BiEDT) and tobramycin | *P. aeruginosa* and *B. cenocepacia* | [78] |
| | PEGylated liposome | Daptomycin and clarithromycin | MRSA | [85] |
| | PG, PC and cholesterol | Clarithromycin and ofloxacin | *M. avium* | [86] |
| | PC, SA, and cholesterol | Ciprofloxacin and vancomycin | MRSA | [84 |
| | PC, PEG-DSPE, and cholesterol | Gentamicin and ceftazidime | *K. pneumoniae* | [83] |
| | DPPC and cholesterol | Isoniazid and rifampicin | *M. turberculosis* | [75] |
| | PG, PC and cholesterol | Streptomycinand and ciprofloxacin | *M. avium* | [87] |
| | PC, PE, SA and cholesterol | Amoxicillin trihydrate and ranitidine bismuth citrate | *H. pylori* | [88] |
| | PAA, PAH, PC, and cholesterol | Amoxicillin and metronidazole | *H. pylori* | [89] |
| Polymeric nanoparticles | PLGA | Rifampin and azithromycin | *C. trachomatis* and *C. pneumoniae* | [95] |
| | PLGA | Rifampicin, isoniazid, pyrazinamide, and ethambutol. | *M. tuberculosis* | [99] |
| | Sodium alginate and chitosan | Rifampicin, isoniazid, pyrazinamide, and ethambutol. | *M. tuberculosis* | [100] |
| | Chitosan and glutamic acid | Amoxicillin, clarithromycin, and omeprazole | *H. pylori* | [97] |
| | Gliadin and Pluronic F-68 | Clarithromycin and omeprazole | *H. pylori* | [98] |
| | Gliadin, lectin and Pluronic F-68 | Amoxicillin, clarithromycin and omeprazole | *H. pylori* | [96] |

DPPC: 1,2-dipalmitoyl-sn-glycero-3- phosphocholine,
DMPG: 1,2-dimyristoyl-sn-glycero-3-phosphoglycerol**,**
DSPC: 1,2-distearoyl-sn-glycero-3-phosphocholine,
DSPE1,2-distearoyl-sn-glycero-3-phosphoethanolamine**,**
DPPC: dipalmitoylphosphatidylcholine**,**
PG: egg yolk phosphatidylglycerol,
PE: phosphatidylethanolamine,
PC: phosphatidylcholine**,** SA: stearylamine**,**
PLGA: poly(lactic acid-co-glycolic acid),
PAA: poly(acrylic acid), PAH: poly(allylamine hydrochloride)

## 1.4 Nanoparticle-enabled antibacterial vaccination

Vaccines can protect against or treat infections by manipulating the host's immune responses, and their success in controlling former epidemics worldwide has

been considered as the most effective public health intervention ever achieved[101, 102]. The vaccine strategy also holds the promise to halt antibiotic resistance by reducing the exposure of bacteria to widely used antimicrobial agents[103, 104]. However, the majority of existing vaccines predominantly drive the generation of neutralizing or opsonizing antibodies against pathogens, a mechanism that is ineffective against a number of infections[105]. Vaccine development against these diseases is further hampered by incomplete understanding of the enormously complex human immune system and the underlying mechanisms of protection[106]. To address these challenges, nanoparticles offer unique advantages for immune modulation against bacterial infections[107, 108].

Nanoparticles have been extensively explored to overcome the instability, undesirable systemic biodistribution, and toxicity frequently associated with the administration of soluble molecules[109, 110]. It has been reported that conjugation of antigens to nanoparticle surfaces facilitated B-cell activation[111], due to a higher quantity of antigens that were delivered to antigen presenting cells (APCs)[112]. With the advancement in nanoparticle engineering, new fabrication techniques including layer-by-layer assembly[113, 114], facile spray-drying process[115], and soft lithography-based PRINT technology[116] have been developed to produce nanoparticle platforms with superior antigen loading efficiency. Recently, natural cellular membrane-coated nanoparticles have also been shown to detain membrane-damaging toxins and divert them away from their cellular targets[117, 118]. Such a toxin-detainment strategy was applied to safely deliver intact staphylococcal α-hemolysin to APCs and induced

superior protective immunity against toxin-mediated adverse effects in mice when compared to vaccination with heat-denatured toxins (Figure 1.3)[119]. This approach maintained a faithful antigenic presentation while removing toxin virulence, therefore avoiding the trade-off between efficacy and safety that remains a major challenge of current toxoid development.

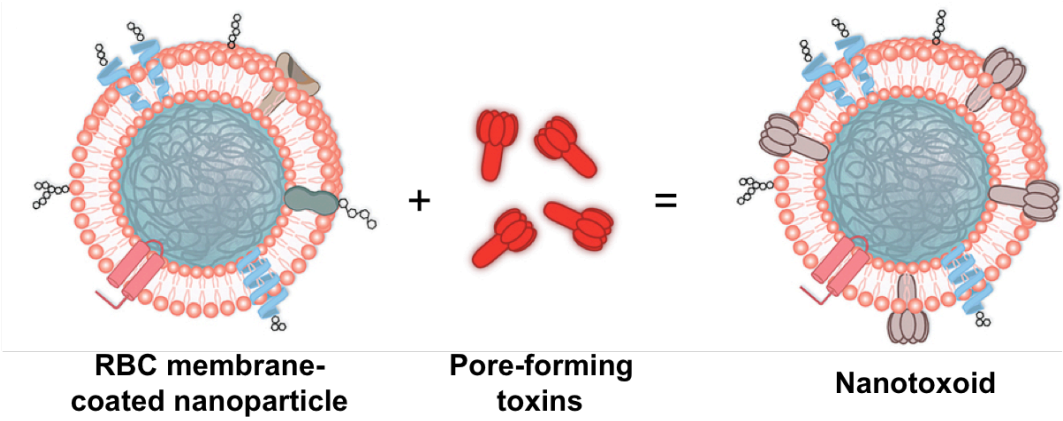


**Figure 1.3** Schematic preparation of nanoparticle-detained toxins, denoted 'nanotoxoid', consisting of substrate-supported RBC membranes into which pore-forming toxins can spontaneously incorporate.

Besides delivering antigens, nanoparticles can concurrently carry adjuvants to mimic natural microbes for enhanced vaccination efficacy[120, 121]. Particularly, various toll-like receptor (TLR) ligands including small molecules, carbohydrates, DNAs, and RNAs, together with antigens have been delivered using nanoparticles, resulting in equivalent immune responses compared to soluble antigen formulations but at significantly reduced dosages[122-125]. More importantly, nanoparticles allow for programmable presentation of adjuvants and antigens to immune cells for desirable responses. For example, combinations of TLR agonists, as opposed to a single

adjuvant, have been concurrently loaded into nanoparticles to mimic the combinatorial TLR activation that occurs in natural infections, therefore resulting in more vigorous immune responses[126-128]. In addition, nanoparticles allow for the sequential presentation of antigens and adjuvants to be programmed for optimal immune responses. For example, encapsulation of antigens and TLR agonists into the same nanoparticles has shown advantages for the induction of effector T-cell responses[124, 129] due to the manner in which antigen processing occurs in dendritic cells[130, 131]. In contrast, delivery of antigens and TLR agonists in separate nanoparticles seemed to benefit antibody responses[132]. Recent advancement in controlling the intra-nanoparticle architecture and adjuvant distribution has provided additional capability for programming nanoparticle-based immune modulation[133]. For example, when an interbilayer-crosslinked multilamellar vesicles were used as synthetic vaccines, the TLR-4 agonist monophosphoryl lipid A (MPLA) was incorporated throughout the vesicle layers and elicited stronger serum IgG titres as compared to the vesicles carrying the same amount of MPLA but attached only on the vesicle surfaces (Figure 1.4)[134].

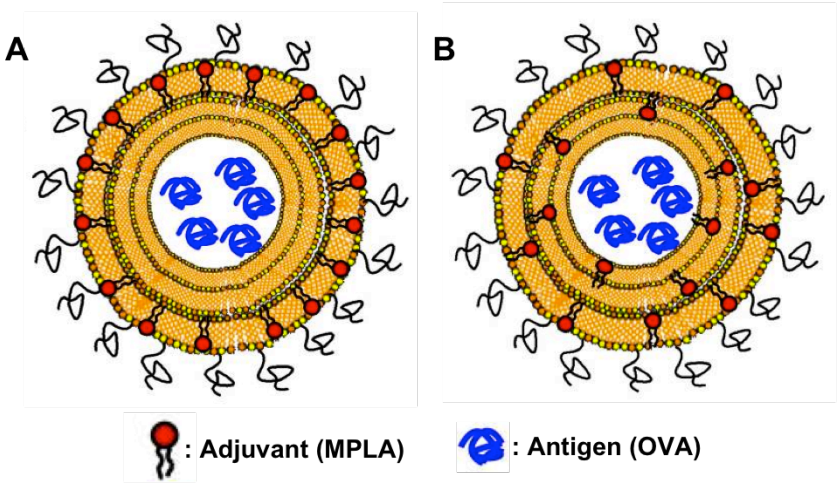


**Figure 1.4** Schematic illustration of interbilayer-crosslinked multilamellar vesicles (ICMVs) for vaccine delivery: (A) OVA-loaded ICMVs with MPLA only on the external surface, and (B) OVA-loaded ICMVs with MPLA throughout the lipid multilayers.

Targeting vaccines to desired sites for safe and effective immune responses is another advantage of using nanoparticles for vaccine delivery. For example, a cationic nanogel loaded with a subunit fragment of *Clostridium botulinum (C. botulinum)* type-A neurotoxin has been shown to facilitate persistent antigen adherence to the nasal epithelium and effective uptake by mucosal dendritic cells[135]. This platform not only elicited strong systemic and mucosal immune responses, but also prevented exposure of the upper respiratory tract and the central nervous system to toxic antigens. As another example, nanoparticles responsive to the pH gradient of the GI tract have been able to protect antigens while in the stomach but release them in the lower GI tract for subsequent translocation across the intestinal epithelium[136]. A similar strategy has also shown promise for targeting antigen-transcytosing M cells overlying Peyer's patches for further enhanced immunity[137]. In addition, nanoparticle-based vaccine platforms

can effectively target lymph node-residing immune cells. It has been shown that smaller nanoparticles transport faster to the lymph node[138], but larger particles are retained longer within the lymph node[139]. Such distinct correlations indicate the importance of size optimization in lymphatic targeting for desired immune responses. At the single-cell level, numerous nanoparticle formulations have been designed to escape endosomes following their uptake by APCs[140-142]. These nanoparticles specifically deposited vaccine payloads into the cytosol and showed promise to enhance CD8+ T-cell priming.

## 1.5 Nanoparticle-based bacterial detection

Rapid and sensitive bacterial detection is crucial for identification of the infection source, allowing for treatment with the appropriate antibiotics and thus preventing the spread of the disease[143, 144]. Bacterial culture and biochemical staining remain the current gold standard in the clinic despite laborious processing, long procedural times and limitations in identifying certain pathogenic species. Among the various existing diagnostic approaches, those based on polymerase chain reaction (PCR) and sequencing have shown particular promise as highly sensitive tools for microbial identification[145, 146]. However, quantitative real-time PCR-based systems are often too expensive in resource-limited settings, and the current sequencing techniques still lack practical applicability for patient care[147, 148]. In this regard, nanoparticles offer unique opportunities for generic, accurate and point-of-care detection of pathogens[149, 150].

Using conventional organic fluorophores for bacterial detection is limited by the molecules' short lifetime and low sensitivity. To overcome these challenges, silica nanoparticles have been used to encapsulate thousands of fluorescent molecules in a single particle, resulting in significantly stronger fluorescence signals[151]. This strategy has resulted in ultra sensitive bacterial detection at a single cell level. Meanwhile, semiconductor quantum dots (QDs) have also emerged as a promising class of fluorophores for bacterial detection. Compared to organic fluorephores, QDs are brighter and more stable; they also exhibit broad absorption and narrow emission spectra, a property useful for simultaneous excitation and detection[152]. Ligand-conjugated QDs have been extensively explored for the detection of various bacteria, including *Escherichia coli* (*E. coli*), *S. typhimurium*, *Mycobacterium bovis (M. bovis)*, and oral bacteria[153-155]. Additional strategies have been explored to further improve the sensitivity of QD-based bacterial detection systems. For example, the binding affinity of QDs coated with zinc(II)-dipicolylamine coordination complexes, a bacterial ligand, has been shown to correlate to the size of the QDs[156]. Based on this observation, QDs with tailored sizes have been developed to distinguish different mutants of the same bacterial species. As another example, streptavidin-coated QDs have been used to label engineered bacteriophages following an *in vivo* amplification and biotinylation process[157]. This method enabled specific detection of as few as 10 bacteria per milliliter in testing samples.

Besides fluorescence-based detection techniques, iron oxide nanoparticles have received much attention, owing largely to their intrinsic magnetic properties[158,159]. Iron

oxide nanoparticles coated with pathogen-specific antibodies have been widely used to isolate living bacteria from human blood samples under a magnetic field[160, 161]. More recently, this technique has been coupled with microfluidic technology and has resulted in high-throughput bacterial detection under various clinical settings[162-164]. Meanwhile, paramagnetic iron oxide nanoparticles that allow for signal readout with magnetic resonance imaging (MRI) systems have become an attractive new option for ultrasensitive bacterial detection. For *in vitro* diagnosis, iron oxide nanoparticles with a diameter of 21 nm have been coupled with a DNA hybridization technique to enhance the capturing of bacterial 16S rRNAs with a miniaturized micro-NMR system, resulting in rapid and specific pathogen profiling in clinical samples (Figure 1.5)[165]. For *in vivo* diagnosis, iron oxide nanoparticles have also been explored to detect a variety of pathogenic bacteria in animal models, where the high spatial resolution and excellent soft tissue contrast of MRI provided information on both bacterial localization and corresponding host responses[166].

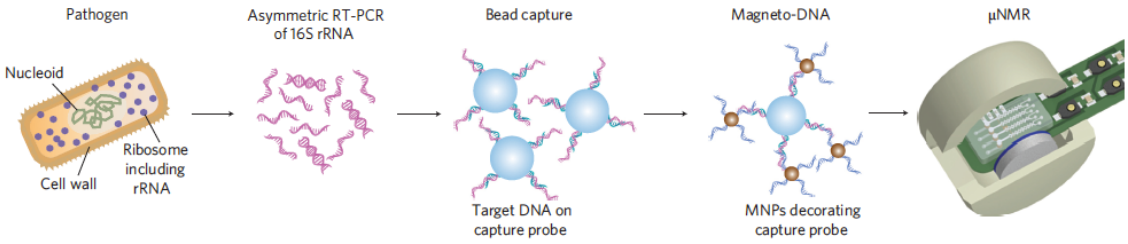


**Figure 1.5.** Magneto-DNA assay for the detection of bacterial 16S rRNA. Total RNA is extracted from the specimen, and the 16S rRNA is amplified by asymmetric RT-PCR. Single-strand DNA of the amplified product is then captured by beads conjugated with capture probes, followed by hybridizing with MNPs to form a magnetic sandwich complex. Samples are subsequently analyzed using a miniaturized micro-NMR (μNMR) system.

Gold nanoparticles are another emerging nanoparticle platform for bacterial detection. These nanoparticles possess strong light scattering properties and change their plasmon resonance spectrum upon aggregation. This phenomenon has been widely explored for the detection of bacteria-specific DNAs, proteins, and live bacteria[167]. For example, individual gold nanoparticles have been precisely cross-linked with switchable linkers, which were designed to break in the presence of target subjects[168]. As a result, this design amplified the pathogen-induced nanoparticle aggregation-dispersion process and allowed for visible detection of *E. coli* at a concentration of 100 CFU/mL. In addition, gold nanoparticles can non-specifically quench fluorescent molecules. Based on this phenomenon, a fluorophore displacement strategy has been developed for bacterial detection[169]. In this strategy, gold nanoparticles adsorbed with fluorescent polymers such as poly(paraphenyleneethynylene) and polylysine selectively interacted with bacteria and released the bound fluorescent polymers which were initially quenched by the gold nanoparticles. The recovered polymer fluorescence allowed for the effective identification of bacteria within minutes.

## 1.6 Conclusions

The advent of nanotechnology, particularly nanoparticle engineering, together with the accumulation of knowledge on infectious diseases, has allowed for significant advancement in the field of antibacterial drug delivery. Major efforts have been devoted to developing various nanoparticle-based delivery platforms including

liposomes, polymeric nanoparticles, dendrimers, and inorganic nanoparticles. These nanoparticle approaches have shown excellent outcomes in treating and detecting bacterial pathogens by enabling targeted, responsive, and combinatorial delivery of antibiotics, effective antibacterial vaccination, and rapid detection of bacteria. It is expected that nanotechnology will continue bringing improvements to antimicrobial delivery systems for efficacious, patient-compliant, and cost effective therapeutics as well as the specific and sensitive detection of various infectious diseases.

Chapter 1, in full, is a reprint of the material as it appears in WIREs Nanomedicine & Nanobiotechnology, 2014, Soracha Thamphiwatana, Weiwei Gao, Pavimol Angsantikul and Liangfang Zhang. The dissertation author was the primary investigator and co-author of this paper.

## 1.7 References


1. Parks T, Hill AV, Chapman SJ. The perpetual challenge of infectious diseases. *New Engl J Med* 2012, 367:90-90.

2. Farmer PE. Chronic infectious disease and the future of health care delivery. *New Engl J Med* 2013, 369:2424-2436.

3. Baxt LA, Garza-Mayers AC, Goldberg MB. Subversion of host innate immune pathways. *Science* 2013, 340:697-701.

4. Modlin RL, Bloom BR. Tb or not tb: That is no longer the question. *Sci Transl Med* 2013, 5:213sr6.

5. Appelbaum PC, Hunter PA. The fluoroquinolone antibacterials: Past, present and future perspectives. *Int J Antimicrob Agents* 2000, 16:5-15.

6. Poulikakos P, Falagas ME. Aminoglycoside therapy in infectious diseases. *Expert Opin Pharm* 2013, 14:1585-1597.

7. Morens DM, Folkers GK, Fauci AS. The challenge of emerging and re-emerging infectious diseases. *Nature* 2004, 430:242-249.

8. Spellberg B, Bartlett JG, Gilbert DN. The future of antibiotics and resistance. *New Engl J Med* 2013, 368:299-302.

9. Moellering RC, Jr. Discovering new antimicrobial agents. *Int J Antimicrob Agents* 2011, 37:2-9.

10. Farokhzad OC, Langer R. Impact of nanotechnology on drug delivery. *ACS Nano* 2009, 3:16-20.

11. Timko BP, Whitehead K, Gao W, Kohane DS, Farokhzad O, Anderson D, Langer R. Advances in drug delivery. *Annu Rev Mater Res* 2011, 41:1-20.

12. Petros RA, DeSimone JM. Strategies in the design of nanoparticles for therapeutic applications. *Nature Reviews Drug Discovery* 2010, 9:615-627.

13. Davis ME, Chen Z, Shin DM. Nanoparticle therapeutics: An emerging treatment modality for cancer. *Nature Reviews Drug Discovery* 2008, 7:771-782.

14. Zhang L, Pornpattananangkul D, Hu CMJ, Huang CM. Development of nanoparticles for antimicrobial drug delivery. *Curr Med Chem* 2010, 17:585-594.
15. Lee WL, Liles WC. Endothelial activation, dysfunction and permeability during severe infections. *Curr Opin Hematol* 2011, 18:191-196.

16. Taylor SL, Wahl-Jensen V, Copeland AM, Jahrling PB, Schmaljohn CS. Endothelial cell permeability during hantavirus infection involves factor xii-dependent increased activation of the kallikrein-kinin system. *PLoS Path* 2013, 9:e1003470.

17. DiStasi MR, Ley K. Opening the flood-gates: How neutrophil-endothelial interactions regulate permeability. *Trends Immunol* 2009, 30:539-545.

18. Swartz MN. Cellulitis. *New Engl J Med* 2004, 350:904-912.
19. Azzopardi EA, Ferguson EL, Thomas DW. The enhanced permeability retention effect: A new paradigm for drug targeting in infection. *J Antimicrob Chemother* 2013, 68:257-274.

20. Boerman OC, Storm G, Oyen WJG, Vanbloois L, Vandermeer JWM, Claessens R, Crommelin DJA, Corstens FHM. Sterically stabilized liposomes labeled with in-111 to image focal infection. *J Nucl Med* 1995, 36:1639-1644.

21. Oyen WJG, Boerman OC, Storm G, vanBloois L, Koenders EB, Claessens R, Perenboom RM, Crommelin DJA, vanderMeer JWM, Corstens FHM. Detecting infection and inflammation with technetium-99m-labeled stealth(r) liposomes. *J Nucl Med* 1996, 37:1392-1397.

22. Boerman OC, Oyen WJG, vanBloois L, Koenders EB, vanderMeer JWM, Corstens FHM, Storm G. Optimization of technetium-99m-labeled peg liposomes to image focal infection: Effects of particle size and circulation time. *J Nucl Med* 1997, 38:489-493.

23. Laverman P, Dams ETM, Storm G, Hafmans TG, Croes HJ, Oyen WJG, Corstens FHM, Boerman OC. Microscopic localization of peg-liposomes in a rat model of focal infection. *J Controlled Release* 2001, 75:347-355.

24. Kaim AH, Wischer T, O'Reilly T, Jundt G, Frohlich J, von Schulthess GK, Allegrini PR. Mr imaging with ultrasmall superparamagnetic iron oxide particles in experimental soft-tissue infections in rats. *Radiology* 2002, 225:808-814.

25. Dillen K, Bridts C, Van der Veken P, Cos P, Vandervoort J, Augustyns K, Stevens W, Ludwig A. Adhesion of PLGA or Eudragit®/PLGA nanoparticles to staphylococcus and, pseudomonas. *Int J Pharm* 2008, 349:234-240.

26. Sambhy V, Peterson BR, Sen A. Antibacterial and hemolytic activities of pyridinium polymers as a function of the spatial relationship between the positive charge and the pendant alkyl tail. *Angew Chem Int Ed* 2008, 47:1250-1254.

27. Kenawy E-R, Worley SD, Broughton R. The chemistry and applications of antimicrobial polymers: A state-of-the-art review. *Biomacromolecules* 2007, 8:1359-1384.

28. Liu L, Xu K, Wang H, Tan JPK, Fan W, Venkatraman SS, Li L, Yang Y-Y. Self-assembled cationic peptide nanoparticles as an efficient antimicrobial agent. *Nat Nanotechnol* 2009, 4:457-463.

29. Nederberg F, Zhang Y, Tan JPK, Xu K, Wang H, Yang C, Gao S, Guo XD, Fukushima K, Li L. Biodegradable nanostructures with selective lysis of microbial membranes. *Nat Chem* 2011, 3:409-414.

30. Choi SK, Myc A, Silpe JE, Sumit M, Wong PT, McCarthy K, Desai AM, Thomas TP, Kotlyar A, Holl MMB. Dendrimer-based multivalent vancomycin nanoplatform for targeting the drug-resistant bacterial surface. *ACS Nano* 2013, 7:214-228.

31. Choi K-H, Lee H-J, Park BJ, Wang K-K, Shin EP, Park J-C, Kim YK, Oh M-K, Kim Y-R. Photosensitizer and vancomycin-conjugated novel multifunctional magnetic particles as photoinactivation agents for selective killing of pathogenic bacteria. *Chem Commun* 2012, 48:4591-4593.

32. Gu HW, Ho PL, Tong E, Wang L, Xu B. Presenting vancomycin on nanoparticles to enhance antimicrobial activities. *Nano Lett* 2003, 3:1261-1263.

33. Qi G, Li L, Yu F, Wang H. Vancomycin-modified mesoporous silica nanoparticles for selective recognition and killing of pathogenic gram-positive bacteria over macrophage-like cells. *ACS Appl Mater Interfaces* 2013, 5:10874-10881.

34. Kell AJ, Stewart G, Ryan S, Peytavi R, Boissinot M, Huletsky A, Bergeron MG, Simard B. Vancomycin-modified nanoparticles for efficient targeting and preconcentration of gram-positive and gram-negative bacteria. *ACS Nano* 2008, 2:1777-1788.

35. Chen J, Zhang C, Liu Q, Shao X, Feng C, Shen Y, Zhang Q, Jiang X. Solanum tuberosum lectin-conjugated PLGA nanoparticles for nose-to-brain delivery: In vivo and in vitro evaluations. *J Drug Targeting* 2012, 20:174-184.

36. Umamaheshwari RB, Jain NK. Receptor mediated targeting of lectin conjugated gliadin nanoparticles in the treatment of helicobacter pylori. *J Drug Targeting* 2003, 11:415-424.

37. Huang P-J, Tay L-L, Tanha J, Ryan S, Chau L-K. Single-domain antibody-conjugated nanoaggregate-embedded beads for targeted detection of pathogenic bacteria. *Chem Eur J* 2009, 15:9330-9334.

38. Tay L-L, Huang P-J, Tanha J, Ryan S, Wu X, Hulse J, Chau L-K. Silica encapsulated sers nanoprobe conjugated to the bacteriophage tailspike protein for targeted detection of salmonella. *Chem Commun* 2012, 48:1024-1026.

39. Chen F, Zhou J, Luo F, Mohammed A-B, Zhang X-L. Aptamer from whole-bacterium selex as new therapeutic reagent against virulent mycobacterium tuberculosis. *Biochem Biophys Res Commun* 2007, 357:743-748.

40. Duan N, Wu S, Chen X, Huang Y, Xia Y, Ma X, Wang Z. Selection and characterization of aptamers against salmonella typhimurium using whole-bacterium systemic evolution of ligands by exponential enrichment (selex). *J Agric Food Chem* 2013, 61:3229-3234.

41. Deysine M, Chua A, Gerboth A. Selective delivery of antibiotics to experimental-infection by autologous white blood-cells. *Surgical Forum* 1979, 30:38-39.

42. Mehta RT, McQueen TJ, Keyhani A, Lopezberestein G. Phagocyte transport as mechanism for enhanced therapeutic activity of liposomal amphotericin-b. *Chemother* 1994, 40:256-264.

43. Briones E, Colino CI, Lanao JM. Delivery systems to increase the selectivity of antibiotics in phagocytic cells. *J Controlled Release* 2008, 125:210-227.

44. Chellat F, Merhi Y, Moreau A, Yahia L. Therapeutic potential of nanoparticulate systems for macrophage targeting. *Biomaterials* 2005, 26:7260-7275.

45. Kelly C, Jefferies C, Cryan S-A. Targeted liposomal drug delivery to monocytes and macrophages. *J Drug Deliv* 2011, 2011:727241-727241.

46. Vyas SP, Kannan ME, Jain S, Mishra V, Singh P. Design of liposomal aerosols for improved delivery of rifampicin to alveolar macrophages. *Int J Pharm* 2004, 269:37-49.

47. Xiong M-H, Li Y-J, Bao Y, Yang X-Z, Hu B, Wang J. Bacteria-responsive multifunctional nanogel for targeted antibiotic delivery. *Adv Mater* 2012, 24:6175-6180.

48. Gao W, Chan JM, Farokhzad OC. Ph-responsive nanoparticles for drug delivery. *Mol Pharm* 2010, 7:1913-1920.

49. Kararli TT. Comparison of the gastrointestinal anatomy, physiology, and biochemistry of humans and commonly used laboratory animals. *Biopharm Drug Disposition* 1995, 16:351-380.

50. Schmid-Wendtner M-H, Korting HC. The ph of the skin surface and its impact on the barrier function. *Skin Pharmacol Physiol* 2006, 19:296-302.

51. Simoes S, Slepushkin V, Düzgünes N, Pedroso de Lima MC. On the mechanisms of internalization and intracellular delivery mediated by ph-sensitive liposomes. *Biochim Biophys Acta* 2001, 1515:23-37.

52. Imbuluzqueta E, Gamazo C, Ariza J, Blanco-Prieto MJ. Drug delivery systems for potential treatment of intracellular bacterial infections. *Front Biosci* 2010, 15:397-417.

53. Chu C-J, Dijkstra J, Lai M-Z, Hong K, Szoka FC. Efficiency of cytoplasmic delivery by ph-sensitive liposomes to cells in culture. *Pharm Res* 1990, 7:824-834.

54. Slepushkin VA, Simões S, Dazin P, Newman MS, Guo LS, de Lima MCP, Düzgüneş N. Sterically stabilized ph-sensitive liposomes intracellular delivery of aqueous contents and prolonged circulation in vivo. *J Biol Chem* 1997, 272:2382-2388.

55. Simões S, Moreira JN, Fonseca C, Düzgüneş N, Pedroso de Lima MC. On the formulation of ph-sensitive liposomes with long circulation times. *Adv Drug Del Rev* 2004, 56:947-965.

56. Lutwyche P, Cordeiro C, Wiseman DJ, St-Louis M, Uh M, Hope MJ, Webb MS, Finlay BB. Intracellular delivery and antibacterial activity of gentamicin encapsulated in ph-sensitive liposomes. *Antimicrob Agents Chemother* 1998, 42:2511-2520.

57. Cordeiro C, Wiseman DJ, Lutwyche P, Uh M, Evans JC, Finlay BB, Webb MS. Antibacterial efficacy of gentamicin encapsulated in ph-sensitive liposomes against an in vivo salmonella enterica serovar typhimurium intracellular infection model. *Antimicrob Agents Chemother* 2000, 44:533-539.

58. Ponnappa BC, Dey I, Tu G-C, Zhou F, Aini M, Cao Q-N, Israel Y. In vivo delivery of antisense oligonucleotides in pH-sensitive liposomes inhibits lipopolysaccharide-induced production of tumor necrosis factor-α in rats. *J Pharmacol Exp Ther* 2001, 297:1129-1136.

59. Tschaikowsky K. Protein kinase c inhibitors suppress lps-induced tnf production in alveolar macrophages and in whole blood: The role of encapsulation into liposomes. *Biochim Biophys Acta* 1994, 1222:113-121.

60. Lee K-D, Oh Y-K, Portnoy DA, Swanson JA. Delivery of macromolecules into cytosol using liposomes containing hemolysin from listeria monocytogenes. *J Biol Chem* 1996, 271:7249-7252.

61. Beauregard KE, Lee K-D, Collier RJ, Swanson JA. Ph-dependent perforation of macrophage phagosomes by listeriolysin o from listeria monocytogenes. *J Exp Med* 1997, 186:1159-1163.

62. Zhang L, Granick S. How to stabilize phospholipid liposomes (using nanoparticles). *Nano Lett* 2006, 6:694-698.

63. Zhang L, Hong L, Yu Y, Bae SC, Granick S. Nanoparticle-assisted surface immobilization of phospholipid liposomes. *J Am Chem Soc* 2006, 128:9026-9027.

64. Pornpattananangkul D, Olson S, Aryal S, Sartor M, Huang C-M, Vecchio K, Zhang L. Stimuli-responsive liposome fusion mediated by gold nanoparticles. *ACS Nano* 2010, 4:1935-1942.

65. Thamphiwatana S, Fu V, Zhu J, Lu D, Gao W, Zhang L. Nanoparticle-stabilized liposomes for ph-responsive gastric drug delivery. *Langmuir* 2013, 29:12228-12233.

66. Pornpattananangkul D, Zhang L, Olson S, Aryal S, Obonyo M, Vecchio K, Huang C-M, Zhang L. Bacterial toxin-triggered drug release from gold nanoparticle-stabilized liposomes for the treatment of bacterial infection. *J Am Chem Soc* 2011, 133:4132-4139.

67. Gao W, Vecchio D, Li J, Zhu J, Zhang Q, Fu V, Li J, Thamphiwatana S, Lu D, Zhang L. Hydrogel containing nanoparticle-stabilized liposomes for topical antimicrobial delivery. *ACS Nano* 2014:10.1021/nn500110a.

68. Radovic-Moreno AF, Lu TK, Puscasu VA, Yoon CJ, Langer R, Farokhzad OC. Surface charge-switching polymeric nanoparticles for bacterial cell wall-targeted delivery of antibiotics. *ACS Nano* 2012, 6:4279-4287.

69. Lin Y-H, Chang C-H, Wu Y-S, Hsu Y-M, Chiou S-F, Chen Y-J. Development of ph-responsive chitosan/heparin nanoparticles for stomach-specific anti-*helicobacter pylori* therapy. *Biomaterials* 2009, 30:3332-3342.

70. Xiong M-H, Bao Y, Yang X-Z, Wang Y-C, Sun B, Wang J. Lipase-sensitive polymeric triple-layered nanogel for "on-demand" drug delivery. *J Am Chem Soc* 2012, 134:4355-4362.

71. Hu C-MJ, Aryal S, Zhang L. Nanoparticle-assisted combination therapies for effective cancer treatment. *Ther Deliv* 2010, 1:323-334.

72. Zhang L, Pornpattananangkul D, Hu C-M, Huang C-M. Development of nanoparticles for antimicrobial drug delivery. *Curr Med Chem* 2010, 17:585-594.

73. Deol P, Khuller G, Joshi K. Therapeutic efficacies of isoniazid and rifampin encapsulated in lung-specific stealth liposomes against mycobacterium tuberculosis infection induced in mice. *Antimicrob Agents Chemother* 1997, 41:1211-1214.

74. Labana S, Pandey R, Sharma S, Khuller G. Chemotherapeutic activity against murine tuberculosis of once weekly administered drugs (isoniazid and rifampicin) encapsulated in liposomes. *Int J Antimicrob Agents* 2002, 20:301-304.

75. Gürsoy A, Kut E, Özkırımlı S. Co-encapsulation of isoniazid and rifampicin in liposomes and characterization of liposomes by derivative spectroscopy. *Int J Pharm* 2004, 271:115-123.

76. Banin E, Lozinski A, Brady KM, Berenshtein E, Butterfield PW, Moshe M, Chevion M, Greenberg EP, Banin E. The potential of desferrioxamine-gallium as an anti-pseudomonas therapeutic agent. *Proc Natl Acad Sci USA* 2008, 105:16761-16766.

77. Halwani M, Yebio B, Suntres Z, Alipour M, Azghani A, Omri A. Co-encapsulation of gallium with gentamicin in liposomes enhances antimicrobial

activity of gentamicin against pseudomonas aeruginosa. *J Antimicrob Chemother* 2008, 62:1291-1297.

78. Halwani M, Blomme S, Suntres ZE, Alipour M, Azghani AO, Kumar A, Omri A. Liposomal bismuth-ethanedithiol formulation enhances antimicrobial activity of tobramycin. *Int J Pharm* 2008, 358:278-284.

79. Alipour M, Suntres ZE, Lafrenie RM, Omri A. Attenuation of pseudomonas aeruginosa virulence factors and biofilms by co-encapsulation of bismuth-ethanedithiol with tobramycin in liposomes. *J Antimicrob Chemother* 2010, 65:684-693.

80. Alipour M, Dorval C, Suntres ZE, Omri A. Bismuth–ethanedithiol incorporated in a liposome–loaded tobramycin formulation modulates the alginate levels in mucoid pseudomonas aeruginosa. *J Pharm Pharmacol* 2011, 63:999-1007.

81. Alhariri M, Omri A. Efficacy of liposomal bismuth-ethanedithiol-loaded tobramycin after intratracheal administration in rats with pulmonary pseudomonas aeruginosa infection. *Antimicrob Agents Chemother* 2013, 57:569-578.

82. Schiffelers RM, Storm G, Kate MT, Stearne-Cullen LE, Hollander JG, Verbrugh HA, Bakker-Woudenberg IA. Liposome-enabled synergistic interaction of antimicrobial agents. *J Liposome Res* 2002, 12:121-127.

83. Schiffelers RM, Storm G, Marian T, Stearne-Cullen LE, den Hollander JG, Verbrugh HA, Bakker-Woudenberg IA. In vivo synergistic interaction of liposome-coencapsulated gentamicin and ceftazidime. *J Pharmacol Exp Ther* 2001, 298:369-375.

84. Kadry AA, Al-Suwayeh SA, Abd-Allah AR, Bayomi MA. Treatment of experimental osteomyelitis by liposomal antibiotics. *J Antimicrob Chemother* 2004, 54:1103-1108.

85. Li Y, Su T, Zhang Y, Huang X, Li J, Li C. Liposomal co-delivery of daptomycin and clarithromycin at an optimized ratio for treatment of methicillin-resistant staphylococcus aureus infection. *Drug Deliv* 2014:1-11.

86. Onyeji C, Nightingale C, Nicolau D, Quintiliani R. Efficacies of liposome-encapsulated clarithromycin and ofloxacin against mycobacterium avium: Intracellulare complex in human macrophages. *Antimicrob Agents Chemother* 1994, 38:523-527.

87. Majumdar S, Flasher D, Friend D, Nassos P, Yajko D, Hadley W, Düzgüneş N. Efficacies of liposome-encapsulated streptomycin and ciprofloxacin against mycobacterium avium: Intracellulare complex infections in human peripheral blood monocyte/macrophages. *Antimicrob Agents Chemother* 1992, 36:2808-2815.

88. Singh DY, Prasad NK. Double liposomes mediated dual drug targeting for treatment of Helicobacter pylori infections. *Die Pharmazie* 2011, 66:368-373.

89. Jain P, Jain S, Prasad K, Jain S, Vyas SP. Polyelectrolyte coated multilayered liposomes (nanocapsules) for the treatment of Helicobacter pylori infection. *Mol Pharm* 2009, 6:593-603.

90. Sengupta S, Eavarone D, Capila I, Zhao G, Watson N, Kiziltepe T, Sasisekharan R. Temporal targeting of tumour cells and neovasculature with a nanoscale delivery system. *Nature* 2005, 436:568-572.

91. Aryal S, Hu CMJ, Zhang L. Combinatorial drug conjugation enables nanoparticle dual‐drug delivery. *Small* 2010, 6:1442-1448.

92. Aryal S, Hu C-MJ, Zhang L. Polymeric nanoparticles with precise ratiometric control over drug loading for combination therapy. *Mol Pharm* 2011, 8:1401-1407.

93. Zhang L, Radovic‐Moreno AF, Alexis F, Gu FX, Basto PA, Bagalkot V, Jon S, Langer RS, Farokhzad OC. Co‐delivery of hydrophobic and hydrophilic drugs from nanoparticle–aptamer bioconjugates. *ChemMedChem* 2007, 2:1268-1271.

94. Kolishetti N, Dhar S, Valencia PM, Lin LQ, Karnik R, Lippard SJ, Langer R, Farokhzad OC. Engineering of self-assembled nanoparticle platform for precisely controlled combination drug therapy. *Proc Natl Acad Sci USA* 2010, 107:17939-17944.

95. Toti US, Guru BR, Hali M, McPharlin CM, Wykes SM, Panyam J, Whittum-Hudson JA. Targeted delivery of antibiotics to intracellular chlamydial infections using PLGA nanoparticles. *Biomaterials* 2011, 32:6606-6613.

96. Ramteke S, Ganesh N, Bhattacharya S, Jain NK. Triple therapy-based targeted nanoparticles for the treatment of Helicobacter pylori. *J Drug Targeting* 2008, 16:694-705.

97. Ramteke S, Ganesh N, Bhattacharya S, Jain NK. Amoxicillin, clarithromycin, and omeprazole based targeted nanoparticles for the treatment of H. pylori. *J Drug Targeting* 2009, 17:225-234.

98. Ramteke S, Jain NK. Clarithromycin-and omeprazole-containing gliadin nanoparticles for the treatment of Helicobacter pylori. *J Drug Targeting* 2008, 16:65-72.

99. Pandey R, Khuller G. Oral nanoparticle-based antituberculosis drug delivery to the brain in an experimental model. *J Antimicrob Chemother* 2006, 57:1146-1152.

100. Ahmad Z, Pandey R, Sharma S, Khuller G. Alginate nanoparticles as antituberculosis drug carriers: Formulation development, pharmacokinetics and therapeutic potential. *Indian J Chest Dis Allied Sci* 2006, 48:171.

101. Plotkin SA. Vaccines: Past, present and future. *Nat Med* 2005, 11:S5-S11.

102. Germain RN. Vaccines and the future of human immunology. *Immunity* 2010, 33:441-450.

103. Wenzel RP, Edmond MB. Managing antibiotic resistance. *New Engl J Med* 2000, 343:1961-1963.

104. Mishra RPN, Oviedo-Orta E, Prachi P, Rappuoli R, Bagnoli F. Vaccines and antibiotic resistance. *Curr Opin Microbiol* 2012, 15:596-602.

105. Levy SB, Marshall B. Antibacterial resistance worldwide: Causes, challenges and responses. *Nat Med* 2004, 10:S122-S129.

106. Fauci AS, Morens DM. The perpetual challenge of infectious diseases. *New Engl J Med* 2012, 366:454-461.

107. Swartz MA, Hirosue S, Hubbell JA. Engineering approaches to immunotherapy. *Sci Transl Med* 2012, 4:148rv9.

108. Irvine DJ, Swartz MA, Szeto GL. Engineering synthetic vaccines using cues from natural immunity. *Nat Mat* 2013, 12:978-990.

109. Tan ML, Choong PFM, Dass CR. Recent developments in liposomes, microparticles and nanoparticles for protein and peptide drug delivery. *Peptides* 2010, 31:184-193.

110. Gu Z, Biswas A, Zhao M, Tang Y. Tailoring nanocarriers for intracellular protein delivery. *Chem Soc Rev* 2011, 40:3638-3655.

111. Villa CH, Dao T, Ahearn I, Fehrenbacher N, Casey E, Rey DA, Korontsvit T, Zakhaleva V, Batt CA, Philips MR. Single-walled carbon nanotubes deliver peptide antigen into dendritic cells and enhance igg responses to tumor-associated antigens. *ACS Nano* 2011, 5:5300-5311.

112. Nembrini C, Stano A, Dane KY, Ballester M, van der Vlies AJ, Marsland BJ, Swartz MA, Hubbell JA. Nanoparticle conjugation of antigen enhances cytotoxic t-cell responses in pulmonary vaccination. *Proc Natl Acad Sci USA* 2011, 108:E989-E997.

113. De Rose R, Zelikin AN, Johnston APR, Sexton A, Chong S-F, Cortez C, Mulholland W, Caruso F, Kent SJ. Binding, internalization, and antigen presentation of vaccine-loaded nanoengineered capsules in blood. *Adv Mater* 2008, 20:4698-+.

114. De Geest BG, Willart MA, Lambrecht BN, Pollard C, Vervaet C, Remon JP, Grooten J, De Koker S. Surface-engineered polyelectrolyte multilayer capsules: Synthetic vaccines mimicking microbial structure and function. *Angew Chem Int Ed* 2012, 51:3862-3866.

115. Dierendonck M, De Koker S, Cuvelier C, Grooten J, Vervaet C, Remon J-P, De Geest BG. Facile two-step synthesis of porous antigen-loaded degradable polyelectrolyte microspheres. *Angew Chem Int Ed* 2010, 49:8620-8624.

116. Perry JL, Herlihy KP, Napier ME, Desimone JM. Print: A novel platform toward shape and size specific nanoparticle theranostics. *Acc Chem Res* 2011, 44:990-998.

117. Hu C-MJ, Zhang L, Aryal S, Cheung C, Fang RH, Zhang L. Erythrocyte membrane-camouflaged polymeric nanoparticles as a biomimetic delivery platform. *Proc Natl Acad Sci USA* 2011, 108:10980-10985.

118. Hu C-MJ, Fang RH, Copp J, Luk BT, Zhang L. A biomimetic nanosponge that absorbs pore-forming toxins. *Nat Nanotechnol* 2013, 8:336-340.

119. Hu C-MJ, Fang RH, Luk BT, Zhang L. Nanoparticle-detained toxins for safe and effective vaccination. *Nat Nanotechnol* 2013, 8:933-938.

120. Peek LJ, Middaugh CR, Berkland C. Nanotechnology in vaccine delivery. *Adv Drug Del Rev* 2008, 60:915-928.

121. Little SR. Reorienting our view of particle-based adjuvants for subunit vaccines. *Proc Natl Acad Sci USA* 2012, 109:999-1000.

122. Diwan M, Elamanchili P, Lane H, Gainer A, Samuel J. Biodegradable nanoparticle mediated antigen delivery to human cord blood derived dendritic cells for induction of primary t cell responses. *J Drug Targeting* 2003, 11:495-507.

123. Diwan M, Elamanchili P, Cao M, Samuel J. Dose sparing of cpg oligodeoxynucleotide vaccine adjuvants by nanoparticle delivery. *Curr Drug Del* 2004, 1:405-412.

124. Heit A, Schmitz F, Haas T, Busch DH, Wagner H. Antigen co-encapsulated with adjuvants efficiently drive protective t cell immunity. *Eur J Immunol* 2007, 37:2063-2074.

125. Demento SL, Eisenbarth SC, Foellmer HG, Platt C, Caplan MJ, Saltzman WM, Mellman I, Ledizet M, Fikrig E, Flavell RA. Inflammasome-activating nanoparticles as modular systems for optimizing vaccine efficacy. *Vaccine* 2009, 27:3013-3021.

126. Zhu Q, Egelston C, Gagnon S, Sui Y, Belyakov IM, Klinman DM, Berzofsky JA. Using 3 tlr ligands as a combination adjuvant induces qualitative changes in t cell responses needed for antiviral protection in mice. *J Clin Invest* 2010, 120:607-616.

127. Mount A, Koernig S, Silva A, Drane D, Maraskovsky E, Morelli AB. Combination of adjuvants: The future of vaccine design. *Expert Rev Vaccines* 2013, 12:733-746.

128. Orr MT, Beebe EA, Hudson TE, Moon JJ, Fox CB, Reed SG, Coler RN. A dual tlr agonist adjuvant enhances the immunogenicity and protective efficacy of the tuberculosis vaccine antigen id93. *Plos One* 2014, 9:e83884.

129. Schlosser E, Mueller M, Fischer S, Basta S, Busch DH, Gander B, Groettrup M. Tlr ligands and antigen need to be coencapsulated into the same biodegradable microsphere for the generation of potent cytotoxic T-lymphocyte responses. *Vaccine* 2008, 26:1626-1637.

130. Blander JM, Medzhitov R. Regulation of phagosome maturation by signals from toll-like receptors. *Science* 2004, 304:1014-1018.

131. Blander JM, Medzhitov R. Toll-dependent selection of microbial antigens for presentation by dendritic cells. *Nature* 2006, 440:808-812.

132. Kasturi SP, Skountzou I, Albrecht RA, Koutsonanos D, Hua T, Nakaya HI, Ravindran R, Stewart S, Alam M, Kwissa M. Programming the magnitude and persistence of antibody responses with innate immunity. *Nature* 2011, 470:543-U136.

133. Gao W, Hu C-MJ, Fang RH, Zhang L. Liposome-like nanostructures for drug delivery. *J Mater Chem* 2013, 1:6569-6585.

134. Moon JJ, Suh H, Bershteyn A, Stephan MT, Liu H, Huang B, Sohail M, Luo S, Um SH, Khant H. Interbilayer-crosslinked multilamellar vesicles as synthetic vaccines for potent humoral and cellular immune responses. *Nat Mat* 2011, 10:243-251.

135. Nochi T, Yuki Y, Takahashi H, Sawada S-i, Mejima M, Kohda T, Harada N, Kong IG, Sato A, Kataoka N. Nanogel antigenic protein-delivery system for adjuvant-free intranasal vaccines. *Nat Mat* 2010, 9:572-578.

136. Zhu Q, Talton J, Zhang G, Cunningham T, Wang Z, Waters RC, Kirk J, Eppler B, Klinman DM, Sui Y. Large intestine-targeted, nanoparticle-releasing oral vaccine to control genitorectal viral infection. *Nat Med* 2012, 18:1291-1296.

137. Fujkuyama Y, Tokuhara D, Kataoka K, Gilbert RS, McGhee JR, Yuki Y, Kiyono H, Fujihashi K. Novel vaccine development strategies for inducing mucosal immunity. *Expert Rev Vaccines* 2012, 11:367-379.

138. Reddy ST, van der Vlies AJ, Simeoni E, Angeli V, Randolph GJ, O'Neill CP, Lee LK, Swartz MA, Hubbell JA. Exploiting lymphatic transport and complement activation in nanoparticle vaccines. *Nat Biotechnol* 2007, 25:1159-1164.

139. Jewell CM, Lopez SCB, Irvine DJ. In situ engineering of the lymph node microenvironment via intranodal injection of adjuvant-releasing polymer particles. *Proc Natl Acad Sci USA* 2011, 108:15745-15750.

140. Hu Y, Litwin T, Nagaraja AR, Kwong B, Katz J, Watson N, Irvine DJ. Cytosolic delivery of membrane-impermeable molecules in dendritic cells using ph-responsive core-shell nanoparticles. *Nano Lett* 2007, 7:3056-3064.

141. Yue H, Wei W, Fan B, Yue Z, Wang L, Ma G, Su Z. The orchestration of cellular and humoral responses is facilitated by divergent intracellular antigen trafficking in nanoparticle-based therapeutic vaccine. *Pharmacol Res* 2012, 65:189-197.

142. Vasdekis AE, Scott EA, O'Neil CP, Psaltis D, Hubbell JA. Precision intracellular delivery based on optofluidic polymersome rupture. *ACS Nano* 2012, 6:7850-7857.

143. Klompas M, Yokoe DS. Automated surveillance of health care-associated infections. *Clin Infect Dis* 2009, 48:1268-1275.

144. Allegranzi B, Nejad SB, Combescure C, Graafmans W, Attar H, Donaldson L, Pittet D. Burden of endemic health-care-associated infection in developing countries: Systematic review and meta-analysis. *Lancet* 2011, 377:228-241.

145. Ottesen EA, Hong JW, Quake SR, Leadbetter JR. Microfluidic digital pcr enables multigene analysis of individual environmental bacteria. *Science* 2006, 314:1464-1467.

146. Dark PM, Dean P, Warhurst G. Bench-to-bedside review: The promise of rapid infection diagnosis during sepsis using polymerase chain reaction-based pathogen detection. *Crit Care* 2009, 13:217.

147. Niemz A, Ferguson TM, Boyle DS. Point-of-care nucleic acid testing for infectious diseases. *Trends Biotechnol* 2011, 29:240-250.

148. Loman NJ, Misra RV, Dallman TJ, Constantinidou C, Gharbia SE, Wain J, Pallen MJ. Performance comparison of benchtop high-throughput sequencing platforms. *Nat Biotechnol* 2012, 30:434-439.

149. Jain KK. Nanotechnology in clinical laboratory diagnostics. *Clin Chim Acta* 2005, 358:37-54.

150. Tallury P, Malhotra A, Byrne LM, Santra S. Nanobioimaging and sensing of infectious diseases. *Adv Drug Del Rev* 2010, 62:424-437.

151. Zhao XJ, Hilliard LR, Mechery SJ, Wang YP, Bagwe RP, Jin SG, Tan WH. A rapid bioassay for single bacterial cell quantitation using bioconjugated nanoparticles. *Proc Natl Acad Sci USA* 2004, 101:15027-15032.

152. Alivisatos P. The use of nanocrystals in biological detection. *Nat Biotechnol* 2004, 22:47-52.

153. Hahn MA, Tabb JS, Krauss TD. Detection of single bacterial pathogens with semiconductor quantum dots. *Anal Chem* 2005, 77:4861-4869.

154. Paquet C, Ryan S, Zou S, Kell A, Tanha J, Hulse J, Tay L-L, Simard B. Multifunctional nanoprobes for pathogen-selective capture and detection. *Chem Commun* 2012, 48:561-563.

155. Abdelhamid HN, Wu H-F. Probing the interactions of chitosan capped cds quantum dots with pathogenic bacteria and their biosensing application. *J Mater Chem* 2013, 1:6094-6106.

156. Leevy WM, Lambert TN, Johnson JR, Morris J, Smith BD. Quantum dot probes for bacteria distinguish escherichia coli mutants and permit in vivo imaging. *Chem Commun* 2008:2331-2333.

157. Edgar R, McKinstry M, Hwang J, Oppenheim AB, Fekete RA, Giulian G, Merril C, Nagashima K, Adhya S. High-sensitivity bacterial detection using biotin-tagged phage and quantum-dot nanocomplexes. *Proc Natl Acad Sci USA* 2006, 103:4841-4845.

158. Katz E, Willner I. Integrated nanoparticle-biomolecule hybrid systems: Synthesis, properties, and applications. *Angew Chem Int Ed* 2004, 43:6042-6108.

159. Gao J, Gu H, Xu B. Multifunctional magnetic nanoparticles: Design, synthesis, and biomedical applications. *Acc Chem Res* 2009, 42:1097-1107.

160. Gupta AK, Naregalkar RR, Vaidya VD, Gupta M. Recent advances on surface engineering of magnetic iron oxide nanoparticles and their biomedical applications. *Nanomed* 2007, 2:23-39.

161. Luis Corchero J, Villaverde A. Biomedical applications of distally controlled magnetic nanoparticles. *Trends Biotechnol* 2009, 27:468-476.

162. Gijs MAM, Lacharme F, Lehmann U. Microfluidic applications of magnetic particles for biological analysis and catalysis. *Chem Rev* 2010, 110:1518-1563.

163. Valencia PM, Farokhzad OC, Karnik R, Langer R. Microfluidic technologies for accelerating the clinical translation of nanoparticles. *Nat Nanotechnol* 2012, 7:623-629.

164. Cooper RM, Leslie DC, Domansky K, Jain A, Yung C, Cho M, Workman S, Super M, Ingber DE. A microdevice for rapid optical detection of magnetically captured rare blood pathogens. *Lab Chip* 2014, 14:182-188.

165. Chung HJ, Castro CM, Im H, Lee H, Weissleder R. A magneto-DNA nanoparticle system for rapid detection and phenotyping of bacteria. *Nat Nanotechnol* 2013, 8:369-375.

166. Hoerr V, Tuchscherr L, Hueve J, Nippe N, Loser K, Glyvuk N, Tsytsyura Y, Holtkamp M, Sunderkoetter C, Karst U. Bacteria tracking by in vivo magnetic resonance imaging. *BMC Biol* 2013, 11:63.

167. Baptista PV, Koziol-Montewka M, Paluch-Oles J, Doria G, Franco R. Gold-nanoparticle-probe-based assay for rapid and direct detection of mycobacterium tuberculosis DNA in clinical samples. *Clin Chem* 2006, 52:1433-1434.

168. Lim S, Koo OK, You YS, Lee YE, Kim M-S, Chang P-S, Kang DH, Yu J-H, Choi YJ, Gunasekaran S. Enhancing nanoparticle-based visible detection by controlling the extent of aggregation. *Sci Rep* 2012, 2:srep00456.

169. Phillips RL, Miranda OR, You C-C, Rotello VM, Bunz UHF. Rapid and efficient identification of bacteria using gold-nanoparticle - poly(para-phenyleneethynylene) constructs. *Angew Chem Int Ed* 2008, 47:2590-2594.

# Chapter 2

## Antibacterial Activities of Liposomal Linolenic acids (LipoLLA) Against Antibiotic-Resistant *Helicobacter pylori (H. pylori)* strains

## 2.1 Introduction

*Helicobacter pylori* (*H. pylori*) colonizes the stomach of more than half of the world's population and is the etiologic agent of various gastric diseases including gastritis and peptic ulcer disease[1]. *H. pylori* infection is also the single most common cause of gastric cancer[2]. Triple therapy, the combination of two antibiotics (clarithromycin plus amoxicillin or metronidazole) and a proton pump inhibitor, remains the standard first-line treatment of *H. pylori* infection worldwide[3]. However, this therapy is associated with poor compliance of patients, side effects of the antibiotics, and high cost. Moreover, the increasing emergence of *H. pylori* strains resistant to some of the antibiotics has resulted in a progressive decline in recent years to unacceptable low eradication rates ranging from 60 to 75%[4-6]. Particularly, resistance prevalence of metronidazole, a cornerstone of the triple-therapy formulation, has reached nearly 40% in developed countries and over 90% in developing countries[7]. In certain geographic regions, *H. pylori* resistance to clarithromycin has sharply decreased the rate of eradication by over 40%[6]. Even in regions where the conventional therapy remains efficacious, poor patient compliance due to the severe side effects associated with multiple antibiotics frequently leads to therapy failure[8]. Therefore, there is an urgent need to develop new antibacterial agents that can effectively eradicate *H. pylori* with minimum drug resistance.

In this regard, a series of free fatty acids (FFAs) including lauric acid, myristoleic acid, linoleic acid, and linolenic acid (LLA) have attracted much attention as they have shown antibacterial activities against a diverse range of bacteria including

*H. pylori*[9]. In addition to their high potency, these lipid-like molecules are ubiquitous and, hence, considered less harmful. Studies have also shown that FFAs induce drug resistance in *H. pylori* at a much lower frequency when compared to conventional antibiotics[10]. While promising results have been reported, the use of FFAs in inhibiting *H. pylori* remains challenging. In particular, medium-chain FFAs that are effective in inhibiting *H. pylori* commonly have low water solubility. If orally administered, the acidic pH in the stomach further decreases their solubility, making these molecules ineffective. Even if a small amount of FFAs can be dissolved, they are subject to oxidation, esterification, and lipid–protein complexation, further compromising their bactericidal activity in vivo[9]. Therefore, to fulfill the therapeutic potential of FFAs, it is essential to develop novel FFA formulations that can overcome these challenges.

Among various approaches, using nanotechnology to formulate nanosized FFA-loaded liposomes is promising. During liposome formulation, the amphiphilic nature of FFAs allows these molecules to be directly incorporated into the hydrophobic membranes at high loading yield[11]. The resulting liposomes can protect FFAs from degradation. We have demonstrated that FFAs such as lauric acid and oleic acid can be loaded into liposomes and form potent antibacterial agents against *Propionibacterium acnes* and drug-resistant *Staphylococcus aureus*, respectively[12, 13]. On the basis of our previous development in FFA-loaded liposomes, in this study, we further address challenges in *H. pylori* treatment with a primary focus on overcoming antibiotic resistance of the bacteria using liposomal formulations. Antibacterial

activities induced by liposome–bacterial membrane fusion have been shown to be less likely to induce drug resistance[14]. In addition, the approach of using liposomal formulations to inhibit *H. pylori* in vitro, if successful, will allow us to implement various established nanotechnological strategies, particularly those tailored for oral drug delivery, for future in vivo development[15, 16].

Herein, we chose LLA as a model FFA to formulate liposomal LLA (LipoLLA) and evaluated its bactericidal activities against various resistant strains of *H. pylori*. On a laboratory strain of *H. pylori*, LipoLLA showed an antibacterial efficacy comparable with free LLA predissolved in organic solvent in inhibiting both spiral and coccoid forms of the bacteria. As compared to amoxicillin, which killed the spiral form but not the coccoid form of the bacteria, LipoLLA and LLA were able to kill both forms. Using a metronidazole-resistant strain of *H. pylori* and seven clinically isolated strains, we further demonstrated that LipoLLA eradicated all strains of bacteria regardless of their resistance status to metronidazole. Finally, we tested LipoLLA in eliciting drug resistance in *H. pylori*. Under our experimental conditions, bacteria did not develop drug resistance when cultured with LipoLLA at various sub-bactericidal concentrations. On the contrary, bacteria acquired resistance to both metronidazole and LLA when cultured with drugs at comparable concentrations. Our findings suggest that LipoLLA holds strong potential to become an effective antimicrobial agent to treat *H. pylori* infection.

## 2.2 Experimental Methods

### 2.2.1 Materials

Hydrogenated l-α-phosphatidylcholine (egg PC), cholesterol, $C_6$-NBD Sphingomyelin ($C_6$NBD), and 1,2-dimyristoyl-sn-glycero-3-phosphoethanolamine-*N*-lissamine rhodamine B sulfonyl (DMPE-RhB) were purchased from Avanti Polar Lipids, Inc. (Alabaster, AL). LLA was purchased from Ultra Scientific (North Kingstown, RI). Brain heart infusion (BHI), Columbia broth, and agar were purchased from Becton Dickinson (Sparks, MD). Alamar blue dye, tetracycline hydrochloride, amoxicillin, glutaraldehyde, along with other common reagents including tris(hydroxymethyl) aminomethane (Tris), 4-(2-hydroxyethyl)-1-piperazineethanesulfonic acid (HEPES), phosphate-buffered saline (PBS), dimethyl sulfoxide (DMSO), dithiothreitol (DTT), and glycerol were obtained from Sigma-Aldrich Co. LLC (St. Louis, MO).

### 2.2.2 *H. pylori* Strains and Bacterial Culture

*H. pylori* Sydney strain 1 (SS1) and seven clinically isolated strains were used in this study. *H. pylori* SS1 is a mouse-adapted strain originally described by Lee et al[17]. Metronidazole-resistant *H. pylori* SS1 ($Mtz^r$ SS1 mutant) and clinical isolates (Shi470, Lithuania75, SouthAfrica7, India7, Gambia94/24, PeCan4, and SJM180) were a kind gift from Dr. Douglas Berg (Washington University, St. Louis, MO). *H. pylori* strains were routinely maintained on Columbia agar supplemented with 5% laked horse blood at 37 °C under microaerobic conditions (10% $CO_2$, 85% $N_2$, and 5%

$O_2$) as previously described[18]. For experiments, broth cultures of *H. pylori* were prepared by subculturing fresh colonies from agar plates into BHI containing 5% fetal bovine serum (FBS) and incubated overnight at 37 °C under microaerobic conditions with moderate reciprocal shaking. $Mtz^r$ SS1 mutant was selected in medium containing 15 μg/mL chloramphenicol and 20 μg/mL kanamycin[19].

### 2.2.3 Preparation of Solutions Containing LLA and LipoLLA

Stock solution containing 5 mg/mL LLA was prepared by dissolving LLA powder in DMSO. The experimental concentrations were achieved by diluting the stock solution of LLA with PBS or BHI growth medium containing 5% FBS. LipoLLA was prepared by a sonication and needle extrusion method as previously described[13]. Specifically, a total of 4 mg of egg PC, cholesterol, and LLA (5:1:4 weight ratio) were dissolved in 1 mL of chloroform. Then, the chloroform was evaporated by blowing argon gas for 10 min, and a thin lipid layer formed. The film was rehydrated by adding 2 mL of PBS or BHI medium. The resulting lipid suspension was vortexed for 1 min, followed by sonication for 3 min in a bath sonicator (Fisher Scientific FS30D) to produce multilamellar vesicles (MLVs). Then, the MLVs were sonicated using a Branson 450 sonifier with a Ti-probe at 20 W for 30 s to produce small unilamellar vesicles (SUVs). The solution containing liposomes was obtained by extruding the SUVs through a 100 nm pore-sized polycarbonate membrane 11 times with a mini-extruder (Avanti Polar Lipids). After the excess free LLA was removed, possibly in the form of LLA micelles, from the solution of

LipoLLA using a Sephadex G75 column, the loading yield of LLA in the synthesized LipoLLA was determined using an Agilent 1100 series LC-MSD-Trap-SL high-performance ion trap mass spectrometer (Agilent Technologies, Santa Clara, CA), equipped with an electrospray ionization source, following a previously published protocol[13]. Finally, the solution containing LipoLLA was sterilized by filtration through a 0.22 μm filter unit (Millipore, Billerica, MA) prior to uses. The hydrodynamic size (diameter, nm) and surface ζ-potential (mV) of LipoLLA were measured using the Malvern Zetasizer ZS (Malvern Instruments, United Kingdom).

### 2.2.4 Bactericidal Activity against Spiral form of *H. pylori* SS1

An overnight broth culture of *H. pylori* SS1 was centrifuged at 5000*g* for 10 min to obtain a bacterial pellet. The pellet was adjusted to an optical density at 600 nm ($OD_{600}$) of 1.0, corresponding to approximately $1 \times 10^8$ colony-forming units (CFU)/mL. Ten microliters/well of bacterial suspension containing $1 \times 10^6$ CFU bacteria was added to a 96-well plate containing 190 μL of BHI medium supplemented with 5% FBS along with various concentrations of LLA or LipoLLA. The plate was incubated at 37 °C under microaerobic conditions on a reciprocal shaker. Several pilot experiments were performed at 2-, 5-, and 10-fold dilutions of LLA and LipoLLA at 0.5, 1, 6, 12, and 24 h of incubation times to pinpoint desired concentration ranges and time points. After incubation for 30 min, a series of 10-fold dilutions of the bacterial suspension (1:10 to $1:10^5$) were prepared, and 5 μL from each diluted sample was inoculated onto a Columbia agar plate supplemented with 5%

laked horse blood. The plates were cultured in the incubator for 4 days before counting colonies.

### 2.2.5 Bactericidal Activity against Coccoid form of *H. pylori* SS1

The coccoid form of *H. pylori* SS1 was generated using a method described elsewhere[20]. Briefly, tetracycline hydrochloride (15 μg/mL) was added to an overnight culture and cultivated for an additional 4 days. The culture was centrifuged at 600*g* for 5 min to pellet any remaining spiral form of the bacteria followed by the centrifugation of the supernatant at 11000*g* for 5 min. The resulting pellet contained mostly the induced coccoid form of *H. pylori* SS1, as confirmed by observation under light microscope. Their viability was confirmed with Alamar blue dye assay[21]. Briefly, 10 μL of Alamar blue dye (10% vol/vol) was added to each well, and the plate was incubated at 37 °C for 4 h. The fluorescence intensity was measured by a fluorescence microplate reader (Synergy Mx, Biotek, Winooski, VT) with an excitation wavelength of 560 nm and an emission wavelength of 600 nm. A higher fluorescence intensity indicates a higher viability of the bacteria in the well. The density of coccoid *H. pylori* SS1 in solution was determined through an $OD_{600}$ measurement.

To test the sensitivity of coccoid *H. pylori* SS1 to LLA and LipoLLA, $1 \times 10^6$ CFU coccoid *H. pylori* SS1 were added to 200 μL of BHI containing amoxicillin (1, 10, or 20 μg/mL), LipoLLA (2 or 4 mg/mL, containing 400 or 800 μg/mL of LLA, respectively), and LLA (400 or 800 μg/mL). The samples were incubated in a 96-well plate at 37 °C with reciprocal shaking for 0.5, 4, or 24 h. After incubation, bacterial

viability in the suspension was measured by Alamar blue dye assay. As a comparison, the same test was carried out in parallel for spiral *H. pylori* SS1 under the same conditions. Finally, the bacterial viability of all samples was normalized to the control sample treated with PBS buffer.

### 2.2.6 LipoLLA–*H. pylori* SS1 Fusion Study

Fluorescence resonance energy transfer (FRET) study was performed to investigate the interaction mechanism between LipoLLA and *H. pylori* SS1. To prepare a FRET-labeled LipoLLA, a fluorescent donor ($C_6$NBD, 0.1 mol %) and a fluorescent acceptor (DMPE-RhB, 0.5 mol %) were simultaneously incorporated into the lipid bilayer membranes of the LipoLLA (0.5 mg/mL) by mixing the donor and the acceptor with egg PC, cholesterol, and LLA prior to the preparation of LipoLLA. Next, the resulting liposomes were diluted with PBS 2-fold into a solution containing 0.25 mg/mL LipoLLA, and 0.25 mL of the diluted solution was mixed with different amounts of *H. pylori* SS1. The total volume of the final solution (LipoLLA + *H. pylori* SS1) was adjusted to 1 mL, resulting in bacterial concentrations of $8.0 \times 10^7$, $1.6 \times 10^8$, $2.4 \times 10^8$, $3.2 \times 10^8$, and $4.0 \times 10^8$ CFU/mL, respectively. After 10 min of incubation at room temperature, samples were centrifuged at 13500 rpm for 1 min to remove the excess amount of LipoLLA followed by resuspension in 1 mL of PBS. Subsequently, emission spectra in the region of 500–700 nm were obtained by exciting the sample at 470 nm using a fluorescent spectrophotometer (BioTek Instrument, United States). The solution containing the same amount of LipoLLA without

incubating with *H. pylori* SS1 was used as a negative control. Fluorescence emission of *H. pylori* SS1 itself at the corresponding concentrations was subtracted from each sample before data plotting.

### 2.2.7 Scanning Electron Microscope (SEM) Imaging of *H. pylori* SS1

The morphology of both spiral and coccoid forms of *H. pylori* SS1 treated with LLA and LipoLLA was examined with SEM. *H. pylori* SS1 was incubated with 200 μg/mL LLA and 1 mg/mL LipoLLA (containing 200 μg/mL LLA) at the same conditions as those for the bactericidal studies. At 30 min, the bacteria were harvested and visualized by an FEI XL30 Environmental SEM. To prepare SEM samples, untreated and treated bacteria were centrifuged to remove the supernatant, and the remaining pellet was fixed with 2% glutaraldehyde for 2 h at room temperature. Post fixing, the sample was centrifuged to remove glutaraldehyde and resuspended in 100 μL of water. Then, 5 μL of the bacterial suspension was dropped onto a polished silicon wafer and allowed to dry overnight in a biosafety cabinet. The samples were then coated with chromium before SEM imaging.

### 2.2.8 Bactericidal Activity against Antibiotics-Resistant *H. pylori* Strains

To test the bactericidal activity of LLA and LipoLLA against antibiotic-resistant strains of *H. pylori*, including seven clinically isolated resistant strains (Shi470, Lithuania75, SouthAfrica7, India7, Gambia94/24, PeCan4, and SJM180) and

metronidazole-resistant *H. pylori* SS1 ($Mtz^r$ SS1 mutant), $1 \times 10^6$ CFU of bacteria from an overnight culture was added to 200 μL of BHI medium containing LLA and LipoLLA at various concentrations and cultured in a 96-well plate. The plate was incubated at 37 °C under microaerobic conditions with reciprocal shaking for 30 min. The bacterial suspension was then subjected to serial dilution and spotted onto Columbia agar plates supplemented with 5% laked horse blood. The plates were cultured in the incubator for 4 days before counting colonies.

### 2.2.9 Resistance Acquisition of *H. pylori* SS1 upon Treatments

To test the drug resistance development of *H. pylori* SS1 upon treatments, $1 \times 10^7$ CFU of bacteria in logarithm growth phase were added to 600 μL of BHI/5% FBS containing various concentrations of metronidazole, LLA, or LipoLLA in a 24-well plate. The plate was incubated at 37 °C under microaerobic conditions with gentle shaking. After 24 h, 100 μL of sample from each well was collected and added to 500 μL of fresh medium containing the same type of drug and drug concentration. Meanwhile, the bacteria from each treatment group were tested for sensitivity to the corresponding drug using the same protocol described in bactericidal studies. This process was repeated for 10 days to observe possible drug resistance of *H. pylori* SS1.

## 2.3 Results and Discussion

In this study, liposome was made of egg PC and cholesterol, and its lipid bilayer structure was illustrated in Figure 2.1. Liposome offers unique

physicochemical properties for delivering FFAs such as LLA for therapeutic applications. Particularly, amphiphilic LLA molecules can be readily entrapped in the hydrophobic lipid membranes of a liposome by mixing LLA with egg PC and cholesterol at desirable ratios prior to liposome preparation. As a result, the use of LipoLLA can overcome the poor solubility of LLA in aqueous solution. For antibacterial applications, the liposome formulations, as compared to other LLA formulations such as micelles and emulsions, can fuse with bacterial membranes and thus directly release the entrapped LLA molecules into bacterial membranes for efficient bactericidal activity[12, 13]. The loading yield of LLA in LipoLLA formulations was determined by liquid chromatography–mass spectrometry following a procedure previously reported[13]. Under our experimental conditions, 40% LLA in the initial mixture of egg PC, cholesterol, and LLA resulted in a final loading yield of approximately 20%. There was a loss of LLA during the experimental processes, including needle sonication, extrusion, and sterilization. A similar loss of FFA during liposome formulation was also observed in our previous study to encapsulate oleic acid into a liposomal formulation[13]. LipoLLA formulated here has a hydrodynamic size (diameter) of 88 ± 3 nm, a polydispersity index of 0.17 ± 0.01, and a surface ζ-potential of −78 ± 4 mV in deionized water, determined by dynamic light scattering measurements. It is expected that these sub-100 nm liposomes can readily fuse with bacterial membranes due to their high surface tension.

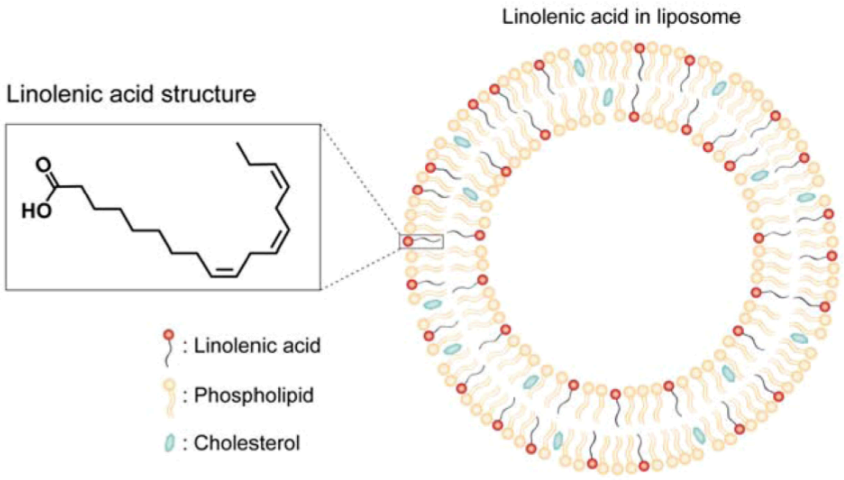


**Figure 2.1** Schematic drawing shows the molecular structure of LLA and the structure of LipoLLA composed of phospholipid, cholesterol, and LLA.

The bactericidal activity of LLA (dissolved in 5% DMSO) and LipoLLA was first tested against a replicating form (also called spiral form) of *H. pylori* SS1 strain. This strain of bacteria was chosen because of its significance and wide applications in *H. pylori* research[22]. When *H. pylori* SS1 was incubated for 30 min in broths containing various concentrations of LLA, the correlation between bacterial viability and LLA concentration was not linear (Figure 2.2A). Specifically, when LLA concentration was below 50 μg/mL, negligible bactericidal activity was observed. Further increasing the LLA concentration above 50 μg/mL led to a sharp decrease in viable bacteria number. When the LLA concentration reached 100 μg/mL, no viable bacteria were detected. For this study, we defined minimal bactericidal concentration (MBC) as the minimum concentration of the bactericidal agent required to kill 3 logs (99.9%) of the bacteria during a 30 min incubation. Therefore, the MBC value for LLA was determined to be 75 μg/mL (equivalent to 0.27 mM). A similar correlation

between bacterial viability and LLA concentration was also observed when LipoLLA at various concentrations was added to bacterial cultures (Figure 2.2B). Specifically, bactericidal activity was negligible when the LLA concentration was below 30 μg/mL. Above this concentration, a rapid decrease in viable bacteria number was observed. When LLA concentration was raised to 100 μg/mL, no viable bacteria were detected. From the correlation between bacterial viability and LLA concentration, the MBC value of LipoLLA was determined to be 67 μg/mL (equivalent to 0.22 mM), at which 99.9% of the bacteria were killed.

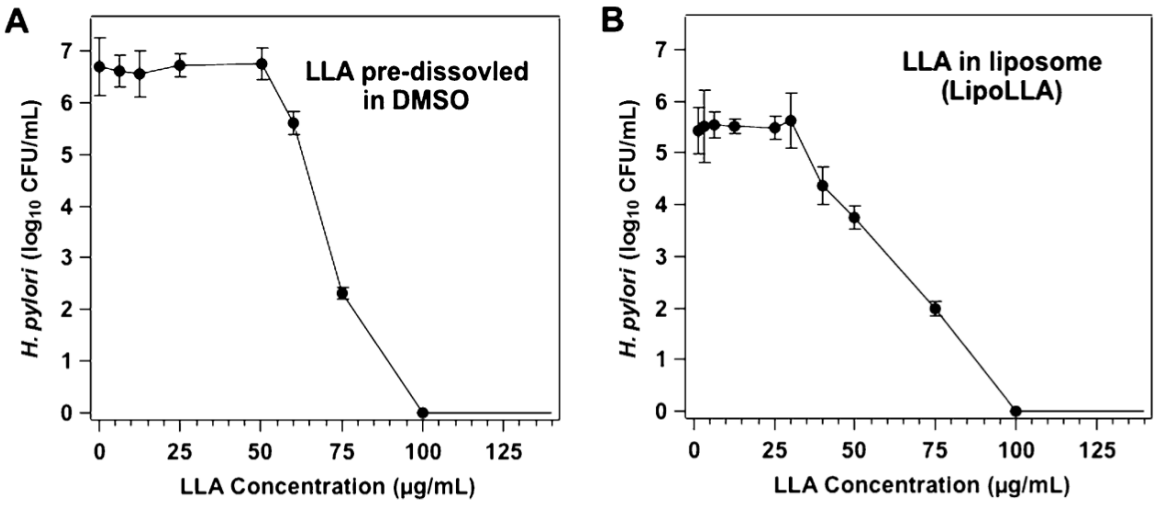


**Figure 2.2** In vitro bactericidal activity of (A) LLA and (B) LipoLLA at different drug concentrations against *H. pylori* SS1. All concentrations refer to LLA concentration, regardless of the formulation. LLA or LipoLLA was incubated with $5 \times 10^6$ CFU/mL *H. pylori* SS1 bacteria at 37 °C under microaerobic conditions for 30 min followed by Columbia agar plate subculture.

The observation of a sharp decrease in viable bacteria at the MBC values implies that the killing of *H. pylori* may involve a highly destructive mechanism such as lysis of the bacterial membranes. This is further supported by a killing time no

longer than 30 min, relatively short when compared to 2.5 h needed for *H. pylori* to complete a replication cycle[9]. To better understand the interaction mechanism between LipoLLA and *H. pylori* bacteria at a molecular level, we labeled LipoLLA with a FRET pair of fluorescence probes and monitored the FRET signal changes upon mixing with the bacteria at various concentrations. FRET is a sensitive technique that precisely detects the distance change between two subjects at the molecular level based on an energy transfer mechanism of two chromophores[23, 24]. Herein, we incorporated a fluorescent donor ($C_6$NBD: excitation/emission = 470 nm/520 nm) and a fluorescent acceptor (DMPE-RhB: excitation/emission = 550 nm/580 nm) into the lipid bilayer membranes of LipoLLA at a molar ratio of 1:5, at which the fluorescence emission from $C_6$NBD was completely quenched by DMPE-RhB. We hypothesize that if the LipoLLA fuses with the bacterial membranes, the spread of the donor and acceptor within the bacterial membranes will alleviate or eliminate the FRET efficiency, resulting in a recovery of the donor florescence. To test this hypothesis, we mixed the FRET-labeled LipoLLA with varying concentrations of *H. pylori* SS1, followed by removal of the excess LipoLLA. The samples were then excited at the wavelength of 470 nm, and the emission spectra at the range of 500–700 nm were obtained. As shown in Figure 2.3, the rise of the emission peak of $C_6$NBD at 520 nm was detected when the concentration of *H. pylori* SS1 increased, indicating an increase of spatial separation between $C_6$NBD and DMPE-RhB upon mixing LipoLLA with *H. pylori* bacteria. These results confirm that the interaction mechanism between the LipoLLA and the bacteria was fusion as opposed to adsorption or aggregation.

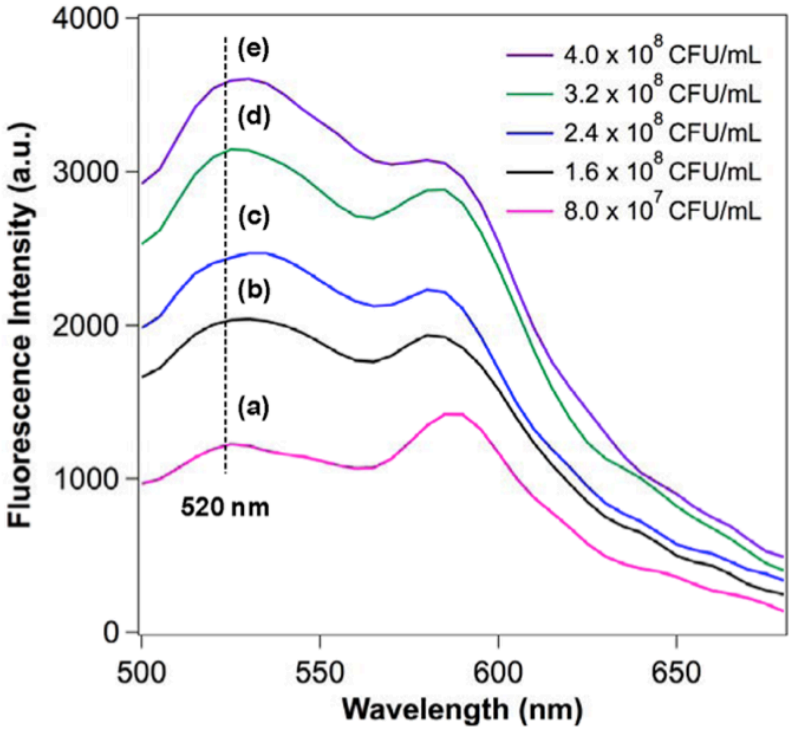


**Figure 2.3** FRET measurements of the fusion between LipoLLA and *H. pylori* SS1. A fluorescent donor ($C_6$NBD, 0.1 mol %) and a fluorescent acceptor (DMPE-RhB, 0.5 mol %) were concurrently incorporated into the lipid bilayer membranes of LipoLLA so that the acceptor completely quenched the fluorescence emission from the donor. The FRET pair-labeled LipoLLA was incubated with *H. pylori* at a concentration of (a–e) $8.0 \times 10^7$, $1.6 \times 10^8$, $2.4 \times 10^8$, $3.2 \times 10^8$, and $4 \times 10^8$ CFU/mL for 10 min. After the excess LipoLLA was removed, all samples were excited at 470 nm. A rise in emission intensity of $C_6$NBD (donor) at 520 nm was observed with the increase of bacterial concentrations, indicating the occurrence of fusion between LipoLLA and *H. pylori* that caused the spatial separation of $C_6$NBD and DMPE-RhB.

After having confirmed that the interaction mechanism between LipoLLA and *H. pylori* is fusion, we further tested the bactericidal activity of LLA and LipoLLA against the dormant form (also called coccoid form) of *H. pylori* SS1 and examined the effects of LLA and LipoLLA on the bacterial membrane morphology upon treatments. *H. pylori* bacteria adopt two major morphologies, spiral and coccoid

forms. Despite the controversy regarding the vitality of nonculturable coccoid form of *H. pylori*, accumulating evidence suggests that *H. pylori* bacteria in coccoid form can play a critical role in disease transmission and subsequent treatment[25]. Particularly, studies have found that *H. pylori* transmitted through oral–oral or oral–fecal routes may survive as coccoid form[26]. The coccoid form of the bacteria was also shown to contribute to the development of relapses following antimicrobial therapy in *H. pylori* infection[27]. Furthermore, in our study, we induced the coccoid form of *H. pylori* by supplementing the culture medium with tetracycline hydrochloride, a method that has been shown to reduce CoA transferase activity and increase α-ketoglutarate oxidoreductase activity of the induced coccoid bacteria[20]. Such changes in enzymatic activities involved in bacterial energy metabolism not only indicate that the bacteria remain viable during the transformation from spiral to coccoid form but also suggest that target-specific antibiotics effective in inhibiting one form of the bacteria may not be effective in another. Hence, for successful therapy, it is essential to develop antimicrobials that can eliminate both forms of *H. pylori*.

Next, we examined the bactericidal activities of LLA and LipoLLA against both spiral and coccoid forms of *H. pylori* SS1, while using amoxicillin as a model anti-*H. pylori* antibiotic as a positive control (see Figure 2.4). We started with 400 μg/mL of LLA as this was the lowest concentration where complete killing of coccoid *H. pylori* was observed at 24 h of incubation time. At concentrations of 400 and 800 μg/mL (referring to LLA), LLA and LipoLLA completely killed *H. pylori* in spiral form at 30 min of incubation time and coccoid form at 24 h of incubation time.

Herein, 1 μg/mL of amoxicillin was selected as the lowest concentration, which is approximately the MIC value of amoxicillin for *H. pylori* in the spiral form[28, 29]. As shown in Figure 2.4, at 0.5 h of incubation time, amoxicillin did not show any inhibition activity against either the spiral or the coccoid form of *H. pylori*, while at 24 h, amoxicillin killed the spiral but not the coccoid *H. pylori*. The lack of efficacy of amoxicillin in inhibiting the coccoid *H. pylori* but not the spiral form can be explained by its mechanism of action, which is to inhibit bacterial cell wall biosynthesis[30]. As the coccoid form is "dormant", the nondividing bacteria will not be affected by amoxicillin. In contrast, the bactericidal activity of LLA results at least in part from the incorporation of LLA into bacterial membranes[10], and the liposome–bacterial membrane fusion would further enhance the antibacterial activity of LipoLLA[12]. Such drug–bacterial membrane interactions are less dependent on the metabolic rate of the bacteria. Hence, when compared to amoxicillin, LLA and LipoLLA show less difference in efficacy when inhibiting spiral and coccoid forms of *H. pylori*. These data therefore provide evidence that LLA and LipoLLA are more effective in killing both forms of *H. pylori* in comparison to existing antibiotics.

The morphology transformation of *H. pylori* from spiral form to coccoid form was examined using SEM, where the image showed typical spiral *H. pylori* cells with normal curved morphology and intact cell membranes (Figure 2.5A). A typical spiral *H. pylori* cell was 2–4 μm long and 0.5–0.8 μm wide with visible sheathed flagella. After the bacteria were treated with 400 μg/mL LLA for 30 min, complete killing of bacteria was confirmed by Alamar blue dye staining assay.

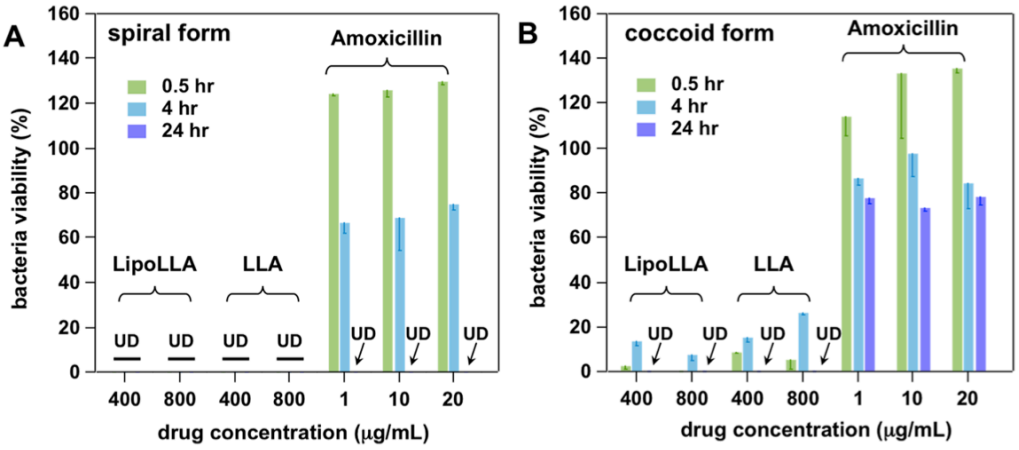


**Figure 2.4** In vitro bactericidal activity of LipoLLA in comparison with LLA and amoxicillin against (A) spiral form and (B) coccoid form of *H. pylori* SS1. Bacterial viability was tested by using Alamar blue dye assay after an incubation period of 0.5, 4, or 24 h. All concentrations of LLA and LipoLLA refer to LLA concentration, regardless of the formulation. Bacterial viability was normalized to the control sample treated with PBS buffer.

Meanwhile, the SEM image showed the bacterial morphology with a complete loss of the normal curved shape, disruption of protoplasmic cylinders, cell lysis, fragmentation of the bacterial cell membranes, and severe clustering (Figure 2.5B). Bacteria treated with LipoLLA under the same conditions had similar morphology as those treated with LLA (Figure 2.5C). Meanwhile, the SEM image of *H. pylori* in coccoid form showed a predominantly non-colonized spherical shape with a diameter around 2 μm (Figure 2.5D). By using Alamar blue dye staining assay to measure viability, a concentration below 400 μg/mL of LLA (predissolved in DMSO or in liposome formulation) was insufficient to completely kill coccoid form of *H. pylori* bacteria. In contrast, treatment with 400 μg/mL LLA for 24 h led to complete killing of bacteria in coccoid form. SEM images showed that the morphology of dead coccoid

form of *H. pylori* bacteria was similar to that of the dead spiral bacteria, where the bacterial membranes were completely disrupted and formed clusters (Figure 2.5E,F). In addition, the bacterial morphology had little discernible difference between the treatments with LLA and LipoLLA. As a control, the bacterial membrane morphology remained intact upon incubation with the same concentration of bare liposomes (without LLA).

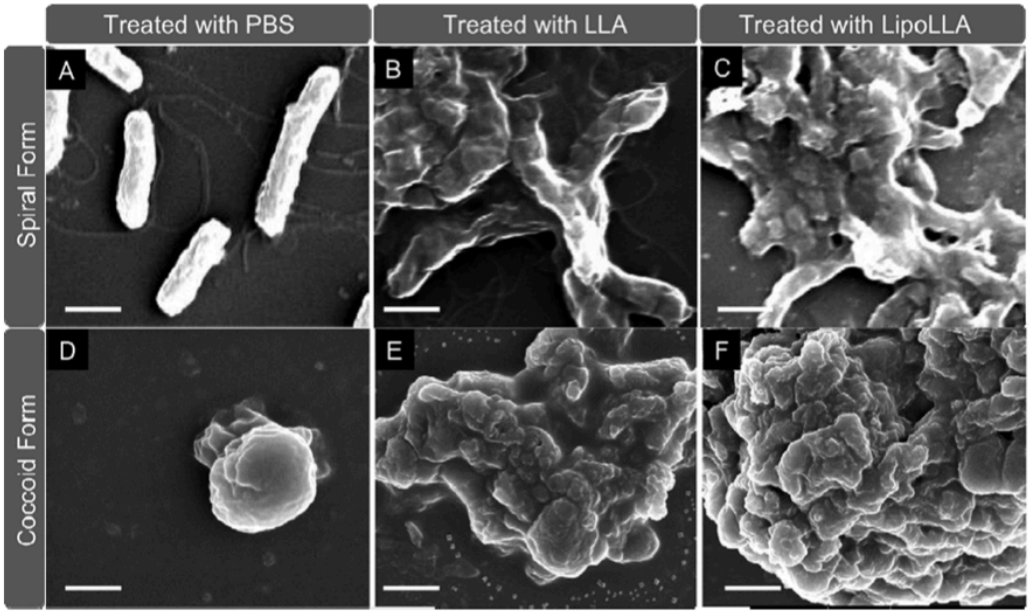


**Figure 2.5** Morphology of *H. pylori* SS1 bacteria in their spiral form (A–C) and coccoid form (D–F) exposed to different treatments. In A and D, bacteria were treated with PBS; in B and E, bacteria were treated with LLA predissolved in DMSO; in C and F, bacteria were treated with LipoLLA. In all experiments, the initial concentration of the bacteria was $5 \times 10^6$ CFU/mL, and the drug concentration was 200 μg/mL (referring to LLA). All samples were treated for 30 min before glutaralderhyde fixation. The scale bar in the image represents 1 μm.

To further evaluate the bactericidal activity of LLA and LipoLLA against *H. pylori*, we next examined their antimicrobial efficacy against a series of clinical

isolates of *H. pylori*, including Shi470, SouthAfrica7, India7, Gambia94/24, PeCan4, Lithuania75, and SJM180. These clinical isolates are normally resistant to existing antibiotics such as metronidazole. In addition, we also developed a metronidazole-resistant strain of *H. pylori* SS1 ($Mtz^r$ SS1 mutant)[19] to be included into this test. All of these antibiotic-resistant *H. pylori* strains were then tested for their susceptibility to LLA and LipoLLA. As shown in Figure 2.6, when the LLA concentration was 100 μg/mL, clinical isolate Shi470 was completely killed, while initial inhibition was observed on other strains. When LLA concentration was raised to 200 μg/mL, all strains, regardless of their resistance status to metronidazole, were completely killed by both LLA and LipoLLA. The nonselective bactericidal activity of LLA and LipoLLA against a broad range of *H. pylori* strains is of great value in developing new treatments for *H. pylori* infection.

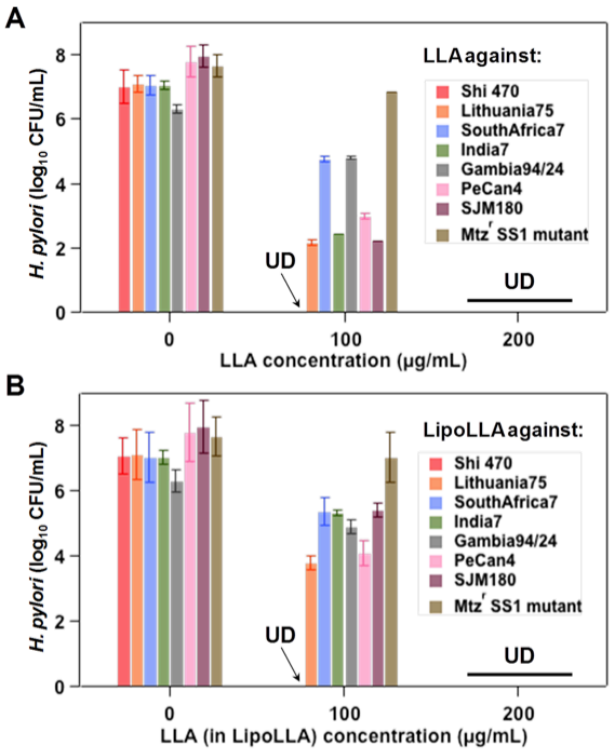


**Figure 2.6** In vitro bactericidal activity of (A) LLA and (B) LipoLLA against various *H. pylori* clinical isolates and a metronidazole-resistant strain of *H. pylori* SS1 ($Mtz^r$ SS1 mutant). In all experiments, $5 \times 10^6$ CFU/mL bacteria were incubated with 0, 100, or 200 μg/mL LLA, either as free LLA predissolved in DMSO or in liposome formulation (LipoLLA). Samples were incubated at 37 °C under microaerobic conditions for 30 min before serial dilution followed by bacterial colony enumeration on Columbia agar plates.

In addition to the efficacy studies conducted to evaluate bactericidal activities of LLA and LipoLLA against *H. pylori* SS1, in both spiral and coccoid forms, and the clinical isolates of *H. pylori* strains, we finally investigated the potential resistance acquisition of *H. pylori* bacteria under the treatments of LLA and LipoLLA. In the study, we used *H. pylori* SS1 as an example to examine the development of drug resistance when the bacteria were cultured with various sub-bactericidal concentrations of LLA or LipoLLA over a span of 10 days. Here, metronidazole, an

anti-*H. pylori* antibiotic in clinic use, was chosen to serve as a positive control. As shown in Table 1.1, *H. pylori* treated with 0.5 or 1 μg/mL metronidazole acquired resistance to the antibiotic on day 3, and by day 4, the bacteria in all concentration groups had developed resistance to metronidazole. In contrast, bacteria treated with LLA at concentrations of 18.8 and 28.2 μg/mL did not acquire drug resistance. However, when the LLA concentration was raised to 37.6 μg/mL (half MBC value of LLA against *H. pylori* SS1), drug resistance was established on day 3. In contrast to both metronidazole and LLA, bacteria treated with LipoLLA in all three different concentration groups including 16.8, 22.4, and 33.6 μg/mL (half MBC value of LipoLLA against *H. pylori* SS1) did not acquire drug resistance during the 10 day period of studies.

**Table 2.1** Resistance Development of *H. pylori* SS1 upon Incubation with Different Levels of Metronidazole, LLA, and LipoLLA over a Span of 10 Days

| | | day | | | | | | | | | |
|---|---|---|---|---|---|---|---|---|---|---|---|
| treatment | LLA concn (Mg/mL) | 1 | 2 | 3 | 4 | 5 | 6 | 7 | 8 | 9 | 10 |
| metronidazole | 0.25 | – | – | – | + | + | + | + | + | + | + |
| | 0.5 | – | – | + | + | + | + | + | + | + | + |
| | 1 | – | – | + | + | + | + | + | + | + | + |
| LLA (p redissolved in DMSO) | 18.8 | – | – | – | – | – | – | – | – | – | – |
| | 28.2 | – | – | – | – | – | – | – | – | – | – |
| | 37.6 | – | – | + | + | + | + | + | + | + | + |
| LipoLLA | 16.8 | – | – | – | – | – | – | – | – | – | – |
| | 22.4 | – | – | – | – | – | – | – | – | – | – |
| | 33.6 | – | – | – | – | – | – | – | – | – | – |

[a]The highest concentrations selected in the LLA group (37.6 μg/mL) and LipoLLA group (168 μg/mL, containing 33.6 μg/mL of LLA) were half of their MBC values, respectively. In the metronidazole group, 1 μg/mL is approximately 1/8 of its reported MIC value. In the table, "–" denotes "nonresistant", and "+" denotes "resistant".

The rapid resistance development of *H. pylori* under the treatment of metronidazole is likely attributed to the fast adaptation of bacteria to target-specific antibiotics through various mechanisms including decreased drug uptake, increased

efflux, decreased drug activation, mutations in biological target, increased oxygen scavenging capabilities, and enhanced activity of DNA repair enzymes[31, 32]. Similar to metronidazole, FFAs have also been hypothesized to inhibit bacteria growth through mechanisms that alternate cell survival signaling pathways. For example, it has been suggested that FFAs may enter the cells and inhibit bacterial growth by creating an acidic environment in cytoplasm that damages pH-sensitive intracellular enzyme activities or amino acid transports[33]. FFAs have also been speculated to participate in chemical processes that generate toxic lipid peroxides, which in turn cause antibacterial activities[34]. These mechanisms are target-specific. Therefore, treated with FFAs, *H. pylori* may still evolve and develop drug resistance. However, FFAs can also inhibit bacteria growth by incorporating themselves into bacterial membranes, disrupting the structural integrity of the cell membrane, and inducing abnormal cell forms and cell lysis[9, 10]. Such antibacterial activities are physical, broad, and unspecific, which may explain a lower frequency of resistance development observed when bacteria are treated with FFAs. For instance, *H. pylori* acquired much less resistance against LLA than metronidazole as shown in Table 2.1

As compared to free FFAs, liposomal formulation confines FFA molecules within the lipid bilayer. During the process of liposome–bacterial membrane fusion, FFA molecules are exclusively distributed into the bacterial membranes, limiting their interaction with cells' intracellular machineries. As liposomal formulation of FFAs limits chemical alterations on cell survival pathways but promotes physical–structural disruption of cell membranes, an even lower rate of resistant was developed when

bacteria were treated with liposomal FFAs. This may explain why LipoLLA did not provoke drug resistance of *H. pylori* during the treatment period.

## 2.4 Conclusions

In this study, we demonstrated the bactericidal activities of LipoLLA and free LLA in treating *H. pylori* infection. Using *H. pylori* SS1 as a model strain, we showed that LipoLLA and free LLA were effective in killing both spiral and coccoid forms of the bacteria. Using a metronidazole-resistant strain of *H. pylori* and seven clinical isolates, we further demonstrated that LipoLLA eradicated all strains of the bacteria regardless of their resistance status to metronidazole. Furthermore, under our experimental conditions, bacteria did not develop noticeable drug resistance when cultured with LipoLLA at various sub-bactericidal concentrations, whereas they acquired resistance to both metronidazole and free LLA at comparable concentrations. While both LipoLLA and free LLA were tested in parallel for their bactericidal activities against *H. pylori* in this study, we expect that LipoLLA holds greater potential to be translated as a new therapeutic option to *H. pylori* infection. This is because of the poor water solubility of LLA, which needs to be predissolved in organic solvents prior to uses. In addition, using LipoLLA to treat H. *pylori* infection is expected less likely to induce bacterial drug resistance because of the liposome–bacterial membrane fusion mechanism, through which the drug molecules are directly introduced to the bacterial membranes rather than intracellular compartments. Moreover, our approach of using LLA-loaded liposomal nanoformulation to treat *H.*

*pylori* infection bridges the accumulated knowledge of antimicrobial activities of FFAs and the fast-emerging field of nanotechnology. As a result, LipoLLA developed in this study would allow us to implement numerous nanotechnology-based strategies, particularly those established to overcome mucosal barrier and gastric conditions[35-39], for more advanced drug delivery to treat *H. pylori* infection.

Chapter 2, in full, is a reprint of the material as it appears in Molecular Pharmaceutics, 2012, Soracha Thamphiwatana, Marygorret Obonyo, Li Zhang, Dissaya Pornpattananangkul, Victoria Fu, and Liangfang Zhang, and, The dissertation author was the primary investigator and author of this paper.

## 2.5 References


1. Hatakeyama M, Brzozowski T. Pathogenesis of Helicobacter pylori infection. *Helicobacter*. 2006, 11:14-20.

2. González CA, Agudo A. Carcinogenesis, prevention and early detection of gastric cancer: where we are and where we should go. *International Journal of Cancer*. 2012, 130:745-53.

3. Gisbert JP, Pajares JM. Treatment of Helicobacter pylori infection: The past and the future. *European journal of internal medicine*. 2010, 21:357-9.

4. Paoluzi OA, Visconti E, Andrei F, Tosti C, Lionetti R, Grasso E. Ten and eight-day sequential therapy in comparison to standard triple therapy for eradicating Helicobacter pylori infection: a randomized controlled study on efficacy and tolerability. *Journal of clinical gastroenterology*. 2010, 44:261-6.

5. Yamaoka Y, Graham D, Lu H. Should triple therapy for Helicobacter pylori infection be abandoned as no longer effective. *US Gastroenterology*. 2008, 4:65-7.

6. Megraud F. H pylori antibiotic resistance: prevalence, importance, and advances in testing. *Gut*. 2004, 53:1374-84.

7. Njume C, Afolayan A, Ndip R. An overview of antimicrobial resistance and the future of medicinal plants in the treatment of Helicobacter pylori infections. *African Journal of Pharmacy and Pharmacology*. 2009, 3:685-99.

8. O'Connor A, Gisbert JP, McNamara D, O'Morain C. Treatment of Helicobacter pylori infection 2011. *Helicobacter*. 2011, 16:53-8.

9. Desbois AP, Smith VJ. Antibacterial free fatty acids: activities, mechanisms of action and biotechnological potential. *Applied microbiology and biotechnology*. 2010, 85:1629-42.

10. Petschow BW, Batema RP, Ford LL. Susceptibility of Helicobacter pylori to bactericidal properties of medium-chain monoglycerides and free fatty acids. *Antimicrobial agents and chemotherapy*. 1996, 40:302-6.

11. Prajapati HN, Dalrymple DM, Serajuddin AT. A comparative evaluation of mono-, di-and triglyceride of medium chain fatty acids by lipid/surfactant/water phase diagram, solubility determination and dispersion testing for application in pharmaceutical dosage form development. *Pharmaceutical research*. 2012, 29:285-305.

12. Yang D, Pornpattananangkul D, Nakatsuji T, Chan M, Carson D, Huang C-M, Zhang L. The antimicrobial activity of liposomal lauric acids against Propionibacterium acnes. *Biomaterials*. 2009, 30:6035-40.

13. Huang C-M, Chen C-H, Pornpattananangkul D, Zhang L, Chan M, Hsieh M-F. Eradication of drug resistant Staphylococcus aureus by liposomal oleic acids. *Biomaterials*. 2011, 32:214-21.

14. Huh AJ, Kwon YJ. "Nanoantibiotics": a new paradigm for treating infectious diseases using nanomaterials in the antibiotics resistant era. *Journal of controlled release*. 2011, 156:128-45.

15. Bhardwaj V, Hariharan S, Bala I, Lamprecht A, Kumar N, Panchagnula R. Pharmaceutical aspects of polymeric nanoparticles for oral drug delivery. *Journal of Biomedical Nanotechnology*. 2005, 1:235-58.

16. Roger E, Lagarce F, Garcion E, Benoit J-P. Biopharmaceutical parameters to consider in order to alter the fate of nanocarriers after oral delivery. *Nanomedicine*. 2010, 5:287-306.

17. Lee A, O'Rourke J, De Ungria MC, Robertson B, Daskalopoulos G, Dixon MF. A standardized mouse model of Helicobacter pylori infection: introducing the Sydney strain. *Gastroenterology*. 1997, 112:1386-97.

18. Obonyo M, Sabet M, Cole SP, Ebmeyer J, Uematsu S, Akira S. Deficiencies of myeloid differentiation factor 88, Toll-like receptor 2 (TLR2), or TLR4 produce specific defects in macrophage cytokine secretion induced by Helicobacter pylori. *Infection and immunity*. 2007, 75:2408-14.

19. Jeong J-Y, Berg DE. Mouse-colonizing Helicobacter pylori SS1 is unusually susceptible to metronidazole due to two complementary reductase activities. *Antimicrobial agents and chemotherapy*. 2000, 44:3127-32.

20. Tsugawa H, Suzuki H, Nakagawa I, Nishizawa T, Saito Y, Suematsu M. Alpha-ketoglutarate oxidoreductase, an essential salvage enzyme of energy metabolism, in coccoid form of Helicobacter pylori. *Biochemical and biophysical research communications*. 2008, 376:46-51.

21. Al-Nasiry S, Geusens N, Hanssens M, Luyten C, Pijnenborg R. The use of Alamar Blue assay for quantitative analysis of viability, migration and invasion of choriocarcinoma cells. *Human reproduction*. 2007, 22:1304-9.

22. Thompson LJ, Danon SJ, Wilson JE, O'Rourke JL, Salama NR, Falkow S. Chronic Helicobacter pylori infection with Sydney strain 1 and a newly

identified mouse-adapted strain (Sydney strain 2000) in C57BL/6 and BALB/c mice. *Infection and immunity*. 2004, 72:4668-79.

23. Ha T. Single-molecule fluorescence resonance energy transfer. *Methods*. 2001, 25:78-86.

24. Bagalkot V, Zhang L, Levy-Nissenbaum E, Jon S, Kantoff PW, Langer R. Quantum dot-aptamer conjugates for synchronous cancer imaging, therapy, and sensing of drug delivery based on bi-fluorescence resonance energy transfer. *Nano letters*. 2007, 7:3065-70.

25. Kusters JG, van Vliet AH, Kuipers EJ. Pathogenesis of Helicobacter pylori infection. *Clinical microbiology reviews*. 2006, 19:449-90.

26. Andersen LP, Rasmussen L. Helicobacter pylori–coccoid forms and biofilm formation. *FEMS Immunology & Medical Microbiology*. 2009, 56:112-5.

27. She FF, Su DH, Lin JY, Zhou LY. Virulence and potential pathogenicity of coccoid Helicobacter pylori induced by antibiotics. *World Journal of Gastroenterology*. 2001, 7:254-8.

28. Megraud F, Lamouliatte H, Boyanova L. Bactericidal effect of amoxicillin on Helicobacter pylori in an in vitro model using epithelial cells. *Antimicrobial agents and chemotherapy*. 1991, 35:869-72.

29. Canton R, de Argila CM, De Rafael L, Baquero F. Antimicrobial resistance in Helicobacter pylori. *Reviews in Medical Microbiology*. 2001, 12:47-61.

30. Schiller NL. Resistance mechanisms in an in vitro-selected amoxicillin-resistant strain of Helicobacter pylori. *Antimicrobial agents and chemotherapy*. 2006, 50:4174-6.

31. Van Zwet A, Thijs J, De Graaf B. Explanations for high rates of eradication with triple therapy using metronidazole in patients harboring metronidazole-resistant Helicobacter pylori strains. *Antimicrobial agents and chemotherapy*. 1995, 39:250-2.

32. Weel J, Van Der Hulst R, Gerrits Y, Tytgat G, Van Der Ende A, Dankert J. Heterogeneity in susceptibility to metronidazole among Helicobacter pylori isolates from patients with gastritis or peptic ulcer disease. *Journal of clinical microbiology*. 1996, 34:2158-62.

33. Sun CQ, O'Connor CJ, Roberton AM. Antibacterial actions of fatty acids and monoglycerides against Helicobacter pylori. *FEMS Immunology & Medical Microbiology*. 2003, 36:9-17.

34. Knapp HR, Melly MA. Bactericidal effects of polyunsaturated fatty acids. *Journal of Infectious Diseases*. 1986, 154:84-94.

35. Lai SK, Wang Y-Y, Hanes J. Mucus-penetrating nanoparticles for drug and gene delivery to mucosal tissues. *Advanced drug delivery reviews*. 2009, 61:158-71.

36. Gao W, Chan JM, Farokhzad OC. pH-responsive nanoparticles for drug delivery. *Molecular pharmaceutics*. 2010, 7:1913-20.

37. Yang M, Lai SK, Wang YY, Zhong W, Happe C, Zhang M. Biodegradable nanoparticles composed entirely of safe materials that rapidly penetrate human mucus. *Angewandte Chemie International Edition*. 2011, 50:2597-600.

38. Lai SK, Wang Y-Y, Hida K, Cone R, Hanes J. Nanoparticles reveal that human cervicovaginal mucus is riddled with pores larger than viruses. *Proceedings of the National Academy of Sciences*. 2010, 107:598-603.

39. Tang BC, Dawson M, Lai SK, Wang Y-Y, Suk JS, Yang M. Biodegradable polymer nanoparticles that rapidly penetrate the human mucus barrier. *Proceedings of the National Academy of Sciences*. 2009, 106:19268-73.

# Chapter 3

## *Helicobacter pylori* Treatment with Liposomal Linolenic Acid *in vivo*

## 3.1 Introduction

*Helicobacter pylori* (*H. pylori*) are the most common bacterial pathogens in the world, infecting over half of the world's population [1, 2]. *H. pylori* infection is responsible for most cases of inflammatory gastritis, peptic ulcer disease, and gastric cancer in the human population [3].Worldwide, the standard treatment of *H. pylori* infection involves two antibiotics (clarithromycin plus amoxicillin or metronidazole) and a proton pump inhibitor, termed triple therapy, which remains the first-line of treatment [4]. However, *H. pylori* eradication rates with triple therapy have significantly decreased varying from 60 to 75% as a result of an increase in emergence of *H. pylori* resistant strains to these antibiotics [5]. Specifically, resistance prevalence of *H. pylori* to metronidazole, which is a key component of the triple-therapy regimen, has increased to approximately 40% in developed countries with even higher prevalence of approximately 90% in developing countries [6]. Although a variety of modified antibiotic regimens aimed to overcome drug resistance are under investigation, they have only shown mixed results [7]. Furthermore, poor patient compliance, adverse side effects, and high cost associated with multiple antibiotics frequently lead to therapy failure [8]. Clearly, new anti-*H. pylori* treatments with both superior therapeutic efficacy and negligible adverse side effects are urgently needed.

Various free fatty acids (FFAs), including lauric acid, myristoleic acid, linoleic acid, and linolenic acid (LLA) with antibacterial activities against a broad range of bacteria including *H. pylori* have recently generated research interest [9, 10]. Intriguingly, when compared to conventional antibiotics, FFAs induce drug resistance in *H. pylori*

at a much lower frequency [11]. In addition, these lipid-like molecules are omnipresent and as such considered safe. Although promising, inhibition of *H. pylori* with FFAs continues to be challenging. Specifically, the majority of medium-chain FFAs effective against *H. pylori* are poorly soluble. Their solubility is further decreased following the oral administration caused by the carboxyl protonation under gastric pH, making these molecules ineffective. Additionally, due to the fact that FFAs are subject to oxidation, esterification, and lipid–protein complexation, further reduces their bactericidal activity in vivo [9].

Use of nanotechnology in which nanosized FFA-loaded liposomes are formulated overcomes the aforementioned challenges. Especially, the amphiphilic properties of FFAs allow for direct incorporation into the hydrophobic membrane of the liposome and thereby achieve a high loading yield [12] and at the same time protect FFAs from degradation. Among various liposomal formulations, liposomal linolenic acid (LipoLLA) has shown significantly enhanced bactericidal activity against *H. pylori* [13]. When tested with *H. pylori SS1*, a laboratory strain of the bacteria, LipoLLA showed an antibacterial efficacy comparable with free LLA pre-dissolved in organic solvent (denoted as LLA) in inhibiting both spiral and coccoid forms of the bacteria. In comparison with amoxicillin, which killed the spiral form but not the coccoid form of the bacteria, LipoLLA and LLA were able to kill both forms. Further tests multiple clinically isolated and metronidazole-resistant strains of *H. pylori*, LipoLLA eradicated all strains of bacteria regardless of their resistance status to metronidazole. Remarkably, bacteria did not develop drug resistance under the experimental

conditions when cultured with LipoLLA at various sub-bactericidal concentrations. In contrast, bacteria acquired resistance to both metronidazole and LLA when cultured with drugs at comparable concentrations. These results suggest that LipoLLA is poised to become an effective antimicrobial agent to treat *H. pylori* infection.

To fulfill the therapeutic potential of FFAs, herein, we systematically evaluate LipoLLA to treat *H. pylori* infection in vivo. By using fluorescence-labeled LipoLLA, we examined its distribution in luminal stomach lining and time-dependent retention inside the mouse stomach following oral administration. By using a mouse model of *H. pylori* infection, we evaluated the therapeutic efficacy of LipoLLA against *H. pylori* in comparison with the standard triple therapy and LLA. To assess host response to LipoLLA treatment, we also examined the levels of proinflammatory cytokines including interleukin-1β (IL-1β), IL-6, and tumor necrosis factor alpha (TNFα) during the treatment. In addition, LipoLLA toxicity in the mouse was evaluated through histological analysis of the gastric tissue and changes in body weight. The findings from this study provide a more clinically related assessments of LipoLLA as a new, effective, and safe anti-*H. pylori* agent.

## 3.2 Experimental Methods

### 3.2.1 Materials

Hydrogenated L-α-phosphatidylcholine (Egg PC), cholesterol, N-[6-[(7-nitro-2-1,3-benzoxadiazol-4-yl)amino]hexanoyl]-phytosphingosine ($C_6$NBD), and 1,2-dimyristoyl-sn-glycero-3-phosphoethanolamine-N-lissamine rhodamine B sulfonyl

(DMPE-RhB) were purchased from Avanti Polar Lipids, Inc. (Alabaster, AL). Linolenic acid (LLA) was purchased from Ultra Scientific (North Kingstown, RI). Sephadex G-75 was purchased from Fisher Scientific (Pittsburgh, PA) Brain heart infusion (BHI), Columbia broth, and agar were purchased from Becton Dickinson (Sparks, MD). All tissue culture reagents, including fetal bovine serum (FBS) and fungizone, were purchased from Life Technology (Grand Island, NY). Lactate dehydrogenase (LDH) cytotoxicity assay kit was purchased from Promega (Madison, WI). Doxycycline, phosphate buffered saline (PBS), dimethyl sulfoxide (DMSO), and glycerol were obtained from Sigma-Aldrich (St. Louis, MO).

### 3.2.2 Preparation and characterization of LLA-loaded liposomes (LipoLLA)

LipoLLA were prepared by using a standard vesicle extrusion method. Briefly, a mixture of Egg PC, cholesterol, and LLA (16 mg with a weight ratio of 6:1:3) were dissolved in 4 mL of chloroform. Then the chloroform was evaporated by blowing ultra pure nitrogen gas until a thin lipid layer formed. The film was rehydrated by adding 2 mL PBS. The mixture was vortexed for 1 min, followed by sonication for 3 min in a bath sonicator (Fisher Scientific FS30D) to produce multilamellar vesicles (MLVs). Then a Branson 450 sonifier with a Ti-probe was used to sonicate the MLVs at 20 W for 1 min to produce small unilamellar vesicles (SUVs). The liposomes were obtained by extruding the SUVs through a 100 nm pore-sized polycarbonate membrane 11 times with a mini-extruder (Avanti Polar Lipids, Alabaster, AL).

Following the extrusion, the suspension was passed through a Sephadex G75 column to remove the unloaded LLA and sterilized by filtering through a 0.22 μm filter unit (Millipore, Billerica, MA). The hydrodynamic size and surface zeta potential of the liposomes were measured by using the Malvern Zetasizer ZS (Malvern Instruments, UK). The mean diameter and zeta potential were determined through dynamic light scattering (DLS) and electrophoretic mobility measurements, respectively. All characterization measurements were repeated three times at 25°C.

### 3.2.3 *Helicobacter pylori* (*H. pylori*) culture and LipoLLA in vitro activity

*H. pylori* Sydney strain 1 (SS1) were used in the present study. The bacteria were maintained on Columbia agar supplemented with 5% laked horse blood at 37°C under microaerobic conditions (10% $CO_2$, 85% $N_2$, and 5% $O_2$), as previously described [14]. Antimicrobial activity of LipoLLA against *H. pylori* was performed as described in our previous study [13]. Briefly, bacteria were inoculated into BHI broth containing 5% FBS and cultured overnight. Prior to the harvesting, the morphology and motility of the bacteria were assessed under microscope. The bacteria were harvested by centrifugation at 5000 × g for 10 min, resuspended in fresh BHI broth, and adjusted to an optical density at 600 nm ($OD_{600}$) of 1.0, corresponding to approximately $1\times10^8$ colony forming units (CFU)/mL. A bacterial suspension containing ~$1\times10^6$ CFU bacteria was mixed with LipoLLA at various pre-determined concentrations in a 96-well plate, incubated at 37$^o$C under microaerobic conditions for

30 min, and a series of 10-fold dilutions of the bacterial suspension inoculated onto Columbia agar plates supplemented with 5% laked horse blood. The agar plates were cultured in the incubator for 4 days before enumerating the colonies.

### 3.2.4 LipoLLA fusion with *H. pylori*

The fusion between LipoLLA and *H. pylori* was examined with fluorescence microscopy. In the study, DMPE-RhB (0.5 mol%) was mixed with Egg PC, LLA, and cholesterol prior to the preparation of LipoLLA and subsequently incorporated into the bilayer membrane of LipoLLA (1 mg/mL). Then 1 mL liposome suspension was mixed with $5\times10^8$ CFU *H. pylori* (determined by $OD_{600}$ measurement, $OD_{600}$ = 1.0 corresponding to ~ $1\times10^8$ CFU/mL). After 10 min incubation, the bacteria were collected by centrifugation at 5,000 ×g for 5 min, followed by fixation with 2% glutaraldehyde in PBS at room temperature for 15 min. The bacteria were then washed and resuspended in 1 mL deionized water. For imaging, 5 μL bacterial suspension was mixed with 5 μL DAPI-containing mounting media and placed on a lysine-coated slide.

### 3.2.5 LipoLLA in vitro cytotoxicity study

The AGS gastric epithelial cell line (ATCC CRL 1739, Manassas, VA, USA) was cultured in RPMI 1640 medium supplemented with 10% heat-inactivated FBS at 37°C in a humidified 5% $CO_2$ atmosphere. For the study, $1\times10^4$ cells/well were grown in 12-well culture plates. Following an overnight culture, cells were incubated with

LLA or LipoLLA at pre-determined concentrations for 24 hours. Cell death was assessed by measuring the release of LDH into the culture medium (CytoTox, Promega Corp., Madison, WI). Untreated cells served as negative controls and the cells treated with 1% Triton X-100 served as positive controls.

### 3.2.6 Gastric retention of LipoLLA

To measure liposome retention, DMPE-RhB (0.5 mol%) was mixed with other lipid components including Egg PC, LLA, and cholesterol prior to the preparation of LipoLLA and subsequently incorporated into the bilayer membrane of LipoLLA (4 mg/mL). C57BL/6 male mice at 8 weeks of age were randomly assigned to 3 groups (n=8) to receive fluorescently labeled liposomes for 4 or 24 hours. One group of mice was left untreated as control. Each mouse in the other two groups was administered 0.3 mL fluorescently labeled liposomes intragastrically by gavage. Mice were sacrificed at the indicated times and the stomachs removed from the abdominal cavity. The stomachs were cut open along the greater curvature, the gastric content was removed, and the gastric fluid containing excess liposomes washed away. Gastric samples of three mice from each group were frozen in OCT compound for confocal imaging. Gastric samples of the remaining five mice from each group were homogenized and the homogenates centrifuged at 5,000 ×g for 10 min to remove tissues or cells debris. Supernatants were collected and measured for fluorescence intensity of liposome-bound DMPE-RhB.

### 3.2.7 Anti-H. pylori efficacy *in vivo*

All animal procedures were approved by the Animal Care Committee at the University of California, San Diego. C57BL/6 male mice at 8 weeks of age were purchased from Jackson Laboratory (Bar Harbor, ME). Each mouse received 0.3 mL of $10^9$ CFU/mL *H. pylori* in BHI broth administered intragastrically by gavage every 48 hrs repeated three times and the infection was allowed to develop for three weeks. The mice were randomly assigned to 5 treatment groups (n=8) to receive LipoLLA, LLA, triple therapy, bare liposomes, or PBS. Mice were first administered omeprazole (a proton pump inhibitor) through oral gavage at a dosage of 400 μmol/kg, followed by a lag time of 30 min before administration of the assigned treatments. LipoLLA, LLA in 5% DMSO (both at 24 mg LLA/kg), and triple therapy formulation (amoxicillin 28.5 mg/kg and clarithromycin 14.3 mg/kg) were administered through oral gavage once daily for consecutive 5 days. Liposomes without LLA and PBS served as two negative control groups. Mouse body weight was monitored during the experiment by weighing the mice daily. Forty eight hrs after the last administration, mice were sacrificed and the stomach was removed from the abdominal cavity. The stomach was cut along the greater curvature and the gastric content removed and rinsed with PBS. The stomachs were cut into three longitudinal sections and each section was weighed. The sections were used for assessment of bacterial colonization, gene expression, and histology/epithelial apoptosis.

For bacterial colonization, a gastric tissue section was suspended in 1 mL of PBS and homogenized for H. pylori recovery. The homogenate was serially diluted

and spotted onto Columbia agar plate containing Skirrow's supplement (10 μg/mL vancomycin, 5 μg/mL trimethoprim lactate, 2500 IU/L polymyxin B) (Oxiod, Hampshire, UK). The plates were then incubated at 37°C under microaerobic conditions for 5 days and bacterial colonies enumerated and adjusted for dilutions.

### 3.2.8 Quantification of inflammatory cytokines

A section of the gastric tissue stored at −80 °C in RNA-stabilizing solution was homogenized in 1 ml Trizol reagent (Invitrogen, Carlsbad, CA, USA) followed by DNase treatment (Turbo DNase, Ambion, Austin, TX, USA) for further purification of RNA samples. RNA concentration was measurement by using a NanoDrop spectrophotometer (NanoDrop Technologies, Inc., Waltham, MA, USA) and the integrity checked by electrophoresis on a 1% agarose gel. Two micrograms of RNA was reverse-transcribed into complementary DNA (cDNA) using the High-capacity cDNA Reverse Transcription kit (Applied Biosystems, Foster City, CA, USA).

Following the transcription, gene expression was determined by real-time PCR using SYBR Green dye (Eurogentec, San Diego, CA) as described in our previous studies [15, 16]. Expression of TNF-α, IL-6, IL-1β, and glyceraldehyde-3-phosphate dehydrogenase (GAPDH) was performed using the following primers: murine (m) TNFα-F, 5'- TTCCAGAACTCCAGGCGGTGC; mTNFα-R, 5'- TGAGTGTGAGGGTCTGGGCCAT; mIL-6-F, 5'- AGACAAAGCCAGAGTCCTTCAGAGA; IL-6-R, 5'- GCCACTCCTTCTGTGACTCCAGC; IL-1β-F, 5'-

AAAAGCCTCGTGCTGTCGGACC; IL-1β-R, 5'-TTGAGGCCCAAGGCCACAGGT; GAPDH-F, 5'-TCAACAGCAACTCCCACTCTTCCA; GAPDH-R, 5'-ACCCTGTTGCTGTAGCCGTATTCA. Real-time PCR conditions consisted of initial 1 cycle at 95$^{o}$C for 5 minutes, followed by 40 cycles of amplification with denaturation at 95$^{o}$C for 15 seconds, annealing at 60$^{o}$C for 20 seconds, and extension at 72$^{o}$C for 40 seconds. A melting curve was generated at for each sample the end of the reaction to ensure specificity. Gene expression levels were normalized to GAPDH, and the data analyzed using a comparative cycle threshold calculations ($\Delta\Delta C_T$; Applied Biosystems). Data were expressed as fold change relative to uninfected mice. Each real-time PCR experiment was run three times.

### 3.2.9 *In vivo* toxicity study

To evaluate LipoLLA toxicity in vivo, C57BL/6 male mice at 6-8 weeks of age were orally administered with 0.3 mL of 8 mg/mL LipoLLA once daily for 5 consecutive days. Mice administered with PBS were used as a negative control. Twenty-four hours after the last oral administration, the mice were sacrificed and the stomachs were removed for histological analysis. The longitudinal sections of gastric tissue were fixed in neutral-buffered 10% formalin and then embedded in paraffin. The tissue sections were stained with hematoxylin and eosin (H&E). Epithelial cell apoptosis was evaluated by the terminal deoxynucleotidyl transferase-mediated deoxyuridine triphosphate nick-end labeling (TUNEL) assay (Boehringer Mannheim, Indianapolis, IN). Sections were visualized by Hamamatsu NanoZoomer 2.0HT and

the images processed using NDP viewing software. Eight mice were used for each test group.

## 3.3 Results

### 3.3.1 LipoLLA formulation and in vitro characterization

Owing to its amphiphilic nature, LA can be readily loaded into liposomes and subsequently fuse with bacteria for antibacterial activity (Figure 3.1A). In the study, LLA, L-α-phosphatidylcholine (EggPC) and cholesterol were first mixed at a weight ratio of 3:6:1 and then extruded to formulate LipoLLA [17]. The resulting liposomes showed a hydrodynamic diameter of 105.7±0.3 nm, comparable to that of the EggPC liposomes made with EggPC and cholesterol only at a weight ratio of 9:1 (Figure 3.1B). The polydispersity index (PDI) of the bare liposomes and LipoLLA were $0.17 \pm 0.01$ and $0.18 \pm 0.01$ respectively, indicating the relatively narrow distribution of liposome sizes. Meanwhile, the surface zeta potential of EggPC liposome was $-8.7 \pm 0.1$ mV in deionized water, whereas the zeta potential of LipoLLA was $-54.9 \pm 1.0$ mV. Such sharp decrease of the surface zeta potential indicates the incorporation of LLA into the lipid bilayers, where the carboxylic acid group is deprotonated to $COO^-$ at near physiological pH of 7.4.

The LipoLLA formulation was further examined for its fusion capability with *H. pylori* bacteria, a mechanism that disrupted the integrity of the bacterial membrane for bactericidal activity[13]. Herein, LipoLLA was labeled with the lipophilic 1,2-dimyristoyl-snglycero-3-phosphoethanolamine-*N*-(lissamine rhodamine B sulfonyl)

(ammonium salt) (DMPE-RhB) fluorophore (excitation/emission = 557 nm/571 nm). Untreated bacteria, used as a control, only showed nucleoids stained with DAPI (blue) (Figure 3.2C). However, when the bacteria were incubated with LipoLLA containing DMPE-RhB, a strong RhB fluorescence signal surrounding the bacterial nucleoid was observed, suggesting the fusion activity had occurred (Figure 3.2D). In addition, the fluorescence signal was exclusively and evenly distributed around the bacterial nucleoids, and the image clearly reflected the characteristic spiral shape of *H. pylori* bacteria. Therefore, the microscopic observation confirms the fusion of LipoLLA with *H. pylori*.

The bactericidal activity of LipoLLA against *H. pylori* was also evaluated in vitro. Bacteria incubated in broths containing varying concentrations of LipoLLA resulted in a non-linear correlation between bacterial viability and LipoLLA concentrations, consistent with LipoLLA-*H. pylori* fusion mechanism (Figure 3.2E) [13]. For this study, we defined minimal bactericidal concentration (MBC) as the minimum concentration of the bactericidal agent required to kill 3 logs (99.9%) of the bacteria during a 30-min incubation. Accordingly, the MBC values for LipoLLA and LLA were determined to be 65 and 80 μg/mL, respectively.

Despite its strong bactericidal activity, LipoLLA showed little toxicity to AGS gastric epithelial cells, as exposure to LipoLLA at concentrations between 30 and 900 μg/mL showed no lactate dehydrogenase (LDH) release (Figure 3.2F). In contrast, exposure to the free LLA resulted in a concentration-dependent increase of LDH release. This comparison suggests the non-toxic nature of LipoLLA to normal cells.

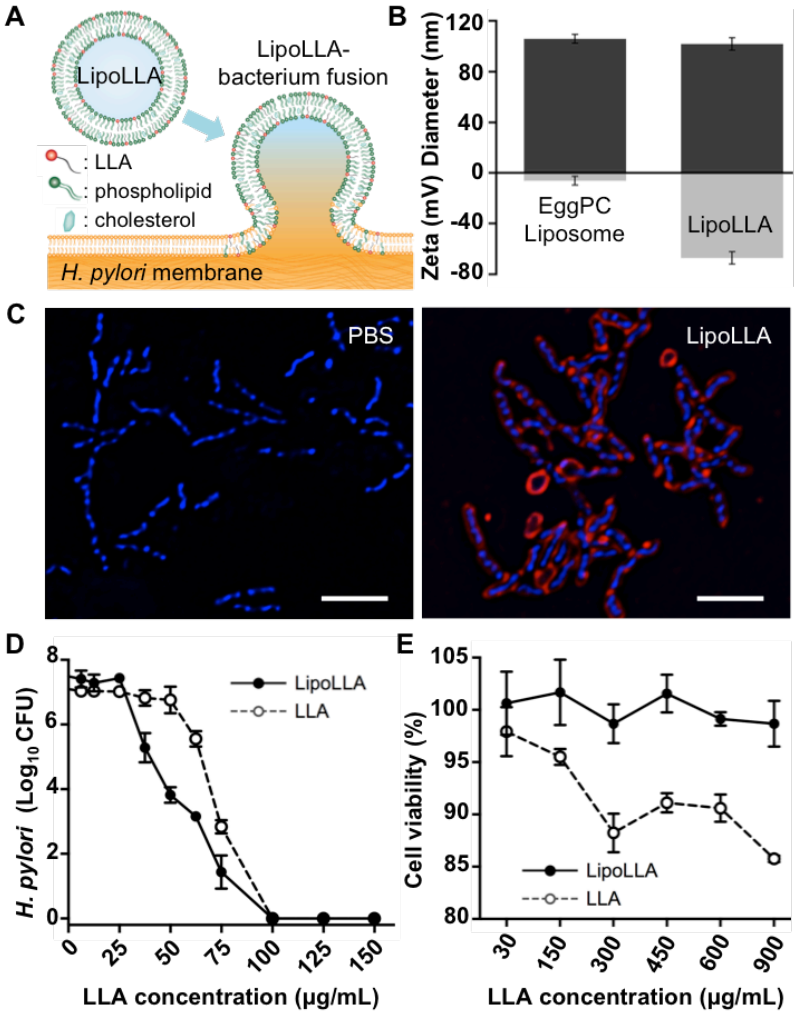


**Figure 3.1** LipoLLA formulation and in vitro characterization. (A) Structure and composition of LipoLLA consisting of phospholipid, cholesterol and LLA. LipoLLA fuses with bacterial membrane for antibacterial activity. (B) Hydrodynamic size (diameter, nm) and surface zeta potential (mV) of EggPC liposome and LipoLLA measured with dynamic light scattering (DLS). (C) Fluorescence study of the fusion interaction between LipoLLA and *H. pylori*. Liposomes were labeled with fluorescent dye RhB (red) and the bacteria were stained with DAPI (blue). Control bacteria were added with PBS free of LLA. Scale bars represent 5 μm. (D) In vitro bactericidal activity of LipoLLA and LLA at different concentrations against *H. pylori*. (E) Viability of human AGS gastric epithelial cells when treated with LipoLLA and LLA at different drug concentrations. In (D) and (E), all concentrations refer to LLA concentration, regardless of the formulation. Error bars represent the standard deviation derived from three independent experiments.

### 3.3.2 Retention and distribution of LipoLLA in mouse stomach

*H. pylori* mainly resides within the adherent mucus layer close to the epithelial surface [18]. Therefore, for effective anti-bacterial treatment, liposome permeation across the mucus layer and its retention by the stomach are critical (Figure 3.2A). To study the retention and distribution of LipoLLA in mouse stomach, we administered the mice orally with the fluorescence-labeled LipoLLA. At 4 and 24 hours after liposome administration, the whole mouse stomach was excised and opened. Then the luminal lining was rinsed with PBS and flattened for fluorescence imaging. As a control group, gastric tissue obtained from untreated mice showed no obvious fluorescence emission (Figure 3.2B). In contrast, strong fluorescence was observed in the gastric tissue collected at 4 hours after the oral gavage, a longer time span compared to reported gastric emptying times of mice (Figure 3.2C) [19]. Hence the apparent presence of the liposomes observed here indicates effective liposome retention in the stomach lining. The image obtained at 24 hours after oral gavage also showed evidence of fluorescent signal throughout the entire stomach, even though the fluorescence intensity decreased slightly (Figure 3.2D). Further quantification of the gastric retention of LipoLLA revealed that approximately 69 μg LipoLLA was retained in the stomach 4 hours after the treatment and the amount decreased to approximately 34 μg at 24 hours after the treatment (Figure 3.2E).

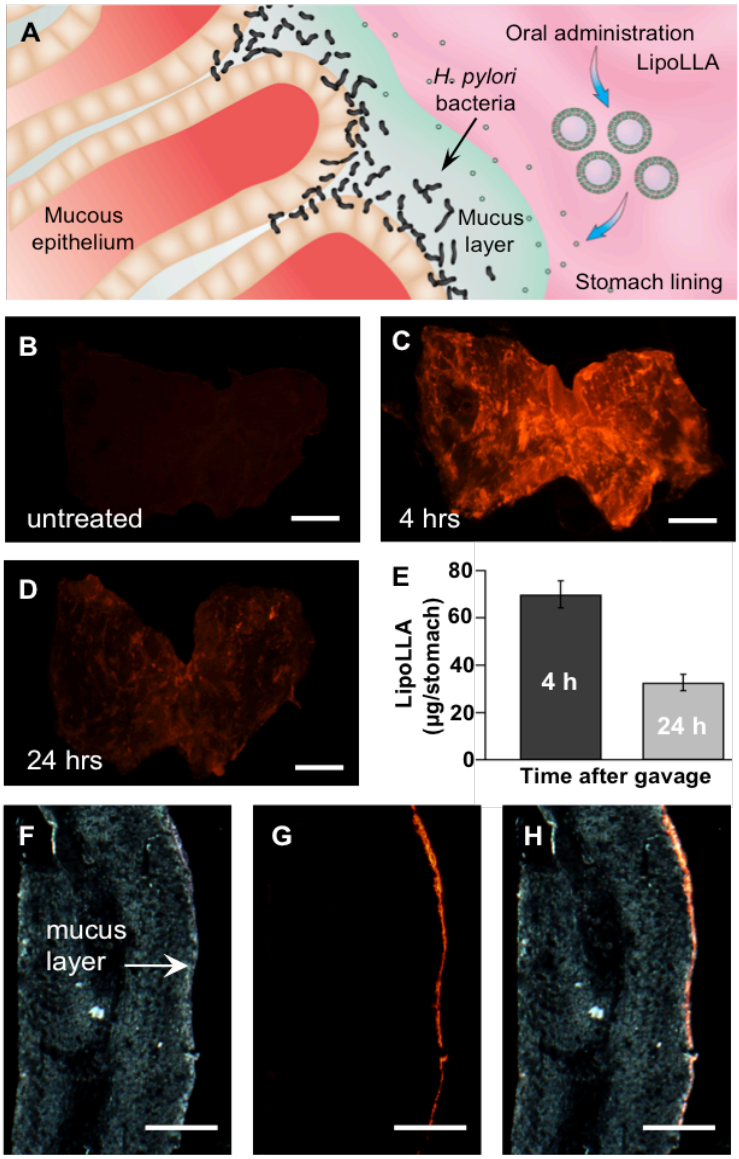


**Figure 3.2** Retention and distribution of LipoLLA in mouse stomach. (A) Anatomic illustration of stomach lining infected by *H. pylori*. (B-D) Fluorescence images of LipoLLA from the luminal lining of freshly excised mouse stomach at 0 (untreated), 4, and 24 hours after oral gavage, respectively. (E) Quantification of LipoLLA retained in the mouse stomach 4 and 24 hours after oral gavage. (F-H) Bright field, fluorescence, and overlay images of a transverse cryosection of a mouse stomach collected 4 hours after the oral gavage. All images are representative of n = 3 mice and the retention is quantified as liposomes per stomach ± SD. The scale bars represent 5 mm in (B-D) and 1 mm in (F-H).

We further studied the LipoLLA tissue distribution by examining the transverse cryosections of mouse stomach collected 4 hours after the oral gavage. The bright field image shows the mucus as a thin layer on the luminal side of the stomach (Figure 3.2F). The fluorescence image obtained from the same sample shows a continuous thin layer of LipoLLA also on the luminal side of the cryosection (Figure 2G). Overlay of the fluorescence image with the bright field image reveals a precise colocalization of the two, therefore confirming the diffusion of LipoLLA toward the gastric epithelium and its retention in the mucus layer (Figure 3.2H).

### 3.3.3 Anti-*H. pylori* efficacy *in vivo*

Next, we sought to evaluate the *in vivo* efficacy of LipoLLA against *H. pylori*. To establish the *H. pylori* infection model, we infected each C57BL/6 mouse with $3\times10^8$ CFU *H. pylori* SS1 in BHI broth by oral gavage three times at 2-day intervals (Figure 3.3A) [20, 21]. At two weeks post inoculation, infected mice were divided into five groups (n=8) and treated with PBS, bare liposome, triple antibiotics, LLA, and LipoLLA, respectively. Proton pump inhibitor was given to all mice 30 min prior to the administration of all formulations in order to neutralize acid in the stomach and prevent potential drug degradation.

In the study, therapeutic efficacy was evaluated by enumerating and comparing *H. pylori* counts in mouse stomach. Following the treatment, quantification of bacterial burden in the mouse stomach showed $1.6 \times 10^8$ and $1.0 \times 10^8$ CFU/g for the two negative control groups treated with PBS and bare liposomes, respectively (Figure

3.3B). Mice treated with triple therapy antibiotics as a positive control showed a bacterial burden of $7.2 \times 10^5$ CFU/g, a significant reduction compared to negative controls. For the mice treated with LLA pre-dissolved in DMSO, a bacterial burden of $7.5 \times 10^6$ CFU/g was quantified. The insignificant decrease of bacterial count in LLA-treated mice compared to the two negative control groups suggests the ineffectiveness of LLA in vivo against *H. pylori* infection. In contrast, when the mice were treated with LipoLLA, the bacterial burden was assessed to be $5.5 \times 10^4$ CFU/g, a significant reduction compared with all other treatment groups. Particularly, LipoLLA reduced *H. pylori* burden in mice compared to the negative controls by approximately 2.5 orders of magnitude whereas triple therapy antibiotics only reduced it by approximately 1.4 orders of magnitude. The superior efficacy observed with LipoLLA demonstrated its significant potential as an effective anti-*H. pylori* agent.

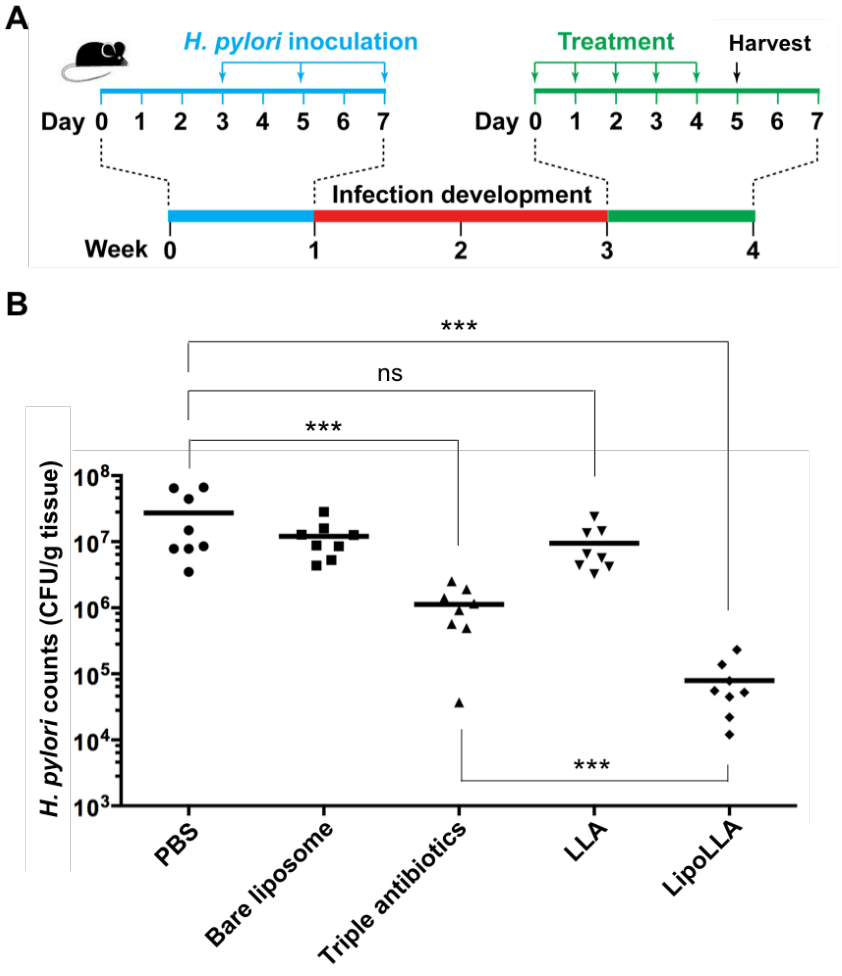


**Figure 3.3** Anti-*H. pylori* efficacy in vivo. (A) The study protocol includes *H. pylori* inoculation and infection development in C57BL/6 mice, followed by the treatments. (B) Quantification of bacterial burden in the stomach of mice treated with PBS, bare liposome, triple antibiotics, LLA, and LipoLLA, respectively. Bars represent median values. *$P < 0.05$, **$P < 0.001$, ***$P < 0.0001$.

### 3.3.4 Proinflammatory response to LipoLLA treatment

The *in vivo* acute toxicity of LipoLLA was evaluated by examining changes in the local immune response using real-time polymerase chain reaction (RT-PCR). We focused on expression of cytokines including interleukin 1β (IL-1β), IL-6, and tumor

necrosis factor alpha (TNFα), which are known to be upregulated during infection with *H. pylori* [14, 22]. A section of the gastric tissue obtained from each mouse was used to analyze the effect of LipoLLA on host immune response by real-time PCR. As shown in Figure 3.4, *H. pylori* infection resulted in upregulation of IL-1β, IL-6, and TNFα as reported in previous studies [14, 22]. However, when infected mice were treated with LipoLLA, mRNA expression of these proinflammatory cytokines was significantly reduced ($P < 0.001$), indicating that no acute toxicity was found in response to treatment with LipoLLA. In addition, these results indicate that LipoLLA had a dampening effect on the assessed proinflammatory cytokines in response to *H. pylori* infection.

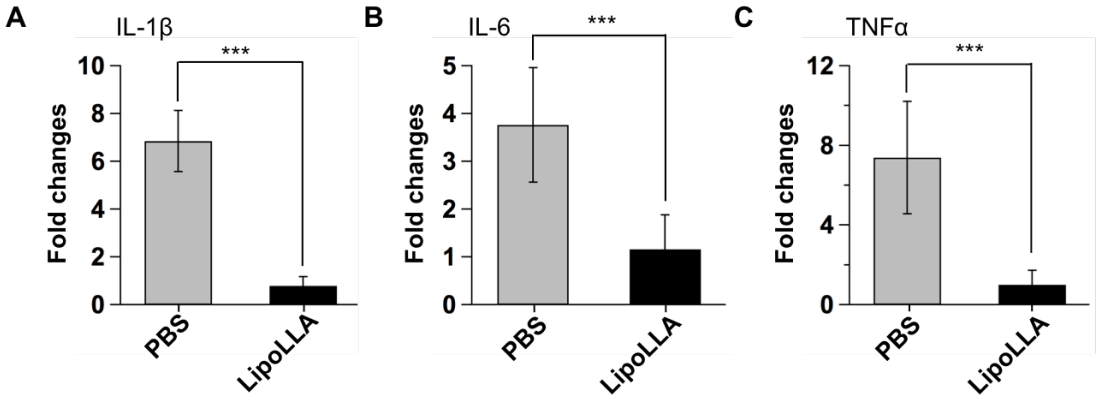


**Figure 3.4** Proinflammatory cytokine production. Comparison of the proinflammatory cytokine IL-1β, IL-6, and TNFα expression levels in from *H. pylori*-infected C57BL/6 mice following the treatment with LLA and LipoLLA, respectively. Data are expressed as fold change relative to uninfected mice. . Error bars represent the standard deviation derived from 8 mice. *$P < 0.05$, **$P < 0.001$, ***$P < 0.0001$.

### 3.3.5 LipoLLA toxicity evaluation *in vivo*

Lastly, we evaluated the toxicity of LipoLLA by using uninfected mice. In the study, mice were orally administered with PBS buffer or LipoLLA once daily for five consecutive days. Mice administered with LipoLLA maintained the same body weight compared to the mice administered with PBS (Figure 3.5A). In the 5-day period, all the mice showed no obvious weight change. In the $6^{th}$ day, all the mice were sacrificed. The longitudinal sections of gastric tissues obtained from mice were collected and stained with hematoxylin and eosin (H&E). The gastric tissues treated with LipoLLA maintained an undisturbed structure with a clear layer of epithelial cells, which was similar to the gastric samples treated with PBS (Figure 3.5 B and C). The LipoLLA toxicity was further evaluated using gastric tissue sections by a terminal deoxynucleotidyl transferase-mediated deoxyuridine triphosphate nick-end labeling (TUNEL) assay to examine the level of gastric epithelial apoptosis as an indicator of gastric mucosal homeostasis [23]. Compared to the PBS control, there was no apparent increase in gastric epithelial apoptosis as indicated by TUNEL staining in LipoLLA - treated mice (Figure 3.5 D and E). The absence of any detectable gastric histopathologic changes and toxicity within a 5-day treatment suggests that orally administered LipoLLA is safe.

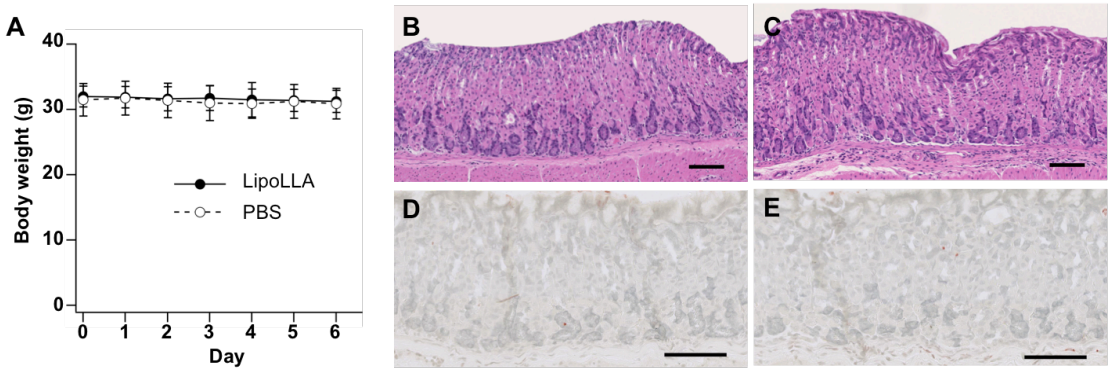


**Figure 3.5** Evaluation of LipoLLA in vivo toxicity. Uninfected mice were orally administered with PBS buffer (B and D) and LipoLLA (C and E), respectively, once daily for 5 consecutive days. (A) Mice administered with LipoLLA maintained the same body weight compared to the mice with PBS. All the mice showed no obvious weight change. (B-E) In the 6th day, mice were sacrificed and sections of the mouse stomach were processed as described in materials and methods and stained with H&E (B and C) or TUNEL (D and E). The scale bars represent 100 μm.

***Statistical analysis***

Data are represented as mean ± standard deviation. A two-tailed Student's *t* test was used to compare two samples. A *P* value of $< 0.05$ was considered statistically significant.

## 3.4 Discussion

In the present study, we evaluated the anti-*H. pylori* efficacy of LipoLLA on a mouse model. Our results demonstrated a significantly improved antimicrobial efficacy of LipoLLA in reducing *H. pylori* bacterial load in a mouse stomach when compared to other treatment regimens including the current worldwide standard treatment of *H. pylori*, triple therapy. Unsaturated fatty acids have been shown to

inhibit *H. pylori in vitro* [11, 24, 25]. However, *in vivo* killing of *H. pylori* has been a challenge until now as also demonstrated by lack of *H. pylori* killing when mice were treated with free LLA in the present study.

To address the increasing challenges in treating *H. pylori* infection, nanotechnology has offered a range of innovative approaches. In particular, a plethora of nanoparticle platforms have been developed, primarily focused on altering the pharmacokinetics of the antibiotics for enhanced potency [26, 27]. Some platforms concurrently encapsulate multiple antibiotics [28], some offer mucoadhesion for prolonged drug retention [29], some are conjugated with bacterium-binding ligand for targeted delivery [30], and some respond to pH gradient between gastric lumen and the adherent mucosal layer for on-site drug delivery [31]. Although promising, these strategies all rely on the conventional antibiotic payloads for bioactivity. Inevitably, they inherit a high susceptibility for drug resistance.

Compared to conventional antibiotics, the superior anti-*H. pylori* activity conferred by LipoLLA can be explained by the unique capability of LipoLLA to fuse rapidly with bacterial membrane and subsequently disrupt membrane integrity, a highly destructive mechanism for bacterial killing with a low susceptibility for resistance development [13]. This mechanism is supported by the sharp decrease in viable bacteria at the MBC values and a killing time no longer than 30 min, relatively short when compared to 2.5 h needed for *H. pylori* to complete a replication cycle [9]. The fusion mechanism is further supported by the microscopic observation, where LipoLLA exclusively distributed throughout the bacterial membrane (Figure 1C). For

in vivo applications, this working mechanism is further ensured by a liposome formulation, where the liposome bilayers protect LLA molecules from the damaging environment of stomach and prevent potential oxidation and enzyme degradation [12, 13].

In this study, LipoLLA also shows promise in targeting gastric mucosal layer for prolonged retention and effective anti-*H. pylori* activity. Herein, we showed that LipoLLA accumulated within the mucus layer and a significant portion was retained for up to 24 hours. The distinct host environment of *H. pylori* is marked by limited drug permeation and retention. However, plenty of nanoparticles, both natural and man-made ones, have shown remarkable capabilities to transport across the mucus mesh for possible entry to the underlying epithelia and prolonged residence time in mucus layer [32, 33]. A comparison of LipoLLA to various mucus-penetrating nanoparticles suggests that a relatively small size of LipoLLA, approximately 100 nm in diameter with a narrow distribution, together with a dense anionic surface charge that minimizes hydrophobic entrapment to mucus, is attributable to the effective LipoLLA retention by gastric mucus [34]. Studies on nanoparticle mucosal transport have also revealed the critical roles played by particle surface chemistry. For example, an equal density of positive and negative charges may be desirable for efficient mucus penetration by minimizing the electrostatic adhesive interactions between particles and mucus. This formulation optimization is currently underway to further improve on the anti-*H.pylori* efficacy of LipoLLA.

In addition to the better efficacy of LipoLLA compared to the commonly used standard triple therapy, our data also show that LipoLLA is safe. Treatment with LipoLLA had no effect on mouse body weight, gastric histopathology, and gastric mucosal integrity. In addition, treatment of mice with LipoLLA did not elicit the host immune response. Interestingly, mice treated with LipoLLA had significantly reduced *H. pylori*-induced proinflammatory cytokines compared to *H. pylori*-infected but untreated mice. Unsaturated fatty acids are reported to play a role in gastric mucosal protection through various pathways including increased synthesis in prostaglandins [35, 36]. The precise mechanism of the reduced expression of inflammatory cytokines is under our current investigation.

## 3.5 Conclusions

In this study, we evaluated the in vivo therapeutic potential of liposomal linolenic acids (LipoLLA) for the treatment of *H. pylori* infection. The formulations of LipoLLA with a size of approximately 100 nm and a surface zeta potential of -54 mV were prone to fuse with bacterial membranes, thereby directly releasing a high dose of linolenic acids into the membranes. LipoLLA penetrated the mucus layer of mouse stomach, and a significant portion was retained in the stomach lining 24 hours after the oral administration. In vivo tests confirmed that LipoLLA were able to kill *H. pylori* and reduce bacterial load in the mouse stomach. The LipoLLA treatment also reduced the levels of proinflammatory cytokines including IL-1β, IL-6, and TNF-α, which

were otherwise elevated in response to *H. pylori* infection. Lastly, toxicity test demonstrated excellent biocompatibility of LipoLLA to normal mouse stomach. Overall, the results from this work indicate that LipoLLA is promising as a new, effective and safe therapeutic agent for the treatment of *H. pylori* infection.

Chapter 3, in full, is in a manuscript submitted to Sciences Translational Medicine, 2014, Soracha Thamphiwatana, Weiwei Gao, Marygorret Obonyo, and Liangfang Zhang, and, The dissertation author was the primary investigator and author of this paper.

## 3.6 References


1. De Francesco V, Giorgio F, Hassan C, Manes G, Vannella L, Panella C. Worldwide H. pylori Antibiotic Resistance: a Systematic Review. *J Gastrointest Liver*. 2010, 19:409-14.

2. McColl KEL. Helicobacter pylori Infection. *New Engl J Med*. 2010, 362:1597-604.

3. Coussens LM, Werb Z. Inflammation and cancer. *Nature*. 2002, 420:860-7.

4. Urgesi R, Cianci R, Riccioni ME. Update on triple therapy for eradication of Helicobacter pylori: current status of the art. *Clin Exp Gastroenterol*. 2012, 5:151-7.

5. Megraud F. H pylori antibiotic resistance: prevalence, importance, and advances in testing. *Gut*. 2004, 53:1374-84.

6. Kaakoush NO, Asencio C, Megraud F, Mendz GL. A Redox Basis for Metronidazole Resistance in Helicobacter pylori. *Antimicrob Agents Chemother*. 2009, 53:1884-91.

7. Suerbaum S, Michetti P. Medical progress: Helicobacter pylori infection. *New Engl J Med*. 2002, 347:1175-86.

8. O'Connor A, Molina-Infante J, Gisbert JP, O'Morain C. Treatment of Helicobacter pylori Infection 2013. *Helicobacter*. 2013, 18:58-65.

9. Desbois AP, Smith VJ. Antibacterial free fatty acids: activities, mechanisms of action and biotechnological potential. *Appl Microbiol Biotechnol*. 2010, 85:1629-42.

10. Jarboe LR, Royce LA, Liu P. Understanding biocatalyst inhibition by carboxylic acids. *Front Microbiol*. 2013, 4.

11. Petschow BW, Batema RP, Ford LL. Susceptibility of Helicobacter pylori to bactericidal properties of medium-chain monoglycerides and free fatty acids. *Antimicrob Agents Chemother*. 1996, 40:302-6.

12. Prajapati HN, Dalrymple DM, Serajuddin ATM. A Comparative Evaluation of Mono-, Di- and Triglyceride of Medium Chain Fatty Acids by Lipid/Surfactant/Water Phase Diagram, Solubility Determination and Dispersion Testing for Application in Pharmaceutical Dosage Form Development. *Pharm Res*. 2012, 29:285-305.

13. Obonyo M, Zhang L, Thamphiwatana S, Pornpattananangkul D, Fu V, Zhang L. Antibacterial Activities of Liposomal Linolenic Acids against Antibiotic-Resistant Helicobacter pylori. *Mol Pharm*. 2012, 9:2677-85.

14. Obonyo M, Sabet M, Cole SP, Ebmeyer J, Uematsu S, Akira S. Deficiencies of myeloid differentiation factor 88, toll-like receptor 2 (TLR2), or TLR4 produce specific defects in macrophage cytokine secretion induced by Helicobacter pylori. *Infect Immun*. 2007, 75:2408-14.

15. Banerjee A, Thamphiwatana S, Carmona EM, Rickman B, Doran KS, Obonyo M. Deficiency of the Myeloid Differentiation Primary Response Molecule MyD88 Leads to an Early and Rapid Development of Helicobacter-Induced Gastric Malignancy. *Infect Immun*. 2014, 82:356-63.

16. Obonyo M, Rickman B, Guiney DG. Effects of Myeloid Differentiation Primary Response Gene 88 (MyD88) Activation on Helicobacter Infection In Vivo and Induction of a Th17 Response. *Helicobacter*. 2011, 16:398-404.

17. Huang C-M, Chen C-H, Pornpattananangkul D, Zhang L, Chan M, Hsieh M-F. Eradication of drug resistant Staphylococcus aureus by liposomal oleic acids. *Biomaterials*. 2011, 32:214-21.

18. Schreiber S, Konradt M, Groll C, Scheid P, Hanauer G, Werling HO. The spatial orientation of Helicobacter pylori in the gastric mucus. *Proc Natl Acad Sci U S A*. 2004, 101:5024-9.

19. Bennink RJ, de Jonge WJ, Symonds EL, van den Wijngaard RM, Spijkerboer AL, Benninga MA. Validation of gastric-emptying scintigraphy of solids and liquids in mice using dedicated animal pinhole scintigraphy. *J Nucl Med*. 2003, 44:1099-104.

20. Obonyo M, Guiney DG, Harwood J, Fierer J, Cole SP. Role of gamma interferon in Helicobacter pylori induction of inflammatory mediators during murine infection. *Infect Immun*. 2002, 70:3295-9.

21. Hase K, Murakami M, Iimura M, Cole SP, Horibe Y, Ohtake T. Expression of LL-37 by human gastric epithelial cells as a potential host defense mechanism against Helicobacter pylori. *Gastroenterology*. 2003, 125:1613-25.

22. Rad R, Brenner L, Krug A, Voland P, Mages J, Lang R. Toll-like receptor-dependent activation of antigen-presenting cells affects adaptive immunity to Helicobacter pylori. *Gastroenterology*. 2007, 133:150-63.

23. Que FG, Gores GJ. Cell death ky apoptosis: Basic concepts and disease relevance for the gastroenterologist. *Gastroenterology*. 1996, 110:1238-43.

24. Khulusi S, Ahmed HA, Patel P, Mendall MA, Northfield TC. The effects of unsaturated fatty-acids on *Helicobacter pylori in vitro*. *J Med Microbiol*. 1995, 42:276-82.

25. Gaby AR. Helicobacter pylori eradication: are there alternatives to antibiotics? *Altern Med Rev*. 2001, 6:355-66.

26. Zhang L, Pornpattananangkul D, Hu CMJ, Huang CM. Development of Nanoparticles for Antimicrobial Drug Delivery. *Curr Med Chem*. 2010, 17:585-94.

27. Gao W, Hu C-MJ, Fang RH, Zhang L. Liposome-like nanostructures for drug delivery. *J Mater Chem B*. 2013, 1:6569-85.

28. Ramteke S, Jain NK. Clarithromycin- and omeprazole-containing gliadin nanoparticles for the treatment of Helicobacter pylori. *J Drug Targeting*. 2008, 16:65-72.

29. Umamaheshwari RB, Ramteke S, Jain NK. Anti-Helicobacter pylori effect of mucoadhesive nanoparticles bearing amoxicillin in experimental gerbils model. *AAPS Pharmscitech*. 2004, 5.

30. Ramteke S, Ganesh N, Bhattacharya S, Jain NK. Triple therapy-based targeted nanoparticles for the treatment of Helicobacter pylori. *J Drug Targeting*. 2008, 16:694-705.

31. Lin Y-H, Chang C-H, Wu Y-S, Hsu Y-M, Chiou S-F, Chen Y-J. Development of pH-responsive chitosan/heparin nanoparticles for stomach-specific anti-Helicobacter pylori therapy. *Biomaterials*. 2009, 30:3332-42.

32. Olmsted SS, Padgett JL, Yudin AI, Whaley KJ, Moench TR, Cone RA. Diffusion of macromolecules and virus-like particles in human cervical mucus. *Biophys J*. 2001, 81:1930-7.

33. Nance EA, Woodworth GF, Sailor KA, Shih T-Y, Xu Q, Swaminathan G. A Dense Poly(Ethylene Glycol) Coating Improves Penetration of Large Polymeric Nanoparticles Within Brain Tissue. *SciTransl Med*. 2012, 4.

34. Lai SK, Wang Y-Y, Hanes J. Mucus-penetrating nanoparticles for drug and gene delivery to mucosal tissues. *Adv Drug Del Rev*. 2009, 61:158-71.

35. Das UN, Begin ME, Ells G. Fatty-acid changes during the induction of differentiation of human promyelocytic leukemia (HL-60) cells by phorbolmyristate acetate. *Prostaglandins Leukot Essent Fatty Acids*. 1992, 46:235-9.

36. Das UN. Essential fatty acids and their metabolites as modulators of stem cell biology with reference to inflammation, cancer, and metastasis. *Cancer Metastasis Rev*. 2011, 30:311-24.

# Chapter 4

## Stimuli-Responsive Liposomes

# 4.1 pH-Responsive Liposomes

## 4.1.1 Introduction

Liposomes have been studied extensively as antimicrobial delivery vehicles mainly because of their unique features, including highly biocompatible lipid materials, unique bilayer structure that can fuse with bacterial membranes, high drug carrying capacity, and readily tunable formulation properties.[1-4] Despite these advantageous features, the applications of liposomes, particularly those with sizes below 100 nm, are often limited by poor stability due to spontaneous fusion among liposomes, causing payload loss and undesired mixing.[5-7] A widely applied approach to stabilize liposomes is to coat their surface with a stealth material such as polyethylene glycol (PEG). The PEG coating reduces the tendency of liposomes to aggregate and fuse with each other through steric stabilization. It also suppresses non-specific interactions of liposomes with blood components (opsonization) for enhanced blood residency time.[8-10] As a result, PEGylated liposomes have found great applications in systemic drug delivery.[11, 12] However, PEGylated liposomes are rarely used for antimicrobial delivery to treat bacterial infections. This is mainly because the polymer coating not only stabilizes liposomes against fusion with each other but also prevents them from fusing with bacterial membranes, to which the antimicrobial payloads need to be delivered.[13-15] Therefore, it would be ideal to engineer advanced liposomal formulations that are stabilized against fusion prior to 'seeing' target bacteria, while their fusion activity resumes once they arrive at the infection sites.

An emerging strategy to stabilize liposomes for effective antimicrobial delivery is to bind tiny charged nanoparticles to liposome surfaces. The non-specific adsorption of charged nanoparticles onto phospholipid bilayers provide steric repulsion that inhibits liposomes from approaching each other and then fusing to form larger vesicles.[16] In addition, the nanoparticle stabilizers are found to cause lipid surface reconstruction at the points where nanoparticles adsorb. Such surface reconstruction reduces liposome surface tension and further enhances liposome stability.[17] More interestingly, stabilization by small nanoparticles leaves a substantial fraction of the liposome surfaces untouched, making it possible to incorporate additional functionalities to the liposomes and allowing for controlled cargo releases.[6, 18] For instance, it has been shown that the uncoated liposome surfaces are highly accessible to bacterial toxins, which can punch holes on the liposomes to release encapsulated drugs at the infectious sites.[6] Furthermore, the charge and charge density of both the nanoparticle stabilizers and the liposomes can be precisely tailored to enable stimulus-responsive binding and detaching of the nanoparticles, thereby allowing an on-demand control over liposome fusion activity for smart cargo delivery.[14] The objective of this study is to develop a unique and robust nanoparticle-stabilized liposome system for gastric antimicrobial delivery with a particular interest in antibiotic delivery to treat *Helicobacter pylori* (*H. pylori*) infection in the stomach.

*H. pylori* infects about half of the people in the world and is of major public health concern. Infection with *H. pylori* is the main cause of chronic gastritis, peptic ulcers, and gastric malignancy.[19-21] However, eradication of *H. pylori* is challenging

regardless of the treatment regimens, partially because the bacteria locate in the stomach mucus lining, which requires drugs to tolerate the highly acidic gastric environment.[22, 23] Herein, we report a novel pH-responsive gold nanoparticle-stabilized liposome system in which small gold nanoparticles (diameter: ~ 10 nm) bind to the surface of liposomes (diameter: ~ 75 nm) and thus stabilize the liposomes at acidic pH values (i.e., gastric pH). These gold stabilizers will detach from the liposomes when the environmental acidity decreases to near neutral value (i.e. pH = 7.4). The resulting free liposomes can then actively fuse with target bacterial membrane. This would be an ideal delivery platform for drug delivery to mucus lining in the stomach for the treatment of *H. pylori* infection. It has been well documented that the pH values in the mucus layer of stomach gradually increase from 1.2 at the gastric lumen side to near 7.4 at the mucus lining, where the *H. pylori* bacteria reside.[22-25]

As shown in the Figure 4.1.1, the gold nanoparticles are surface modified with chitosan (p*K*a ≈ 6), denoted as AuChi, which exhibit a strong positive charge at gastric pH but are deprotonated at neutral pH.[26] The liposomes are comprised of hydrogenated L-aphosphatidylcholine (Egg PC) and 1,2-dioleoyl-*sn*-glycero-3-phosphate (sodium salt) (DOPA), a phospholipid with strong negative charge during the pH range of 1.2 to 7.4.[27, 28] We demonstrate that under gastric pH AuChi tightly bind to the liposome surfaces, thereby effectively inhibiting drug release and liposome fusion with *H. pylori* bacteria. Once the pH level is increased to neutral pH, AuChi detach from the liposomes. The resulting free liposomes can rapidly fuse with the

bacterial membranes of *H. pylori*, release the encapsulated antibiotics, and kill the bacteria with a superior efficacy as compared to the free antibiotic counterpart.

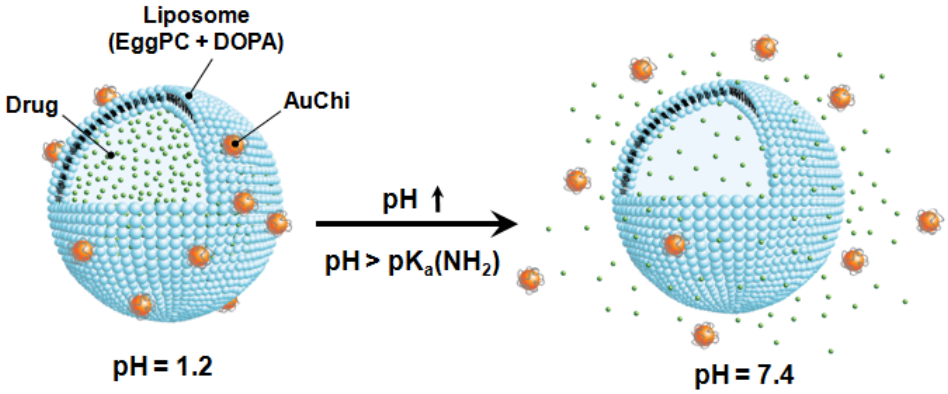


**Figure 4.1.1** Schematic illustration of a phospholipid liposome stabilized by chitosan-modified gold nanoparticles (AuChi-liposome) for pH-responsive gastric drug delivery. At gastric pH (pH = 1.2), the liposome is stabilized by binding of protonated AuChi nanoparticles. At physiological condition (pH = 7.4), AuChi nanoparticles are deprotonated and thus detach from the liposome, resulting in bare liposome with restored fusion and drug release properties.

## 4.1.2 Experimental Methods

### 4.1.2.1 Materials.

Hydrogenated L-α-phosphatidylcholine (Egg PC), 1,2-dioleoyl-*sn*-glycero-3-phosphate (sodium salt) (DOPA) and 1,2-dimyristoyl-*sn*-glycero-3-phosphoethanolamine-N-lissamine rhodamine B sulfonyl (DMPE-RhB) were purchased from Avanti Polar Lipids, Inc. (Alabaster, AL). Rhodamine B and Doxycycline were purchased from Sigma Aldrich (St Louis, MO). Brain Heart Infusion (BHI) broth and Columbia agar were purchased from Becton Dickinson

(Sparks, MD). Hydrogen tetrachloroaurate ($HAuCl_4$) and sodium borohydride ($NaBH_4$) were purchased from ACROS Organics (Geel, Belgium). Chitosan-50 was purchased from Wako Pure Chemical Industries, Ltd. (Osaka, Japan).

### 4.1.2.2 AuChi Preparation and Characterization

AuChi were prepared by a sodium borohydride reduction technique as previously described.[6] Briefly, an aqueous solution of $HAuCl_4$ (0.1 mM, 50 mL) was reduced by 5 mg of $NaBH_4$ to form gold nanoparticles. To functionalize nanoparticles with chitosan, the nanoparticle suspension was incubated overnight with 0.1% w/v chitosan dissolved in 0.1 M acetic acid. Following the reaction, the AuChi nanoparticle suspension was washed three times by using an Amicon Ultra-4 centrifugal filter with a molecular weight cutoff of 10 kDa (Millipore, Billerica, MA). The hydrodynamic size, size distribution, and surface charge of AuChi nanoparticles were characterized by dynamic light scattering (DLS) (Malvern Zetasizer ZS, Malvern Instruments, Worcestershire, UK).

### 4.1.2.3 Liposome preparation

Liposomes were prepared by following a previously described extrusion method.[19] Specifically, 3 mg of lipid mixture (EggPC/DOPA=80/20 wt%) were dissolved in 1 mL chloroform and the organic solvent was evaporated by blowing nitrogen gas over the solution for 15 min to form a dried lipid film. The lipid film was rehydrated with 2 mL of deionized water containing either rhodamine B (RhB) or

doxycycline at desired concentrations, followed by 1 min of vortexing and 3 min of sonication in a bath sonicator (Fisher Scientific FS30D, Pittsburgh, PA) to produce multilamellar vesicles (MLVs). Then the obtained MLVs were sonicated for 1 minute at 20 W by a titanium probe (Branson 450 sonifier, Danbury, CT) to produce unilamellar vesicles. Following the sonication, the solution was extruded through a 100 nm pore-sized polycarbonate membrane for 11 times to form narrowly distributed small unilamellar vesicles (SUVs). After the extrusion, the liposomes were purified by dialysis with a 20 kDa molecular weight cut-off to remove unencapsulated dyes or drugs.

#### 4.1.2.4 AuChi-liposome formulation

To prepare AuChi-liposome, the pH of both AuChi and liposome solutions was adjusted to 6.5 using HCl. Then the liposomes and AuChi at desired molar ratio were mixed together, followed by 12 hr of vortexing. To quantify the adsorption of AuChi nanoparticles onto liposomes, RhB-labeled liposomes were prepared by mixing 0.5 mol% of DMPE-RhB with lipid components prior to liposome preparation. Mixing AuChi nanoparticles with the fluorescent liposomes resulted in the quenching of fluorescence intensity. It was found that the quenching effect reached the maximum at an AuChi-to-liposome molar ratio of 300:1 at pH = 1.2, indicating the saturation of AuChi nanoparticles on liposome surfaces. Hydrodynamic size, size distribution, and surface charge of AuChi-liposome were characterized with DLS. To test the quenching effect at different pH values, the solution was adjusted to desired pH levels

using HCl and NaOH and measured by an Orion 3-star plus portable pH meter. The fluorescence emission spectra of RhB in the range of 550-650 nm were measured by using a fluorescent spectrophotometer (Infinite M200, TECAN, Switzerland) at an excitation wavelength of 470 nm.

### 4.1.2.5 AuChi-liposome fusion with H. pylori bacteria

A fluorescence method was used to study the fusion of AuChi-liposome with bacteria at pH = 1.2 and 7.4, respectively. Specifically, *H. pylori* Sydney strain 1 (SS1) bacteria were maintained on Columbia agar supplemented with 5% laked horse blood at 37$^{o}$C under microaerobic conditions (10% $CO_2$, 85% $N_2$, and 5% $O_2$). For experiments, broth cultures of *H. pylori* were prepared by sub-culturing fresh colonies from agar plates into BHI containing 5% fetal bovine serum (FBS) overnight at 37$^{o}$C under microaerobic conditions with moderate reciprocal shaking. Then, $5\times10^8$ CFU/mL of *H. pylori* bacteria (determined by $OD_{600}$ measurement, $OD_{600}$ = 1.0 corresponding to ~ $1\times10^8$ CFU/mL) were mixed with 0.5 mM fluorescently labeled AuChi-liposome (containing 0.5 mol% of DMPE-RhB). The solutions were adjusted to desired pH values. After 30 min incubation, the bacteria pellet was collected by centrifugation at 4,000 ×g for 5 min. After removing the supernatant, the bacteria were resuspended in 1 mL PBS and the fluorescence intensity of DMPE-RhB was measured. Bare liposomes containing the same amount of DMPE-RhB were used as controls. The experiment was carried out in triplicate and average value was reported.

### 4.1.2.6 Drug release study

Doxycycline-loaded AuChi-liposome were prepared by mixing 1 mM of doxycycline with the rehydration solution during the preparation of liposomes. The unencapsulated doxycycline molecules were then removed by dialyzing AuChi-liposome suspension for 12 hr. Then the liposome suspension was adjusted to pH = 1.2 and 7.4, respectively The samples were loaded into multiple dialysis cups with 400 μL in each and dialyzed against PBS at 37°C up to 24 hr with a frequent change of buffer solution. At each time point, three dialysis cups were collected to quantify the remaining drugs inside the liposomes. Specifcially, the liposomes remained in the cup were disrupted by adding 1% Triton X-100 and the solution was filtered with an Amicon centrifugal filter unit with a molecular weight cutoff of 100 kDa (Millipore, Billerica, MA) at 7000 rpm for 10 min. Following the centrifugation, the amount of doxycycline in filtrate was quantified by measuring absorbance at 345 nm using spectrophotometer (Infinite M200, TECAN, Switzerland). The acquired doxycycline absorbance was compared with a linear standard curve of doxycycline at different concentrations at the desired pH to calculate the amount of doxycycline released from the liposomal formulations. Doxycycline-loaded AuChi-liposome at t=0 (prior to dialysis) was used to determine the initial drug loading yield.

### 4.1.2.7 Antibacterial activity of AuChi-liposome

An overnight broth culture of *H. pylori* was centrifuged at 4000 ×g for 5 min to obtain a bacterial pellet. The pellet was washed and adjusted to an $OD_{600}$ value of 1.0,

corresponding to approximately $1\times10^8$ CFU/mL. Then 10 μL bacterial suspension containing $1\times10^6$ CFU bacteria was added to 190 μL of bacteria culture medium containing doxycycline-loaded AuChi-liposome at desired concentrations. The mixture was incubated at pH = 7.4 with gentle shaking at 37°C under microaerobic conditions. After 12 hr incubation, a series of 10-fold dilutions of the bacterial suspension (1:10 to $1:10^5$) was prepared, and 5 μL from each diluted sample was inoculated onto a Columbia agar plate supplemented with 5% laked horse blood. The plates were cultured in the incubator for 4 days before colony counting. Free doxycycline served as a positive control, while empty AuChi-liposome (without doxycycline) and PBS served as negative controls. All experiments were repeated three times.

## 4.1.3 Results and Discussion

The preparation of AuChi-stabilized liposomes, denoted as AuChi-liposome, can be divided into three steps. First, AuChi nanoparticles were synthesized by following a previously established protocol, where gold hydrosol was first made by using sodium borohydride reduction of $AuHCl_4$ and then stabilized by adding chitosan in ambient condition.[6, 29] Measurements of AuChi nanoparticles with dynamic light scattering (DLS) showed a diameter of about 10 nm with a nearly uniform size distribution (Figure 4.1.2). The electrophoretic mobility measurements with DLS showed that the surface zeta potential of AuChi was 43.4 ± 1.0 mV, a strong positive charge implying the presence of cationic amine groups of chitosan on the particle

surfaces. In the second step, liposomes consisting of Egg PC and DOPA (in a weight ratio of 80:20) were prepared by vesicle extrusion technique in deionized water at pH = 6.[30] The subsequent DLS measurements of liposomes showed a diameter of 76.1 ± 1.0 nm and a surface zeta potential of -61.1 ± 2.3 mV. The strong negative zeta potential verifies the incorporation of DOPA into the lipid bilayers as liposomes formulated without DOPA showed a similar size but a less negative zeta potential of -7.6 ± 0.4 mV.

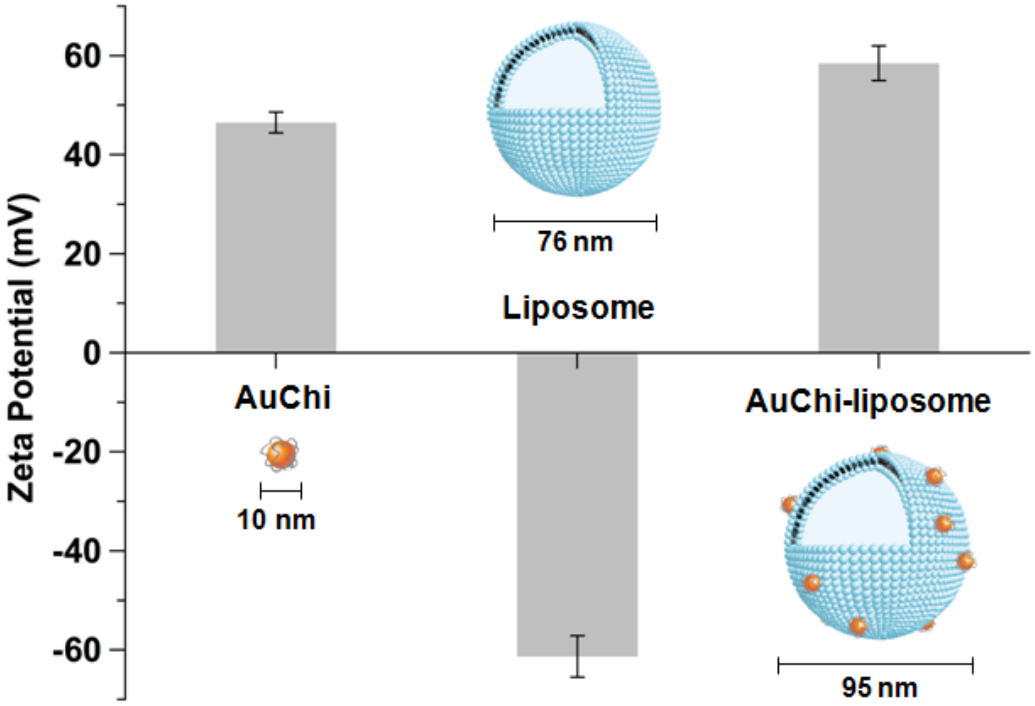


**Figure 4.1.2** The surface zeta potential and hydrodynamic size of AuChi, bare liposome (without AuChi), and AuChi-liposome with an AuChi-to-liposome molar ratio of 300:1 measured by dynamic light scattering (DLS).

Lastly, the resulting cationic AuChi nanoparticles and the anionic liposomes were mixed at a molar ratio of 300:1 under gentle bath sonication for 10 min. The pH value of the mixture solution was then adjusted to 1.2, simulating gastric pH. Following the preparation, DLS measurements showed that the AuChi-liposome had a diameter of 95.2 ± 1.3 nm and a surface zeta potential of 57.4 ± 0.7 mV. Compared to bare liposomes, the observed approximate 20 nm diameter increase of particle size is likely due to the adsorption of AuChi onto the liposome surfaces. The switch of zeta potential from -61.1 to 57.4 mV also confirms the binding of positively charged AuChi nanoparticles to the liposomes.

The formation of AuChi-liposome complex at gastric pH was first verified through a fluorescent assay based upon the distance-dependent fluorescence quenching phenomenon of gold nanoparticles.[31, 32] To this end, a fluorescence labeled lipid molecule, 1,2-dimyristoyl-*sn*-glycero-3 phosphoethanolamine-N-lissamine rhodamine B sulfonyl (DMPE-RhB, excitation/emission = 550/590 nm), was incorporated into the liposome membranes prior to the preparation of AuChi-liposome. The pH value of the AuChi-liposome suspension was then set at pH = 1.2 and 7.4, simulating the gastric pH and physiological condition, respectively, and the florescence intensity of the suspensions was monitored. As shown in Figure 4.1.3A, the fluorescence intensity at pH = 1.2 was over 5-fold lower than that at pH = 7.4, indicating that much more AuChi adsorbed on the liposome surfaces at acidic pH while they detached at neutral pH. To further verify the binding of AuChi to the anionic liposomes, the AuChi-liposome solutions at different pH values were subject

to an external centrifugal force (2000 ×*g*) for 10 min. As shown in Figure 4.1.3B, at pH = 1.2, no particle precipitate was observed and the suspension remained red, the characteristic color of gold nanoparticles. In contrast, a large amount of particle precipitates and a clear supernatant were observed at pH = 7.4. The obtained supernatant was then measured with DLS for the size and surface zeta potential, which were found to be similar to those of the corresponding bare liposomes. These results suggest that AuChi strongly bound to liposomes at acidic pH, thus inseparable from the liposomes by low centrifugal force, but they readily detached from the liposomes and precipitated from the suspension by centrifugation at neutral pH.

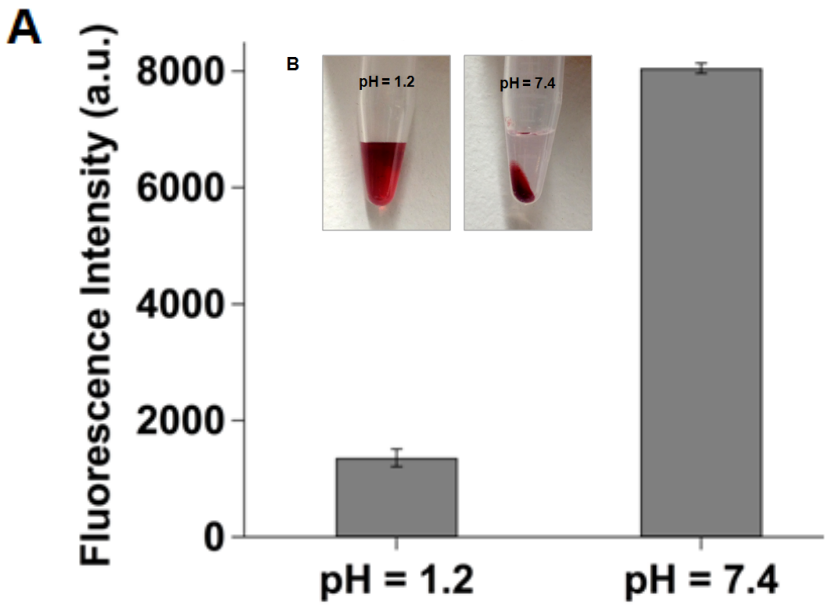


**Figure 4.1.3** (A) Fluorescence intensity of rhodamine B (RhB)-doped AuChi-liposome at pH = 1.2 and 7.4, respectively. 0.5 mol% of DMPE-RhB was incorporated into the liposome membranes prior to AuChi stabilization. The binding of AuChi on the liposome would quench the fluorescent probes within the membranes while detaching of AuChi would induce fluorescence recovery. (B-inset) AuChi-liposome solutions after centrifugation to precipitate free AuChi nanoparticles. Dark red color indicates the presence of AuChi in the solution at pH = 1.2 and the sedimentation of AuChi at pH = 7.4.

To examine the pH-responsive stability of the AuChi-liposome, we next examined their fusion ability with bacterial membranes. Fluorescence labeled AuChi-liposome (0.5 mM, containing 0.5 mol% DMPE-RhB) were prepared and mixed with *H. pylori* bacteria ($5\times10^8$ CFU/mL) at pH = 1.2 and 7.4, respectively. The mixture suspensions were incubated at 37°C for 30 min. Then the bacteria were thoroughly washed, collected and resuspended in 1× PBS (pH = 7.4). The fluorescence intensity of the bacterial suspensions was then measured to quantify the fusion ability of the liposomes. Fluorescence labeled bare liposomes (without AuChi) were tested in parallel as a control. Figure 4.1.4 shows that *H. pylori* bacteria incubated with bare liposomes had comparable fluorescence intensity at pH = 1.2 and 7.4. In contrast, a much weaker fluorescence emission was obtained from the bacteria incubated with AuChi-liposome at pH = 1.2, suggesting a significantly reduced liposome fusion with the bacteria. However, when the pH was increased from 1.2 to 7.4, AuChi-liposome resumed their fusion ability to an extent comparable to that of the bare liposomes. The observed differential fusion activity of AuChi-liposome at different pH values proves the stabilization effect conferred by the binding of AuChi nanoparticles.

We further evaluated the stability of the AuChi-liposome by examining the drug release kinetics from the liposomes at different pH values. Small AuChi adsorbed onto the liposome surfaces can inhibit liposome fusion, which in principle can minimize undesirable drug leakage from liposomes. Moreover, the membrane-bound AuChi may locally modulate the stiffness and morphology of the lipid bilayers, hindering diffusion of drug molecules across the liposomal membranes.[17] Using

doxycycline as a model antibiotic drug, we loaded it inside the AuChi-liposome with a drug concentration of 1 mM and then monitored its release profile from the liposomes. As shown in Figure 4.1.5, at pH = 1.2, AuChi-liposome only released approximately 10% of encapsulated doxycycline within 24 hr. In contrast, at pH = 7.4, over 90% of doxycycline was released within 24 hr. The significant decrease of drug release rate from the liposomes at pH = 1.2, corresponding to the strong binding of AuChi to the liposomes, confirms the stabilization of liposomes by surface adsorption of AuChi nanoparticles.

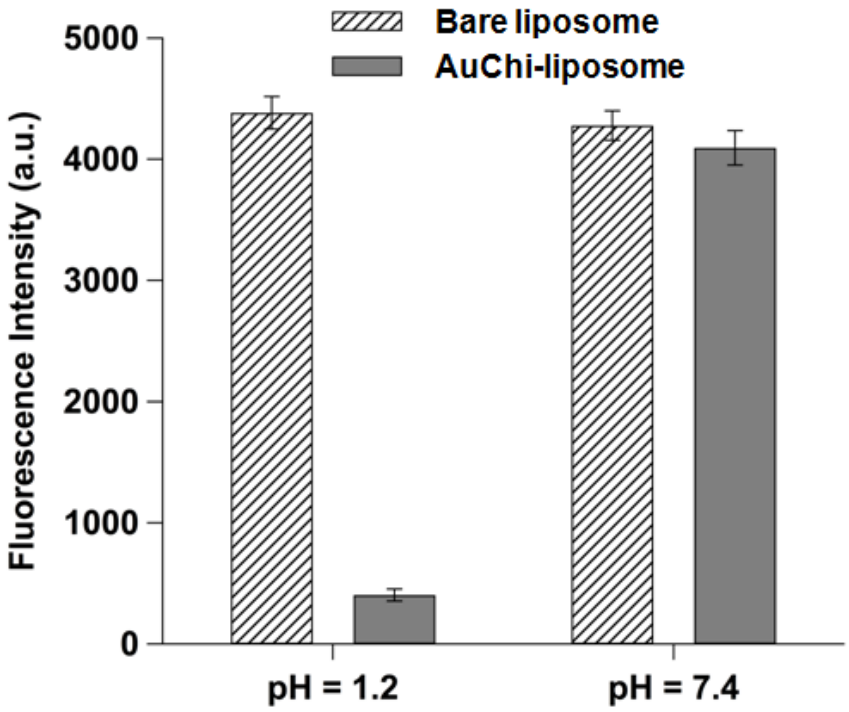


**Figure 4.1.4** Fusion ability of AuChi-liposome with *H. pylori* bacteria at pH = 1.2 and 7.4, respectively. Fluorescently labeled AuChi-liposome (0.5 mM) was incubated with *H. pylori* bacteria ($5\times10^8$ CFU/mL) at pH = 1.2 or 7.4 for 30 min. After incubation, the bacteria pellet was collected and then measured for fluorescence intensity. The same amount of fluorescently labeled bare liposome was tested in parallel as a control. Data represent mean ± SD (n = 3).

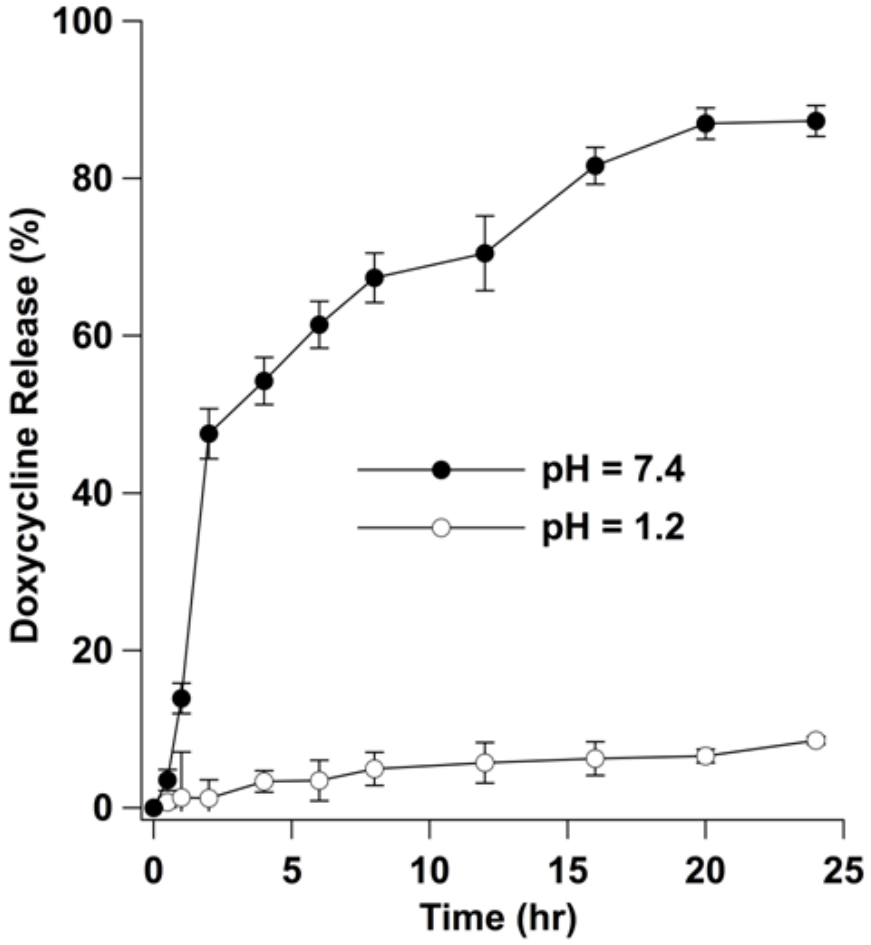


**Figure 4.1.5** Accumulative doxycycline release profile from doxycycline-loaded AuChi-liposome at pH = 1.2 and 7.4, respectively. The released doxycycline was quantified by measuring the UV absorbance at 345 nm using a spectrophotometer and then compared to a linear standard curve to calculate the amount of doxycycline released from the AuChi-liposome.

After having verified the pH-responsive stability of the AuChi-liposome, we finally tested the antimicrobial activity of doxycycline-loaded AuChi-liposome against *H. pylori* bacteria *in vitro*. While both the fusion activity and drug release property of liposomes were effectively inhibited by the adsorption of AuChi at gastric pH, these functions would resume upon detaching of AuChi at a physiological condition.

Subsequently, the drug-loaded liposomes would fuse with bacteria membranes to release therapeutic cargos. In the study, doxycycline-loaded AuChi-liposome at various doxycycline concentrations (ranging from 10 to 150 μg/mL) were mixed with *H. pylori* bacteria ($5\times10^6$ CFU/mL) at pH = 7.4. The samples then were incubated at 37°C under microaerobic conditions for 30 min, followed by serial dilution of each sample for bacterial colony enumeration. For comparison, the same concentration of empty AuChi-liposome (without drug) and free doxycycline we tested in parallel as controls and bacteria incubating in PBS served as a negative control. As shown in Figure 4.1.6, empty AuChi-liposome at all tested concentrations did not show any inhibitory effect against *H. pylori*, as their incubation with the bacteria resulted in a comparable colony formation to the PBS control. Free doxycycline showed a dose-dependent antimicrobial activity, but complete killing was not observed under the experimental conditions. In contrast, doxycycline-loaded AuChi-liposome showed an enhanced therapeutic efficacy against *H. pylori* at all tested concentrations. Particularly, eradication of *H. pylori* bacteria was achieved at a doxycycline concentration of 100 μg/mL. Such significant improvement on the drug's bactericidal efficacy is likely due to the rapid fusion between drug-loaded liposomes and bacterial membranes. Through the fusion process, all drug molecules entrapped in the liposomes are exclusively distributed into the bacteria, which may cause instant killing of the bacteria without inducing bacterial antibiotic resistance.[19, 33]

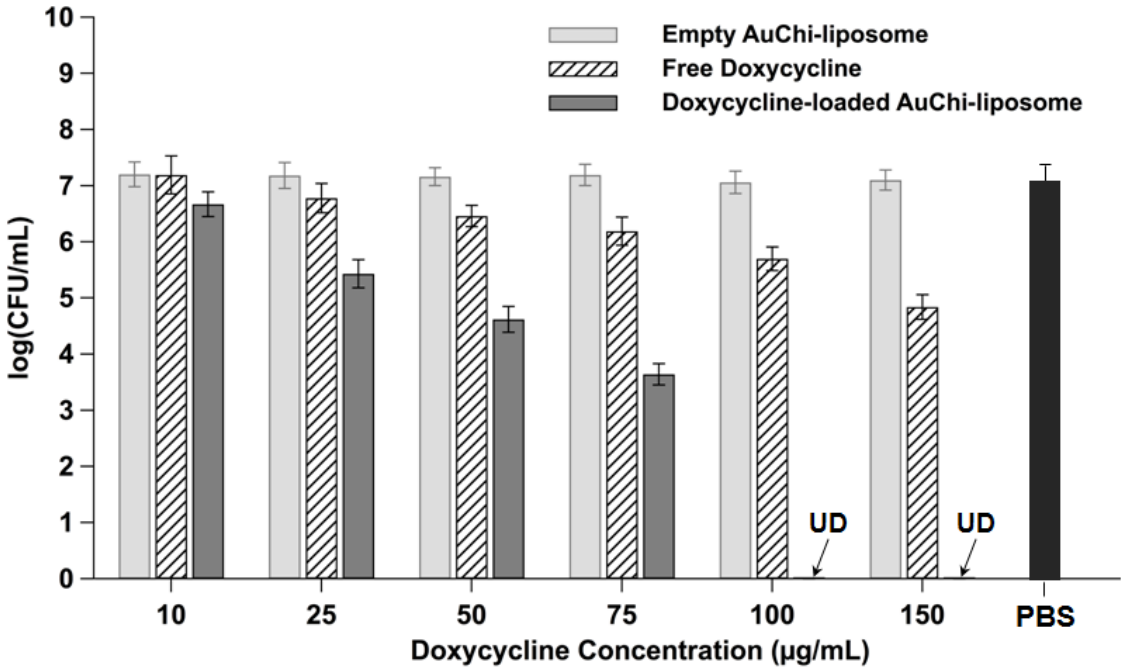


**Figure 4.1.6** Antimicrobial activity of doxycycline-loaded AuChi-liposome against *H. pylori* bacteria at various doxycycline concentrations. Doxycycline-loaded AuChi-liposome were incubated with *H. pylori* bacteria ($5\times10^6$ CFU/mL) at 37°C under microaerobic condition for 30 min, followed by serial dilution and bacterial colony enumeration on Columbia agar plates. Equivalent amounts of empty AuChi-liposome and free doxycycline were tested in parallel for comparison. PBS was used as a negative control. Data represent mean ± SD (n = 3).

## 4.1.4 Conclusions

In conclusion, by attaching chitosan-modified gold nanoparticles to the outer surface of anionic liposomes, a robust liposome-based gastric drug delivery system was developed. Such system has pH-responsive stability and fusion activity. Specifically, at gastric pH small gold nanoparticles spontaneously bound to the liposome surface, effectively inhibiting drug release and liposome fusion with *H.*

*pylori* bacteria. Once the pH level was increased to neutral pH (i.e., pH value at the mucus lining of stomach), gold nanoparticles detached and resulted in free liposomes with both fusion and drug release properties restored. Using doxycycline as a model antibiotic, the gold nanoparticle-stabilized liposome formulation exhibited superior antibacterial efficacy against *H. pylori* bacteria when compared with the same concentrations of free doxycycline. These results indicate that the use of small charged nanoparticles to stabilize liposomes represents a promising strategy for developing effective antibacterial regimes, especially for the treatment of stomach bacterial infections such as *H. pylori* infection.

## 4.1.5 References


1. Torchilin VP. Recent advances with liposomes as pharmaceutical carriers. *Nat Rev Drug Discov*. 2005, 4:145-60.

2. Huang C-M, Chen C-H, Pornpattananangkul D, Zhang L, Chan M, Hsieh M-F. Eradication of drug resistant *Staphylococcus aureus* by liposomal oleic acids. *Biomaterials*. 2011, 32:214-21.

3. Yang D, Pornpattananangkul D, Nakatsuji T, Chan M, Carson D, Huang CM, Zhang L. The antimicrobial activity of liposomal lauric acids against Propionibacterium acnes. *Biomaterials*. 2009, 30:6035-40.

4. Zhang L, Pornpattananangkul D, Hu CM, Huang CM. Development of nanoparticles for antimicrobial drug elivery. *Curr Med Chem*. 2010, 17:585-94.

5. Marrink S, Mark AE. The mechanism of vesicle fusion as revealed by molecular dynamics simulations. *J Am Chem Soc*. 2003, 125:11144-5.

6. Pornpattananangkul D, Zhang L, Olson S, Aryal S, Obonyo M, Vecchio K, Zhang L. Bacterial toxin-triggered drug release from gold nanoparticle-stabilized liposomes for the treatment of bacterial infection. *J Am Chem Soc* 2011, 133:4132-9.

7. Haluska CK, Riske KA, Marchi-Artzner V, Lehn J-M, Lipowsky R, Dimova R. Time scales of membrane fusion revealed by direct imaging of vesicle fusion with high temporal resolution. *Proc Natl Acad Sci USA*. 2006, 103:15841-6.

8. Moghimi SM, Szebeni J. Stealth liposomes and long circulating nanoparticles: critical issues in pharmacokinetics, opsonization and protein-binding properties. *Prog Lipid Res*. 2003, 42:463-78.

9. Knop K, Hoogenboom R, Fischer D, Schubert US. Poly(ethylene glycol) in drug delivery: pros and cons as well as potential alternatives. *Angew Chem Int Edit* 2010, 49:6288-308.

10. Woodle MC. Controlling liposome blood clearance by surface-grafted polymers. *Adv Drug Deliv Rev*. 1998, 32:139-52.

11. Zhang L, Gu FX, Chan JM, Wang AZ, Langer RS, Farokhzad OC. Nanoparticles in medicine: therapeutic applications and developments. *Clin Pharmacol Ther* 2008, 83:761-9.

12. Davis ME, Chen Z, Shin DM. Nanoparticle therapeutics: an emerging treatment modality for cancer. *Nat Rev Drug Discov*. 2008, 7:771-82.

13. Castro GA, Ferreira LA. Novel vesicular and particulate drug delivery systems for topical treatment of acne. *Expert Opin Drug Deliv*. 2008, 5:665-79.

14. Pornpattananangkul D, Olson S, Aryal S, Sartor M, Huang C-M, Vecchio K, Zhang L. Stimuli-responsive liposome fusion mediated by gold nanoparticles. *ACS Nano*. 2010, 4:1935-42.

15. Sinico C, Fadda AM. Vesicular carriers for dermal drug delivery. *Expert Opin Drug Deliv*. 2009, 6:813-25.

16. Zhang L, Granick S. How to stabilize phospholipid liposomes (using nanoparticles). *Nano Lett*. 2006, 6:694-8.

17. Wang B, Zhang L, Bae SC, Granick S. Nanoparticle-induced surface reconstruction of phospholipid membranes. *Proc Natl Acad Sci USA*. 2008, 105:18171-5.

18. Zhang L, Dammann K, Bae SC, Granick S. Ligand-receptor binding on nanoparticle-stabilized liposome surfaces. *Soft Matter*. 2007, 3:551-3.

19. Obonyo M, Zhang L, Thamphiwatana S, Pornpattananangkul D, Fu V, Zhang L. Antibacterial activities of liposomal linolenic acids against antibiotic-resistant *Helicobacter pylori*. *Mol Pharm*. 2012, 9:2677-85.

20. Peek RM, Jr., Blaser MJ. Helicobacter pylori and gastrointestinal tract adenocarcinomas. *Nat Rev Cancer*. 2002, 2:28-37.

21. Suerbaum S, Michetti P. Helicobacter pylori infection. *New Engl J Med*. 2002, 347:1175-86.

22. Furuta T, Graham DY. Pharmacologic aspects of eradication therapy for Helicobacter pylori Infection. *Gastroenterol Clin North Am*. 2010, 39:465-80.

23. Graham DY, Fischbach L. Helicobacter pylori treatment in the era of increasing antibiotic resistance. *Gut*. 2010, 59:1143-53.

24. Ito T, Kobayashi D, Uchida K, Takemura T, Nagaoka S, Kobayashi I. Helicobacter pylori invades the gastric mucosa and translocates to the gastric lymph nodes. *Lab Invest*. 2008, 88:664-81.

25. Necchi V, Candusso ME, Tava F, Luinetti O, Ventura U, Fiocca R. Intracellular, intercellular, and stromal invasion of gastric mucosa,

preneoplastic lesions, and cancer by Helicobacter pylori. *Gastroenterology*. 2007, 132:1009-23.

26. Lin Y-H, Chang C-H, Wu Y-S, Hsu Y-M, Chiou S-F, Chen Y-J. Development of pH-responsive chitosan/heparin nanoparticles for stomach-specific anti-Helicobacter pylori therapy. *Biomaterials*. 2009, 30:3332-42.

27. Tocanne JF, Teissie J. Ionization of phospholipids and phospholipid-supported interfacial lateral diffusion of protons in membrane model systems. *Biochim Biophys Acta*. 1990, 1031:111-42.

28. Hafez IM, Ansell S, Cullis PR. Tunable pH-sensitive liposomes composed of mixtures of cationic and anionic lipids. *Biophys J*. 2000, 79:1438-46.

29. Aryal S, B KCR, Dharmaraj N, Bhattarai N, Kim CH, Kim HY. Spectroscopic identification of S-Au interaction in cysteine capped gold nanoparticles. *Spectrochim Acta A*. 2006, 63:160-3.

30. Mayer LD, Hope MJ, Cullis PR. Vesicles of variable sizes produced by a rapid extrusion procedure. *Biochim Biophys Acta*. 1986, 858:161-8.

31. Gao W, Hu C-M, Fang RH, Luk BT, Jing Su, Zhang L. Surface functionalization of gold nanoparticles with red blood cell membranes. *Adv Mater* 2013, 25:3549-53.

32. Raikar US, Tangod VB, Mastiholi BM, Fulari VJ. Fluorescence quenching using plasmonic gold nanoparticles. *Opt Commun*. 2011, 284:4761-5.

33. Huh AJ, Kwon YJ. Nanoantibiotics: a new paradigm for treating infectious diseases using nanomaterials in the antibiotics resistant era. *J Control Release*. 2011, 156:128-45.

# 4.2 Virulence Factor-Responsive Liposomes

## 4.2.1 Introduction

Liposomes are an established drug carrier with well-documented advantages including highly biocompatible lipid materials, readily tunable formulation properties, and high drug carrying capacity[1-3]. Owing particularly to their distinguishable bilayer structure, liposomes are prone to fusion with bacterial membranes, making them a suitable delivery system for various antimicrobial treatments[4-6]. To further improve on the therapeutic efficacy of liposomal drugs, a myriad of environmentally responsive liposomal formulations have been developed that possess preferential liposome-bacterium fusion ability or triggered drug release at infection sites upon external stimulation[7, 8]. Common stimuli include temperature, pH, redox potential, and enzymatic activities, and these stimulus-responsive liposomal systems hold great promise to improve the current treatment regimes of bacterial infection[9-12].

Recently, nanoparticle-stabilized liposomes have emerged as a new and robust liposomal delivery system that involves the attachment of small charged nanoparticles onto the outer surfaces of phospholipid liposomes for liposome stabilization and triggered cargo release. The nonspecific adsorption of charged nanoparticles onto phospholipid bilayers provided steric repulsion that inhibited liposome fusion. It also reduced liposome surface tension and thus further enhanced liposome stability[13, 14]. Intriguingly, the charge and charge density of both the nanoparticle stabilizers and the liposomes could be precisely tailored to enable stimulus-responsive binding and

detachment of the nanoparticles, thereby allowing for an on-demand control over liposome fusion activity for smart drug delivery. For instance, cationic liposomes bound with negatively charged gold nanoparticles only fused with bacteria at acidic pH, which made them suitable for treating various skin pathogens that thrive in acidic infection sites such as the case with *Propionibacterium acnes*[15]. Conversely, anionic liposomes stabilized by positively charged gold nanoparticles were highly stable in gastric acid, but capable of fusing with bacteria at physiological pH, making them suitable to treat gastric pathogens such as *Helicobacter pylori* (*H. pylori*)[16]. Even in the absence of such stimulus-induced detachment of the nanoparticle stabilizers, these liposomes still had a substantial fraction of their surface areas exposed and highly accessible to membrane-targeting biochemical molecules such as bacterial toxins and enzymes. In a previous study, it has been shown that pore-forming toxins could effectively punch holes in the exposed lipid membranes to trigger antibiotic release from the nanoparticle-stablized liposomes[17]. Herein, we report their responsiveness to hydrolytic enzymes secreted by bacteria and demonstrate that the enzyme-triggered drug release subsequently kills or inhibits the growth of the enzyme-secreting bacteria. While in principle the enzyme-triggered antibiotic release from nanoparticle-stablized liposomes can be applied to a broad range of pathogens that secrete membrane-damaging enzymes, particular interest is focused on *H. pylori* in this work.

*H. pylori* infects nearly half of the world population and is of a significant public health concern. Infection with *H. pylori* is the primary cause of chronic gastritis, peptic ulcers, and gastric malignancy[6, 18, 19]. However, eradication of *H. pylori* is

challenging regardless of the treatment regimens, owing partly to the rapid emergence of *H. pylori* strains resistant to the antibiotics[20, 21]. *H. pylori* bacteria are known to secrete phospholipase A2 ($PLA_2$), a family of enzymes capable of hydrolyzing membrane phospholipids, causing mucosal damage and benefiting bacterial survival[22, 23]. Such enzymatic activity can be utilized as an environment cue to disrupt membrane integrity for triggered payload release from liposomes[24, 25]. In this study, we synthesized liposomes with lipid composition sensitive to $PLA_2$ and stabilized them with small chitosan-modified gold nanoparticles (AuChi). The adsorbed AuChi were effective in preventing liposome fusion and drug leakage, while leaving a considerable fraction of liposome surfaces accessible to $PLA_2$ enzyme. As shown in Figure 4.2.1, the cationic AuChi bind to the negatively charged liposome surfaces through electrostatic attraction and thus stabilize liposomes against fusion and avoid undesirable antibiotic leakage. When the stabilized liposomes are in the vicinity of *H. pylori* bacteria, the bacterium-secreted $PLA_2$ degrades phospholipids, compromises the membrane integrity, and subsequently releases the antibiotic payload. Such on-site release of antibiotics enables localized and rapid killing of *H. pylori* bacteria. We first demonstrated liposome stabilization upon AuChi adsorption and then examined the payload release kinetics of the AuChi-stabilized liposome (AuChi-liposome) in the presence of both purified $PLA_2$ and *H. pylori* culture, respectively. We further demonstrated that the released antibiotics from the liposomes in the presence of *H. pylori* were effective in inhibiting the growth of the bacteria.

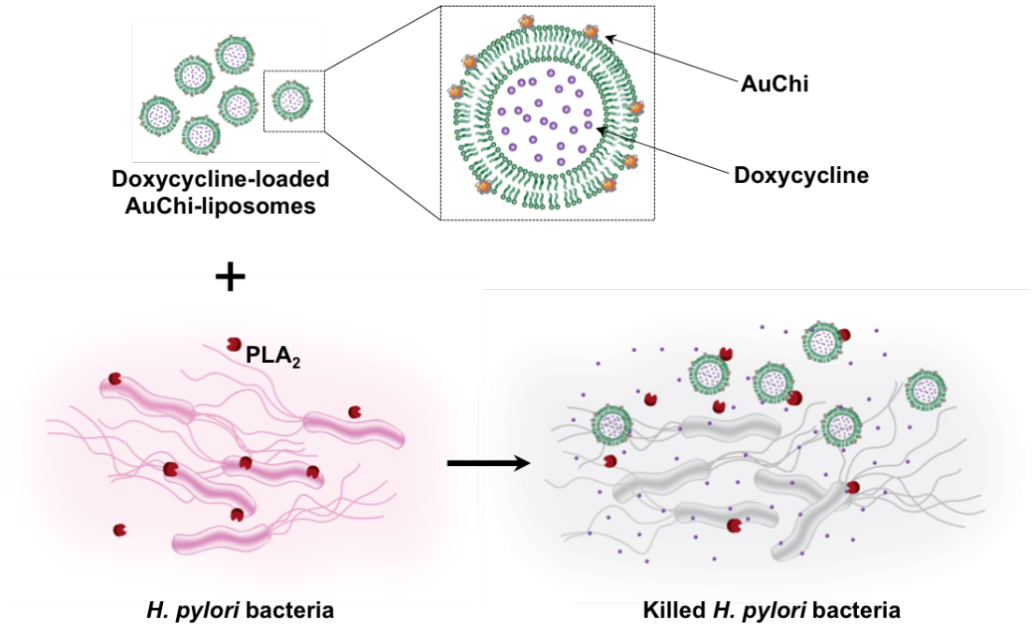


**Figure 4.2.1** Schematic illustration of phospholipase A2 ($PLA_2$)-triggered antibiotic release from liposomes stabilized by chitosan-modified gold nanoparticles (AuChi-liposome) to treat bacteria (e.g., *H. pylori*) that secrete the enzyme. Antibiotic (*e.g.* doxycycline)-loaded liposomes are prohibited from fusion by absorbing AuChi nanoparticles onto their surface. Once the AuChi-liposomes encounter bacteria-secreted $PLA_2$, the enzyme cleaves the phospholipids that form the liposome membranes and thus release the encapsulated antibiotics, which subsequently kill or inhibit the growth of the bacteria.

## 4.2.2 Experimental Methods

### 4.2.2.1 Materials

1,2-distearoyl-*sn*-glycero-3-phosphocholine (DSPC), 1,2-dioctadecanoyl-sn-glycero-3-phospho-(1'-rac-glycerol) (sodium salt) (DSPG), and 1,2-dimyristoyl-*sn*-glycero-3-phosphoethanolamine-N-lissamine rhodamine B sulfonyl (DMPE-RhB) were purchased from Avanti Polar Lipids, Inc (Alabaster, AL). 8-aminonaphthalene-1,3,6-trisulfonic acid disodium salt (ANTS) and *p*-xylene-bis-pyridinium bromide

(DPX) were purchased from Life Technology (Carlsbad, CA). Rhodamine B, doxycycline, phospholipase $A_2$ (*Apis mellifera*), and quinacrine dihydrochloride were purchased from Sigma Aldrich (St Louis, MO). Brain-heart infusion (BHI) broth and Columbia agar were purchased from Becton Dickinson (Sparks, MD). Hydrogen tetrachloroaurate ($HAuCl_4$) and sodium borohydride ($NaBH_4$) were purchased from ACROS Organics (Geel, Belgium). Chitosan-50 was purchased from Wako Pure Chemical Industries, Ltd. (Osaka, Japan).

### 4.2.2.2 Preparation of chitosan-modified gold nanoparticles (AuChi)

AuChi nanoparticles were prepared by sodium borohydride reduction technique as previously described [15, 16]. Briefly, an aqueous solution of $HAuCl_4$ (0.1 mM, 50 mL) was first reduced by 5 mg of $NaBH_4$ to form gold nanoparticles, followed by overnight incubation with 0.1% w/v chitosan that was pre-dissolved in 0.1 M acetic acid. The resulting AuChi nanoparticles were purified three times by using an Amicon Ultra-4 centrifugal filter with a molecular weight cut-off of 10 kDa and the final pH was adjusted to 6.5 by adding HCl. The nanoparticle size and surface zeta potential were determined by dynamic light scattering (DLS) measurements (Malvern Zetasizer ZS, Malvern Instruments, Worcestershire, UK).

### 4.2.2.3 Preparation of AuChi-stabilized liposomes (AuChi-liposomes)

Anionic liposomes were prepared by using a vesicle extrusion method. Briefly, DSPC, a zwitterionic phospholipid, and DSPG, an anionic phospholipid, were

dissolved in chloroform and mixed at 9:1 molar ratio. The organic solvent was evaporated under a stream of nitrogen gas until the thin lipid film was formed. Then the dry lipid film was hydrated with deionized water, or 2 mM rhodamine B (RhB), or 20mM doxycycline, followed by 2 min of vortexing and 30 min of bath sonication (Fisher Scientific FS30D, Pittsburgh, PA) to produce multilamellar vesicles (MLVs). The solution was then sonicated for 1 min at 20 W by a titanium probe (Branson 450 sonifier, Danbury, CT) to produce unilamellar vesicles. Following the sonication, the solution was extruded through a 100 nm pore-sized polycarbonate membrane for 11 times at 60°C to form narrowly distributed small unilamellar vesicles (SUVs). The liposomes were purified by gel filtration through a Sephadex G-75 column. To prepare fluorescently labeled liposomes, DMPE-RhB (0.5% mol) was added to the lipid mixture prior to liposome preparation. To prepare AuChi-liposomes, the liposomes and AuChi were mixed at 1:300 molar ratio, followed by 12 hrs of vortexing. Hydrodynamic size, size distribution, and surface charge of the liposomes and AuChi-liposomes were characterized by DLS (Malvern Zetasizer ZS, Malvern Instruments, Worcestershire, UK). All measurements were repeated three times at 25°C.

#### 4.2.2.4 *Helicobacter pylori (H. pylori)* bacterial culture

*H. pylori* Sydney strain 1 (SS1) were routinely maintained on Columbia agar supplemented with 5% laked horse blood at 37°C under microaerobic conditions (10% $CO_2$, 85% $N_2$, and 5% $O_2$) [6]. For experiments, broth cultures of *H. pylori* were prepared by sub-culturing fresh colonies from agar plates into BHI containing 5% fetal

bovine serum (FBS) overnight at 37°C under microaerobic conditions with moderate reciprocal shaking.

### 4.2.2.5 Liposome stability assay

A fluorescence method was used to study the fusion of AuChi-liposome with *H. pylori* bacteria. Specifically, $5\times10^8$ CFU *H. pylori* bacteria (determined by $OD_{600}$ value, $OD_{600}$ = 1.0 corresponding to approximately $1\times10^8$ CFU/mL) was washed three times with PBS by repeated centrifugation at 4,000 ×g. The bacteria pellet was collected and then mixed with 0.5 mM fluorescently labeled AuChi-liposome (containing 0.5 mol% of DMPE-RhB) at pH 6.5. After 10 min incubation, the bacteria pellet was collected by centrifugation at 4,000 ×g for 5 min and then resuspended in 1 mL PBS. The bacteria were then measured for fluorescence intensity at the range of 550-700 nm (DMPE-RhB's fluorescence emission range). DMPE-RhB-labeled bare liposomes (without AuChi stabilizer) were used as a control. The experiment was carried out in triplicate and average value was reported.

#### 4.2.2.6 Phospholipase $A_2$ ($PLA_2$)-triggered drug release from AuChi-liposomes

RhB was used as a model drug for release study. RhB-loaded AuChi liposomes were formulated as described above and the unencapsulated RhB molecules were removed by gel filtration through a Sephadex G-75 column. The samples were added with $PLA_2$ (at a final enzyme concentration of 0-100 μg/mL) and the mixtures were incubated at 37°C. At predetermined time points, released RhB was separated by

filtration using an Amicon Ultra-4 centrifugal filter with a molecular weight cut-off of 10 kDa at 14,000 × g for 20 min. RhB emission intensity at 585 nm was measured. To obtain 100% drug release, freshly prepared RhB-loaded AuChi-liposome suspension was disrupted by Triton-X-100 (1% v/v) to completely release the encapsulated drug, followed by drug quantification. Percentage of released drug was defined as following: Percentage of released drug (%) = $(I_{PLA_2} - I_{PBS})/(I_{Triton\text{-}X\text{-}100} - I_{PBS})\times 100$, in which $I_{PLA_2}$, $I_{PBS}$, and $I_{Triton\text{-}X\text{-}100}$ represent fluorescence emission intensity at 585 nm of the samples incubated with $PLA_2$, PBS, and Triton-X-100, respectively. The experiment was performed in triplicate.

### 4.2.2.7 AuChi-liposome drug release in *H. pylori* bacterial culture

In the study, 190 μL of RhB-loaded AuChi-liposome was added with 10 μL of overnight broth from *H. pylori* cultures originally containing $1\times10^7$ CFU/mL and $1\times10^8$ CFU/mL bacteria, respectively. The mixture was incubated for 1, 12, and 24 hrs under gentle shaking. After incubation, released RhB was separated by the same filtration process as described above. Quinacrine dihydrochloride (final concentration 0.13 μM), a $PLA_2$ inhibitor, was used to inhibit $PLA_2$ activity. RhB-loaded AuChi-liposome incubated in 5% (v/v) fresh BHI broth without being used for *H. pylori* culture was taken as a negative control. To obtain 100% drug release, Triton-X-100 (1% v/v) was added to disrupt liposomes. The experiments were repeated there times.

#### 4.2.2.8 Anti-*H. pylori* activity study

Doxycycline-loaded AuChi-liposomes were prepared as described. Free doxycycline molecules were removed by using a Sephadex G-75 column. Then 10 μL bacterial suspension containing $1\times10^7$ CFU *H. pylori* bacteria was added to 190 μL of doxycycline-loaded AuChi-liposome. The mixture was incubated with gentle shaking at 37°C under microaerobic conditions. After 12 hrs incubation, a series of 10-fold dilutions of the bacterial suspension (1:10 to $1:10^5$) was prepared, and 5 μL from each diluted sample was inoculated onto a Columbia agar plate supplemented with 5% laked horse blood. The plates were cultured in the incubator for 4 days before colony counting. Free doxycycline served as a positive control, while empty AuChi-liposome (without doxycycline) and PBS (1X, pH=6.5) served as negative controls. All experiments were repeated three times.

## 4.2.3 Results and Discussion

The preparation of AuChi-liposome can be divided into three steps. First, AuChi were synthesized by an ex-situ stabilization technique as previously described[16, 17]. Briefly, gold hydrosol made with a sodium borohydride reduction method was stabilized by adding calculated amount of chitosan under ambient condition, resulting the formation of AuChi. Dynamic light scattering (DLS) measurements of AuChi showed a diameter of approximately 10 nm with a narrow size distribution and a strong positive surface charge of 35.5 ± 0.9 mV, indicating the presence of cationic

amine groups of chitosan on gold surfaces. Second, 1,2-distearoyl-*sn*-glycero-3-phosphocholine (DSPC) and 1,2-dioctadecanoyl-*sn*-glycero-3-phospho-(1'-rac-glycerol) (sodium salt) (DSPG) in a molar ration of 9:1, a composition known to susceptible to $PLA_2$ degradation[26, 27], were used to formualte anionic liposomes following a standard extrusion method in deionized water[6]. DLS measurements of the liposomes showed a diameter of 84.7 ± 0.8 nm with polydispersity index of 0.12 ± 0.02 and a surface zeta potential of −54.7 ± 2.6 mV. Lastly, the anionic liposomes were mixed with cationic AuChi nanoparticles at a liposome-to-AuChi molar ratio of 1:300 under bath sonication for 10 min[16, 17]. The resulting AuChi-liposomes showed a diameter of 95.0 ± 2.7 nm. The slight size increase of AuChi-liposomes compared to bare liposomes corresponds to the adsorption of AuChi onto the liposome surface. Liposome surface change also switched from the strong negative value of the bare liposomes to 36.9 ± 1.3 mV of AuChi-liposomes, further confirming the binding of positively charged AuChi to the negatively charged liposomes through electrostatic interactions (Figure 4.2.2).

Adsorbed AuChi nanoparticles are expected to stabilize liposomes that are otherwise prone to fusion and drug leakage[16, 17, 28]. To test this, we first used a bacterium-liposome fusion assay[6, 16]. Specifically, 0.5 mM AuChi-liposomes containing 0.5 mol% DMPE-RhB were prepared and incubated with $5 \times 10^8$ CFU/mL *H. pylori* bacteria at 37°C for 30 min. Following the incubation, the bacteria pellets were collected and resuspended in PBS solution. The fusion ability of liposomes was then quantified by measuring the fluorescence intensity of the bacterial suspension. *H.*

*pylori* bacteria incubated with bare liposomes without AuChi stabilizers showed strong fluorescence intensity In contrast, a much weaker florescence signal was detected from the bacteria incubated with AuChi-liposomes, indicating a significantly reduced liposome fusion activity upon the adsorption of small AuChi nanoparticles (Figure 4.2.3A). We next tested the inhibition of drug leakage by AuChi nanoparticles. For this study, rhodamine B (RhB) was used as a model drug. As shown in Figure 4.2.3B, bare liposomes released all the fluorescence dye in 48 hrs. In contrast, less than 2% of the encapsulated RhB was released in the same time span from AuChi-liposomes. Together, these results confirm strong stabilization effects conferred by adsorbing AuChi stabilizers onto the liposome surface.

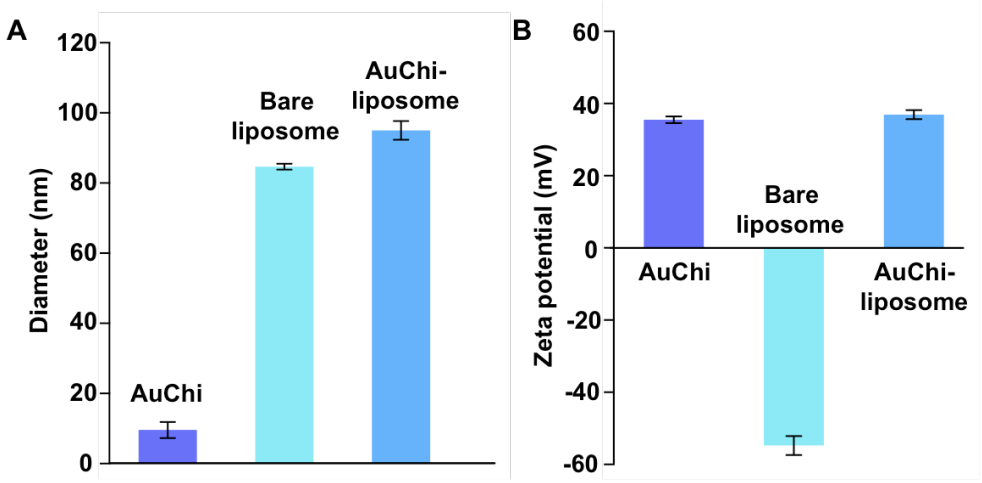


**Figure 4.2.2** (A) Hydrodynamic size (diameter, nm) and (B) surface zeta potential of AuChi, bare liposome (without AuChi), and AuChi-liposome with an AuChi-to-liposome molar ratio of 300:1

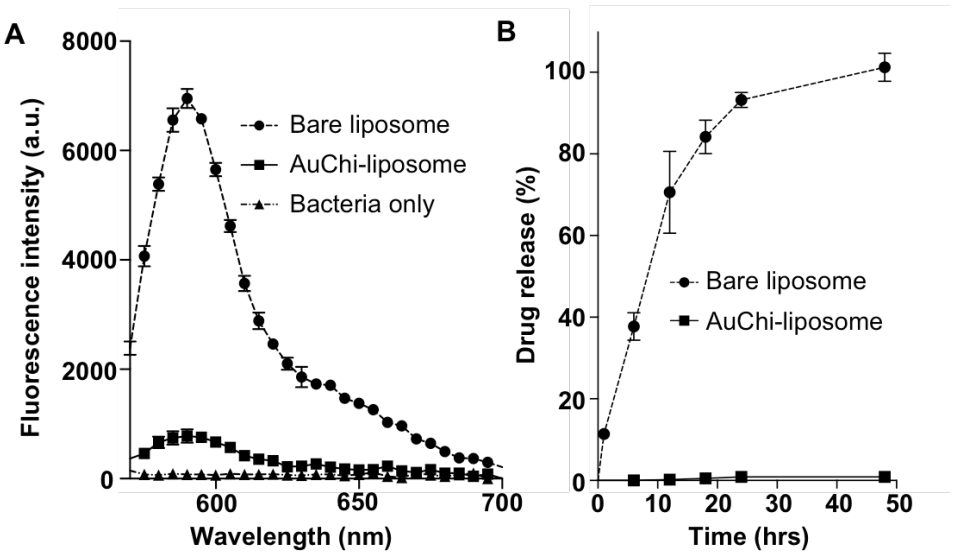


**Figure 4.2.3** (A) Fusion ability of bare liposome and AuChi-liposome with *H. pylori* bacteria. Fluorescently labeled liposome (bare liposome or AuChi-liposome) was incubated with $5\times10^8$ CFU *H. pylori* bacteria at pH 6.5 for 10 min. After incubation, the bacteria pellet was collected and quantified for fluorescence intensity at the range of 550-700 nm. The same amount of bacteria without incubating with any liposome formulations was tested in parallel serving as background signal. (B) Accumulative drug release profile from bare liposome and AuChi-liposome. RhB was used as a model drug loaded inside the liposome. The released RhB was quantified by measuring the fluorescence intensity at 585 nm.

We next proceeded to examine whether the drug release from AuChi-liposomes could be triggered by $PLA_2$. By adding purified $PLA_2$ into the RhB-loaded AuChi-liposome solutions, we found that the drug release rates increased with the increase of $PLA_2$ concentrations. When $PLA_2$ concentration was at 1, 10, and 100 μg/mL, approximately 5, 50, and 67% of encapsulated RhB molecules were released within 24 hrs, respectively (Figure 4.4.4A). In addition, accumulative RhB release profiles showed gradual increases with time without a burst release, implying that drug release kinetics from AuChi-liposomes in the presence of $PLA_2$ is dominated by diffusional liposome efflux [29, 30]. Therefore, we attempted to use a diffusion-dominant

Higuchi model to analyze the drug release profiles: $M_t = Kt^{1/2}$, where $M_t$ is drug release at time $t$ in hours and $K$ is the Higuchi constant [31, 32]. Plotting the drug release percentage against the square root of time yielded linear fittings with $R^2 = 0.97$ and 0.98 for 10 and 100 μg/mL $PLA_2$, respectively (Figure 4B). The goodness of the fit indicates a diffusion-controlled liposome release mechanism. On the basis of this analysis, the Higuchi constants of drug release with 10 and 100 μg/mL of $PLA_2$ were determined to be 10.57 ± 0.25, and 14.74 ± 0.26 $h^{-1/2}$, respectively.

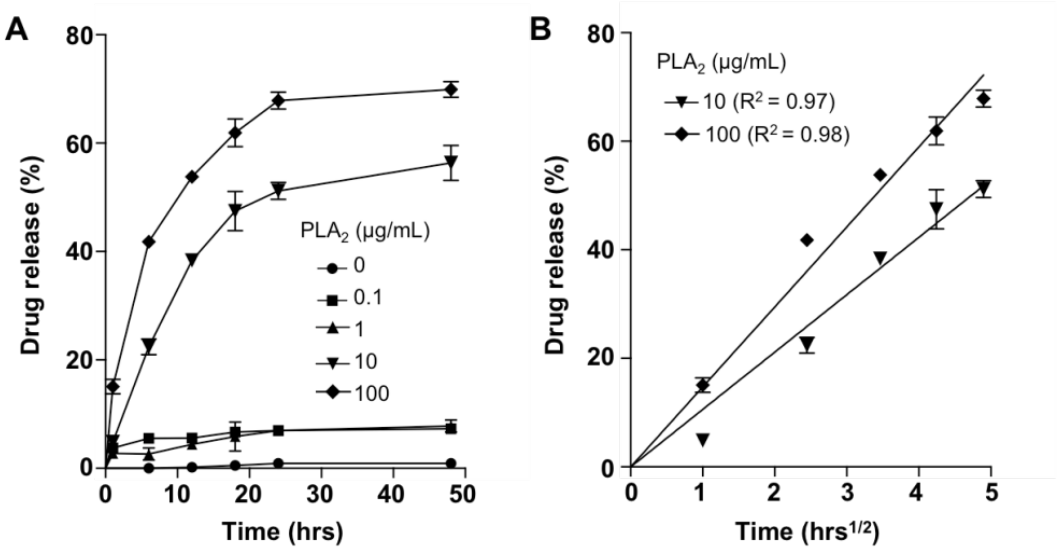


**Figure 4.2.4** (A) Accumulative drug release kinetics from AuChi-liposome in the presence of various $PLA_2$ enzyme concentrations. (B) The drug release percentage was plotted against the square root of time, which yielded linear fittings using a diffusion-dominant Higuchi model.

.

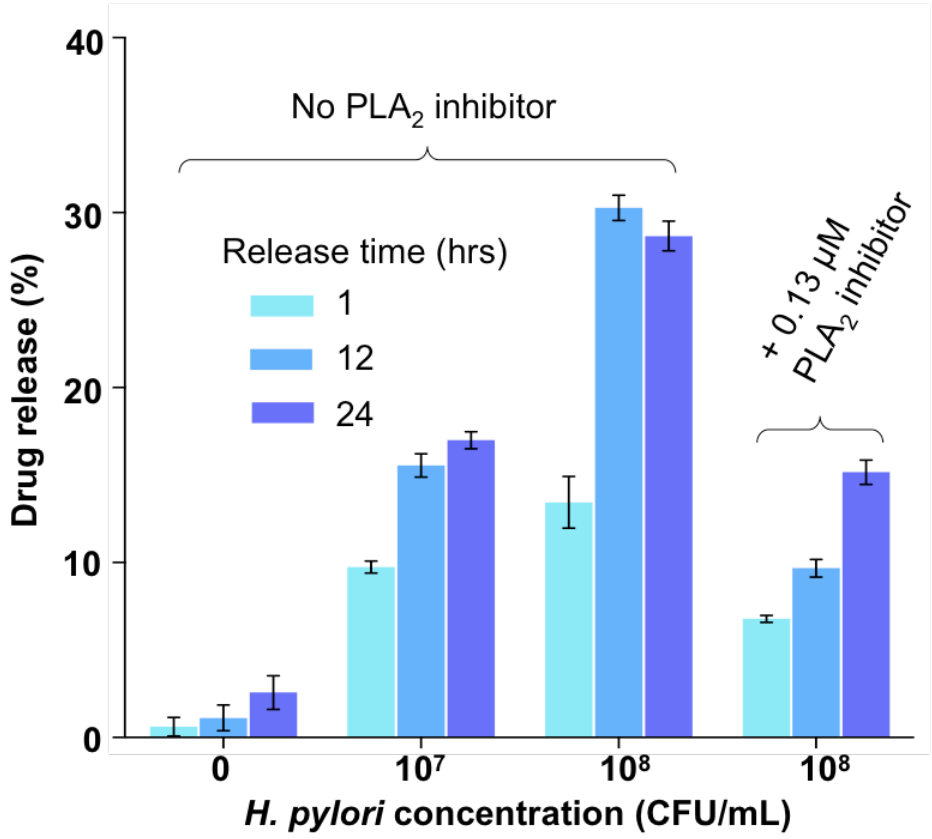


**Figure 4.2.5** Drug release from AuChi-liposome at 1 hr, 12 hrs, and 24 hrs post incubation with 0, $1\times10^7$ and $1\times10^8$ CFU/mL *H. pylori* bacteria culture, respectively. As a control group, quinacrine dihydrochloride (0.13 μM), a $PLA_2$ inhibitor, was added to the bacterial culture to inhibit $PLA_2$ activity. Data represent mean ±SD (n = 3).

To further verify that *H. pylori*-secreted $PLA_2$ can indeed trigger drug release from AuChi-liposomes, we incubated RhB-loaded AuChi-liposomes with *H. pylori* culture and monitored the release of RhB from the liposomes. As shown in Figure 4.2.5, when AuChi-liposomes were incubated in fresh culture medium without *H. pylori* bacteria, less than 5% RhB was released in 24 hrs, confirming that AuChi-liposomes were stable. However, when the AuChi-liposomes were incubated in

bacterial culture containing $1\times10^7$ CFU/mL *H. pylori* bacteria, 9.8%, 15.5%, and 17.0% of RhB was released in 1, 12, and 24 hrs, respectively. The drug release rate further increased when the bacterial concentration was increased. Specifically, when the bacterial concentration was increased to $1\times10^8$ CFU/mL, AuChi-liposomes released 13.4%, 30.3% and 28.7% of RhB in 1, 12, and 24 hrs, respectively. To further confirm that $PLA_2$ was indeed responsible for the accelerated drug release, 0.13 μM quinacrine dihydrochloride, a $PLA_2$ inhibitor, was added to the culture containing $1\times10^8$ CFU/mL *H. pylori*. Under this condition, a reduced drug release rate was observed; AuChi-liposomes released 6.8%, 9.7% and 15.1% of RhB in 1, 12, and 24 hrs, respectively. The incomplete inhibition of RhB release in the presence of quinacrine dihydrochloride was likely due to other *H. pylori*-secreted virulence factors such as CagA, VacA, and TlyA, which are all known to damage phospholipid membranes through various mechanisms[33-36].

After having verified the responsive drug release from AuChi-liposomes in the presence of both purified $PLA_2$ and $PLA_2$ secreted by *H. pylori* bacteria, we finally tested the antimicrobial activity of doxycycline-loaded AuChi-liposome against *H. pylori* bacteria. In the study, doxycycline-loaded AuChi-liposomes with a doxycycline concentration of 0.2 mM were incubated with *H. pylori* bacteria ($5\times10^7$ CFU/mL) in 5% BHI for 12 hrs, followed by serial dilution of each sample for bacterial colony enumeration. For comparison, the same concentration of free doxycycline was tested in parallel as a positive control, and empty AuChi–liposomes (without drug) and PBS (1X) served as negative controls. As shown in Figure 4.2.6, empty AuChi–liposome

did not show any inhibitory effect against *H. pylori*, as their incubation with the bacteria resulted in a comparable colony formation to the PBS (1X) control, whereas free doxycycline resulted a complete bacterial killing under the experimental condition. In contrast, doxycycline-loaded AuChi–liposomes showed excellent antimicrobial efficacy against *H. pylori* and such anti-*H. pylori* efficacy was significantly weakened when $PLA_2$ inhibitor (0.13 μM) was added to the bacterial culture. The incomplete killing of *H. pylori* by AuChi-liposomes was likely due to the partial release of docycycline during the 12 hrs of incubation time. With bacterial enzyme-triggered drug release mechanism, the doxycycline-loaded AuChi-liposomes confer distinct advantages to treat bacterial infections. For example, with a high stability, the formulation improves on the shelf-time of the liposomal drug with minimum drug leakage prior to administration. In addition, AuChi-liposomes allow antibiotics to be delivered in a bacterium-targeted fashion: antibiotic payloads will only be released at the infection sites where the bacteria secrete hydrolytic enzymes. More importantly, by using cues from the target bacteria to trigger drug release, the dosage of the antibiotics is self-regulated by the severity of the infections: the more bacteria present at the infection site, the more drugs will be released to treat the bacteria.

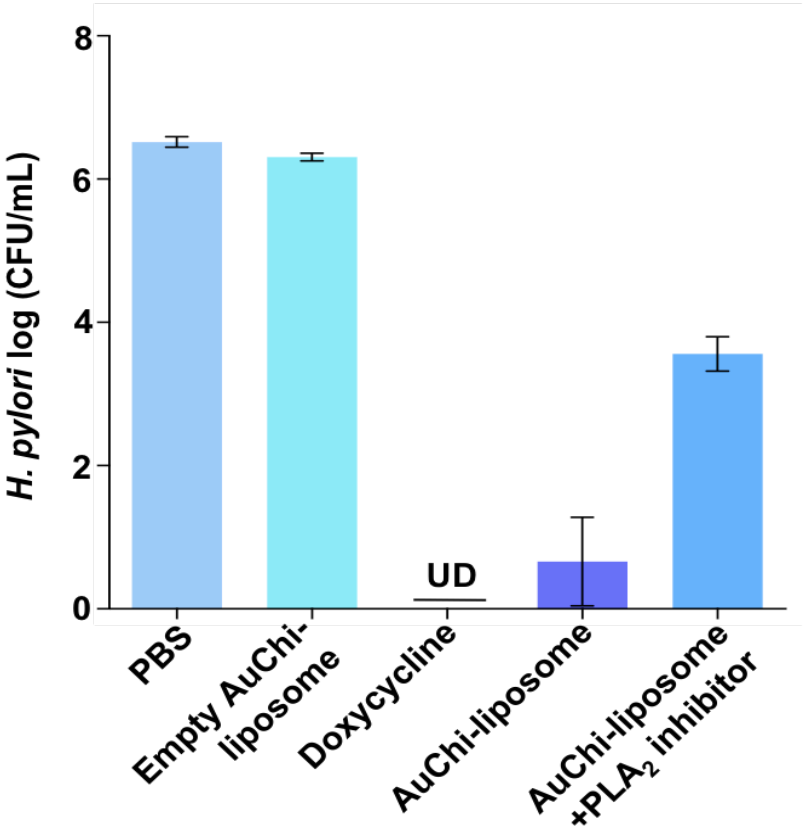


**Figure 4.2.6** Antimicrobial activity of doxycycline-loaded AuChi-liposome against *H. pylori* bacteria. Doxycycline-loaded AuChi-liposome was incubated with *H. pylori* bacteria ($5\times10^7$ CFU/mL) in 5% TSB for 24 hrs before the bacterium enumeration. To test the effect of $PLA_2$ on the observed antimicrobial activity, $PLA_2$ inhibitor (0.13 μM) was added the doxycycline-loaded AuChi-liposome and *H. pylori* mixture solution. Free doxycycline (0.2 mM) served as a positive control. Empty AuChi-liposome without doxycycline and PBS (pH = 6.5) served as two negative control groups. Data represent mean ±SD (n = 3).

## 4.2.4 Conclusions

In conclusion, we formulated a $PLA_2$-degradable liposome formulation and further adsorbed AuChi nanoparticles onto the liposome surfaces. The resulting

AuChi-liposomes were stable under storage conditions but were susceptible to $PLA_2$ degradation at infection site. Such liposomal formulation effectively prevented undesirable liposome fusion and drug leakage. However, the presence of $PLA_2$, either in purified form or in *H. pylori* culture, caused rapid drug release due to the enzymatic degradation of phospholipids and the subsequent damage of liposome integrity. When incubated with *H. pylori* bacteria *in vitro*, AuChi-liposomes effectively inhibited the bacterial growth. Although aimed for anti-*H. pylori* treatment in this particular study, the critical role played by $PLA_2$ has been increasingly recognized in various disease pathogenesis including bacterial infections, viral infections, and cancer development[37-40]. Therefore, $PLA_2$-responsive AuChi-liposomes hold great potential for preferential drug delivery with minimized side effects and targeted therapeutic efficacy to treat a wide range of diseases.

Chapter 4, in full, is a reprint of the material as it appears in Langmuir, 2013, Soracha Thamphiwatana, Victoria Fu, Jingying Zhu, Dainnan Lu, Weiwei Gao, and Liangfang Zhang, and, in full, on the material submitted for publication as it may appear in Journal of Materials Chemistry B, 2014, Soracha Thamphiwatana, Weiwei Gao, Marygorret Obonyo, and Liangfang Zhang. The dissertation author was the primary investigator and author of these papers.

## 4.2.5 References


1. Torchilin VP. Recent advances with liposomes as pharmaceutical carriers. *Nat Rev Drug Discov*. 2005, 4:145-60.

2. Allen TM, Cullis PR. Liposomal drug delivery systems: From concept to clinical applications. *Adv Drug Del Rev*. 2013, 65:36-48.

3. Gao W, Hu C-MJ, Fang RH, Zhang L. Liposome-like nanostructures for drug delivery. *J Mater Chem B*. 2013, 1:6569-85.

4. Yang D, Pornpattananangkul D, Nakatsuji T, Chan M, Carson D, Huang C-M, Zhang L. The antimicrobial activity of liposomal lauric acids against Propionibacterium acnes. *Biomaterials*. 2009, 30:6035-40.

5. Zhang L, Pornpattananangkul D, Hu C-M, Huang CM. Development of Nanoparticles for Antimicrobial Drug Delivery. *Curr Med Chem*. 2010, 17:585-94.

6. Obonyo M, Zhang L, Thamphiwatana S, Pornpattananangkul D, Fu V, Zhang L. Antibacterial Activities of Liposomal Linolenic Acids against Antibiotic-Resistant Helicobacter pylori. *Mol Pharm*. 2012, 9:2677-85.

7. Gao W, Chan JM, Farokhzad OC. pH-Responsive Nanoparticles for Drug Delivery. *Mol Pharm*. 2010, 7:1913-20.

8. Mura S, Nicolas J, Couvreur P. Stimuli-responsive nanocarriers for drug delivery. *Nat Mater*. 2013, 12:991-1003.

9. Gao W, Zhang L. Anticancer agents unleash the forces within. *Nat Chem*. 2012, 4:971-2.

10. De la Rica R, Aili D, Stevens MM. Enzyme-responsive nanoparticles for drug release and diagnostics. *Adv Drug Del Rev*. 2012, 64:967-78.

11. Chan A, Orme RP, Fricker RA, Roach P. Remote and local control of stimuli responsive materials for therapeutic applications. *Adv Drug Del Rev*. 2013, 65:497-514.

12. Ta T, Porter TM. Thermosensitive liposomes for localized delivery and triggered release of chemotherapy. *J Controlled Release*. 2013, 169:112-25.

13. Zhang L, Granick S. How to stabilize phospholipid liposomes (using nanoparticles). *Nano Lett*. 2006, 6:694-8.

14. Wang B, Zhang L, Bae SC, Granick S. Nanoparticle-induced surface reconstruction of phospholipid membranes. *Proc Natl Acad Sci USA*. 2008, 105:18171–5.

15. Pornpattananangkul D, Olson S, Aryal S, Sartor M, Huang C-M, Vecchio K, Zhang L. Stimuli-Responsive Liposome Fusion Mediated by Gold Nanoparticles. *ACS Nano*. 2010, 4:1935-42.

16. Thamphiwatana S, Fu V, Zhu J, Lu D, Gao W, Zhang L. Nanoparticle-Stabilized Liposomes for pH-Responsive Gastric Drug Delivery. *Langmuir*. 2013, 29:12228-33.

17. Pornpattananangkul D, Zhang L, Olson S, Aryal S, Obonyo M, Vecchio K, Zhang L. Bacterial Toxin-Triggered Drug Release from Gold Nanoparticle-Stabilized Liposomes for the Treatment of Bacterial Infection. *J Am Chem Soc*. 2011, 133:4132-9.

18. Peek RM, Blaser MJ. Helicobacter pylori and gastrointestinal tract adenocarcinomas. *Nat Rev Cancer*. 2002, 2:28-37.

19. Suerbaum S, Michetti P. Medical progress: Helicobacter pylori infection. *New Engl J Med*. 2002, 347:1175-86.

20. Iwanczak F, Iwanczak B. Treatment of Helicobacter pylori Infection in the Aspect of Increasing Antibiotic Resistance. *Adv Clin Exp Med*. 2012, 21:671-80.

21. Wu W, Yang Y, Sun G. Recent Insights into Antibiotic Resistance in Helicobacter pylori Eradication. *Gastroenterol Res Pract*. 2012, 2012:Article ID 723183.

22. Nardone G, Holicky EL, Uhl JR, Sabatino L, Staibano S, Rocco A. In Vivo and In Vitro Studies of Cytosolic Phospholipase A2 Expression in Helicobacter pylori Infection. *Infect Immun*. 2001, 69:5857–63.

23. Lusini P, Figura N, Valassina M, Roviello F, Vindigni C, Trabalzini L. Increased phospholipase activity in Helicobacter pylori strains isolated from patients with gastric carcinoma. *Dig Liver Dis*. 2005, 37:232-9.

24. Andresen TL, Davidsen J, Begtrup M, Mouritsen OG, Jorgensen K. Enzymatic release of antitumor ether lipids by specific phospholipase A2 activation of liposome-forming prodrugs. *J Med Chem*. 2004, 47:1694-703.

25. Jorgensen K, Vermehren C, Mouritsen OG. Enhancement of phospholipase A(2) catalyzed degradation of polymer grafted PEG-liposomes: Effects of lipopolymer-concentration and chain-length. *Pharm Res*. 1999, 16:1491-3.

26. Andresen TL, Jensen SS, Kaasgaard T, Jorgensen K. Triggered activation and release of liposomal prodrugs and drugs in cancer tissue by secretory phospholipase A2. *Curr Drug Del*. 2005, 2:353-62.

27. Zhu G, Mock JN, Aljuffali I, Cummings BS, Arnold RD. Secretory Phospholipase A(2) Responsive Liposomes. *J Pharm Sci*. 2011, 100:3146-59.

28. Gao W, Vecchio D, Li J, Zhu J, Zhang Q, Fu V, Thamphiwatana S, Zhang L. Hydrogel Containing Nanoparticle-Stabilized Liposomes for Topical Antimicrobial Delivery. *ACS Nano*. 2014, 8:2900-7.

29. Jensen SS, Andresen TL, Davidsen J, Hoyrup P, Shnyder SD, Bibby MC. Secretory phospholipase A(2) as a tumor-specific trigger for targeted delivery of a novel class of liposomal prodrug anticancer etherlipids. *Mol Cancer Ther*. 2004, 3:1451-8.

30. Aili D, Mager M, Roche D, Stevens MM. Hybrid Nanoparticle-Liposome Detection of Phospholipase Activity. *Nano Lett*. 2011, 11:1401-5.

31. Higuchi T. Rate of release of medicaments from ointment bases containing drugs in suspension. *J Pharm Sci*. 1961, 50:874-5.

32. Siepmann J, Peppas NA. Higuchi equation: Derivation, applications, use and misuse. *Int J Pharm*. 2011, 418:6-12.

33. Dorrell N, Martino MC, Stabler RA, Ward SJ, Zhang ZW, McColm AA. Characterization of Helicobacter pylori PldA, a phospholipase with a role in colonization of the gastric mucosa. *Gastroenterology*. 1999, 117:1098-104.

34. Martino MC, Stabler RA, Zhang ZW, Farthing MJG, Wren BW, Dorrell N. Helicobacter pylori pore-forming cytolysin orthologue TlyA possesses in vitro hemolytic activity and has a role in colonization of the gastric mucosa. *Infect Immun*. 2001, 69:1697-703.

35. Hatakeyama M, Higashi H. Helicobacter pylori CagA: a new paradigm for bacterial carcinogenesis. *Cancer Sci*. 2005, 96:835-43.

36. Jones KR, Whitmire JM, Merrell DS. A tale of two toxins: Helicobacter pylori CagA and VacA modulate host pathways that impact disease. *Front Microbiol*. 2010, 1:article 115.

37. Sitkiewicz I, Stockbauer KE, Musser JM. Secreted bacterial phospholipase A(2) enzymes: better living through phospholipolysis. *Trends Microbiol*. 2007, 15:63-9.

38. Murakami M, Taketomi Y, Sato H, Yamamoto K. Secreted phospholipase A(2) revisited. *J Biochem*. 2011, 150:233-55.

39. Dennis EA, Cao J, Hsu Y-H, Magrioti V, Kokotos G. Phospholipase A(2) Enzymes: Physical Structure, Biological Function, Disease Implication, Chemical Inhibition, and Therapeutic Intervention. *Chem Rev*. 2011, 111:6130-85.

40. Murakami M, Lambeau G. Emerging roles of secreted phospholipase A(2) enzymes: An update. *Biochimie*. 2013, 95:43-50.

# Chapter 5

## Conclusions

## 5.1 LipoLLA Against Antibiotic-Resistant *H. pylori* strains

*Helicobacter pylori* (*H. pylori*) infection with its vast prevalence is responsible for various gastric diseases including gastritis, peptic ulcers, and gastric malignancy. While effective, current treatment regimens are challenged by a fast-declining eradication rate due to the increasing emergence of *H. pylori* strains resistant to existing antibiotics. Therefore, there is an urgent need to develop novel antibacterial strategies against *H. pylori*. In this study, we developed a liposomal nanoformulation of linolenic acid (LipoLLA) and evaluated its bactericidal activity against resistant strains of *H. pylori*. Using a laboratory strain of *H. pylori*, we found that LipoLLA was effective in killing both spiral and coccoid forms of the bacteria via disrupting bacterial membranes. Using a metronidazole-resistant strain of *H. pylori* and seven clinically isolated strains, we further demonstrated that LipoLLA eradicated all strains of the bacteria regardless of their antibiotic resistance status. Furthermore, under our experimental conditions, the bacteria did not develop drug resistance when cultured with LipoLLA at various sub-bactericidal concentrations, whereas they rapidly acquired resistance to both metronidazole and free linolenic acid (LLA). Our findings suggest that LipoLLA is a promising antibacterial nanotherapeutic to treat antibiotic-resistant *H. pylori* infection.

## 5.2 *H. pylori* Treatment with LipoLLA *in vivo*

*Helicobacter pylori* (*H. pylori*) infection is marked with its vast prevalence and strong association with various gastric diseases including gastritis, peptic ulcers, and gastric cancer. Due to the rapid emergence of *H. pylori* strains resistant to existing antibiotics, current treatment regimens show a rapid decline of their eradication rates. There is a clear urgency to develop novel antibacterial strategies against *H. pylori*. Herein, we investigated the *in vivo* therapeutic potential of liposomal linolenic acid (LipoLLA) for the treatment of *H. pylori* infection. The LipoLLA formulation with a size of approximately 100 nm were prone to fuse with bacterial membranes, thereby directly releasing a high dose of linolenic acids into the bacterial membranes. LipoLLA penetrated the mucus layer of mouse stomach, and a significant portion of the administered LipoLLA was retained in the stomach lining up to 24 hours after the oral administration. In vivo tests further confirmed that LipoLLA was able to kill *H. pylori* and reduce bacterial load in the mouse stomach. LipoLLA treatment was also shown to reduce the levels of proinflammatory cytokines including interleukin-1β (IL-1β), IL-6, and tumor necrosis factor alpha, which were otherwise elevated due to the *H. pylori* infection. Finally, toxicity test demonstrated excellent biocompatibility of LipoLLA to normal mouse stomach. Collectively, results from this work indicate that LipoLLA is a promising, new, effective, and safe therapeutic agent for the treatment of *H. pylori* infection.

## 5.3 pH-Responsive Liposomes

We report a novel pH-responsive gold nanoparticle-stabilized liposome system for gastric antimicrobial delivery. By adsorbing small chitosan-modified gold nanoparticles (diameter ~ 10 nm) onto the outer surface of negatively charged phospholipid liposomes (diameter ~ 75 nm), we show that at gastric pH the liposomes have excellent stability with limited fusion ability and negligible cargo releases. However when the stabilized liposomes are present in an environment with neutral pH, the gold stabilizers detach from the liposomes resulting in free liposomes that can actively fuse with bacterial membranes. Using *Helicobacter pylori* as a model bacterium and doxycycline as a model antibiotic, we demonstrate such pH-responsive fusion activity and drug release profile of the nanoparticle-stabilized liposomes. Particularly, at neutral pH the gold nanoparticles detach and thus the doxycycline-loaded liposomes rapidly fuse with bacteria and cause superior bactericidal efficacy as compared to the free doxycycline counterpart. Our results suggest that the reported liposome system holds a substantial potential for gastric drug delivery; it remains inactive (stable) in the stomach lumen but actively interact with bacteria once reaches the mucus layer of the stomach where the bacteria may reside.

## 5.4 Virulence Factor-Responsive Liposomes

Adsorbing small charged nanoparticles onto liposome surfaces to stabilize them against fusion and payload leakage has resulted in a new class of liposomes capable of environment-responsive drug delivery. Herein, we engineered a liposome formulation with a lipid composition sensitive to bacterium-secreted phospholipase A2 ($PLA_2$) and adsorbed chitosan-modified gold nanoparticles (AuChi) onto the liposome surface. The resulting AuChi-stabilized liposomes (AuChi-liposomes) showed prohibited fusion activity and negligible drug leakage. However, upon exposure to either purified $PLA_2$ enzyme or $PLA_2$ secreted by *Helicobacter pylori* (*H. pylori*) bacteria in culture, AuChi-liposomes rapidly released the encapsulated payloads and such responsive release was retarded by adding quinacrine dihydrochloride, a $PLA_2$ inhibitor. When loaded with doxycycline, AuChi-liposomes effectively inhibited *H. pylori* growth. Overall, the AuChi-liposomes allowed for smart "on-demand" antibitoic delivery: the more enzymes or bacteria present at the infection site, the more drug will be released to treat the infection. Given the strong association of $PLA_2$ with a diverse range of diseases, the present liposomal delivery technique holds broad application potential for tissue microenvironment-responsive drug delivery.